Hilmar Hofmann

Characteristics and implications of surface gravity waves in the littoral zone of a large lake (Lake Constance)

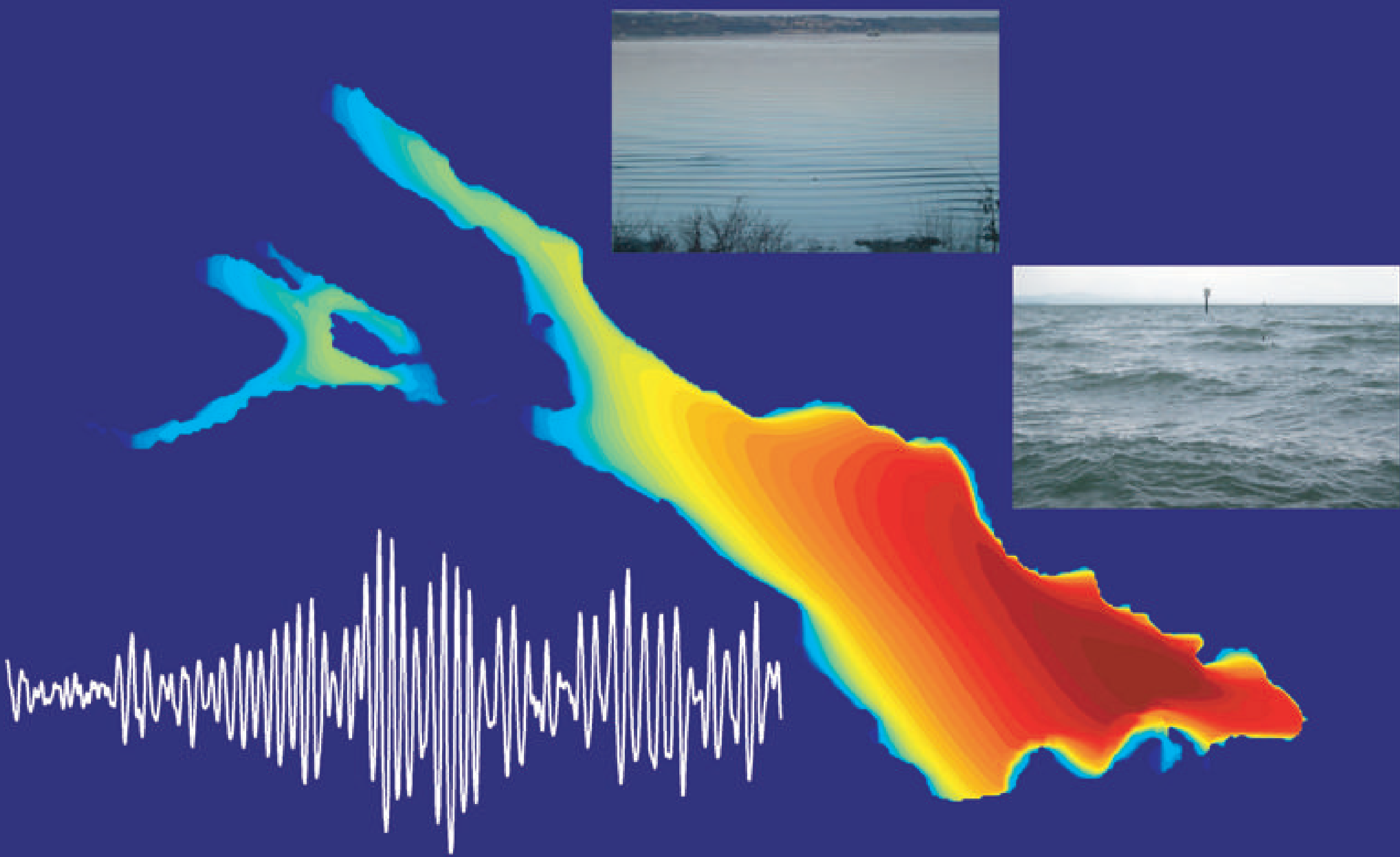

Cuvillier Verlag Göttingen

Characteristics and implications of surface gravity waves in the littoral zone of a large lake (Lake Constance)

Dissertation

Zur Erlangung des akademischen Grades des
Doktors der Naturwissenschaften (Dr. rer. nat.)
an der
Universität Konstanz
Mathematisch-Naturwissenschaftliche Sektion
Fachbereich Biologie

vorgelegt von

Hilmar Hofmann

Konstanz, 2007

Tag der mündlichen Prüfung: 23.06.2008
Referent: Prof. Dr. Frank Peeters
Referent: Dr. habil. Klaus Jöhnk
Referent: Prof. Dr. habil. Karl-Otto Rothhaupt

Bibliografische Information der Deutschen Nationalbibliothek
Die Deutsche Nationalbibliothek verzeichnet diese Publikation in der Deutschen Nationalbibliografie; detaillierte bibliografische Daten sind im Internet über http://dnb.ddb.de abrufbar.
1. Aufl. - Göttingen : Cuvillier, 2008
Zugl.: Konstanz, Univ., Diss., 2007

978-3-86727-714-3

Nonnenstieg 8, 37075 Göttingen
Telefon: 0551-54724-0
Telefax: 0551-54724-21
www.cuvillier.de

1. Auflage, 2008
Gedruckt auf säurefreiem Papier

978-3-86727-714-3

Table of contents

Summary

The central issue of this thesis is to provide a detailed characterization of the surface wave field in a lacustrine ecosystem including small-amplitude wind and ship waves with their specific implications on physical processes and biological conditions (e.g., sediment resuspension and light climate). Therefore, surface waves were measured during different seasons (long-term approach), wind regimes, and water levels in the littoral zone of Lake Constance.

A review of water level fluctuations revealed their different temporal and spatial scales. In the case of Lake Constance, seasonal water level fluctuations are next to high-frequency surface waves an important factor, since they change the section of the shore and thus the sediment composition exposed to high-energetic surface waves.

The measurement of the surface wave field showed that wind and ship waves can be distinguished by their properties. Wind waves are characterized by small wave heights and short wave periods. Their range is determined by the prevailing wind speed and the effective fetch length at the specific site. The occurrence of wind waves is rather sporadically and infrequent. Ship waves occur very frequently at regular time intervals, have higher wave periods and longer wave lengths than wind waves, and are generated by regular car and passenger ferries, passenger ships, and a newly introduced catamaran ferry. In contrast to wind waves, the occurrence of ship waves follows a diurnal and a seasonal pattern, because of the pronounced ship traffic at daytime especially during the tourist season in summer. On Lake Constance, ship waves are as important as wind waves and during summer they even dominate the wave field. Since ship waves are generated all around Lake Constance and due to their ability to travel over long distances, the results obtained at the study site Littoral Garden are representative for most of the southern and southwestern shores.

According to the different temporal patterns of wave generation, wind-wave induced resuspension occurs sporadically and less frequent than ship-wave induced resuspension. The periodic and regular occurrence of ship waves, especially of passenger ships during daytime and in summer, cause a substantial increase of the suspended sediment concentration in the shallow littoral, and hence cause a diurnal cycle as well as a seasonal pattern in the suspended sediment concentration and resuspension. Ship-wave induced resuspension is known to prevent sediment consolidation and may significantly contribute to erosion. The continuous interplay between seasonal water level fluctuations and surface waves under the condition of decreasing mean water levels can further support sediment erosion.

Simultaneous, high-frequent measurements of surface wave field and underwater light climate revealed amplitudes and temporal scales of the fluctuations in the light intensity, which are caused by the process of wave focusing, the change in the surface elevation, and resuspension. Wave focusing is induced by wind-generated ripple waves. It causes fluctuations of the underwater light intensity with large amplitudes and high frequencies that are far above the pure effect of surface elevation. On the other hand, wave-induced resuspension dramatically reduces the underwater light intensity in the littoral zone due to the shading effect of suspended particles, and thus limits the availability of light for the growth of phytoplankton and biofilms.

Measurements of the surface wave field and the related currents were also performed in a wave mesocosm, which is used for various biological investigations focusing on implications of waves on biota in the shallow littoral. The comparison of a typical wave in the mesocosm with waves in the field revealed the limitations as well as the advantages of mesocosm experiments compared to field experiments. Since the wave heights and periods and also the magnitude of other wave-related parameters in the wave mesocosm are much smaller than in the field, the implications on biota determined during biological experiments may underestimate the actual impact of wave motion in the field.

In conclusion, this thesis is the first long-term investigation that gives a detailed characterization of the surface wave field including small-amplitude waves with a high temporal resolution in a lacustrine environment. In Lake Constance, wind as well as ship waves contribute to the overall wave field, whereas ship waves are as important as wind waves on an annual scale and even dominate the wave field during summer. The specific occurrence and properties of wind and ship waves cause different temporal patterns and have various implications on sediment resuspension and the underwater light climate, which in turn affect biotic processes in the littoral ecosystem. This thesis demonstrates the strong linkages between physical processes and biological conditions, which supports the need of integrated research.

Zusammenfassung

Zentrales Thema dieser Dissertation ist eine detaillierte Charakterisierung des Oberflächenwellenfeldes in einem limnischen Ökosystem, bei der sowohl Wind- als auch Schiffswellen und ihre jeweiligen Auswirkungen auf physikalische Prozesse und biologische Bedingungen berücksichtigt werden (z. B. die Resuspension von Sedimenten und das Unterwasser-Lichtklima). Dazu wurden Oberflächenwellen während unterschiedlicher Jahreszeiten (langfristige Messungen), Windregime und Wasserständen im Litoral des Bodensees gemessen.

Die umfassende Darstellung von Wasserspiegelschwankungen zeigte deren unterschiedliche zeitliche und räumliche Skalen auf. Im Fall des Bodensee bilden saisonale Wasserspiegelschwankungen neben Oberflächenwellen einen wichtigen Faktor, da sie den Abschnitt des Ufers und somit die Zusammensetzung der Sedimente verändern, die den energiereichen Oberflächenwellen ausgesetzt werden.

Die Messung des Wellenfeldes im Bodensee ergab, dass Wind- und Schiffwellen anhand ihrer Eigenschaften unterschieden werden können. Windwellen haben geringe Wellenhöhen und kurze Wellenperioden, die von der vorherrschenden Windgeschwindigkeit und der Wirklänge des Windes am jeweiligen Standort bestimmt werden. Sie treten relativ sporadisch und selten auf. Schiffswellen kommen dagegen sehr häufig und in regelmäßigen Zeitabständen vor, und besitzen größere Wellenperioden und Wellenlängen als Windwellen. Sie werden von Auto- und Passagierfähren, Passagierschiffen und einer neu eingeführten Katamaranfähre erzeugt. Im Gegensatz zu Windwellen, kann man bei Schiffswellen ein ausgeprägtes diurnales und saisonales Muster beobachten, das durch das fast ausschließliche Auftreten des Schiffsverkehrs am Tag und während der touristischen Kursschifffahrt im Sommer erzeugt wird. Im Bodensee sind Schiffswellen im Jahresmittel ebenso bedeutend wie Windwellen, und während des Sommers dominieren sie sogar das Wellenfeld. Das ubiquitäre Auftreten von Schiffswellen im Bodensee und ihre Eigenschaft sich über lange Strecken

auszubreiten, machen die Ergebnisse der Untersuchungen im Litoralgarten auf die meisten der südlich und südwestlich gelegenen Ufer des Bodensees übertragbar.

Das zeitlich unterschiedliche Auftreten von Wind- und Schiffswellen spiegelt sich in der Resuspension von Sedimenten wider. Die durch Windwellen hervorgerufene Resuspension tritt sporadischer und seltener auf als die durch Schiffswellen erzeugte. Das periodische und regelmäßige Auftreten von Schiffswellen verursacht eine deutliche Konzentrationszunahme von suspendierten Partikeln in der Flachwasserzone, besonders am Tag und im Sommer wenn die meisten Passagierschiffe verkehren. Die regelmäßige Resuspension durch Schiffswellen kann die Konsolidierung des Sediments verhindern und so zur Erosion beitragen. Auch die kontinuierliche Interaktion von saisonalen Wasserspiegelschwankungen und Oberflächenwellen kann zur verstärkten Erosion von Sedimenten führen, besonders wenn man berücksichtigt, dass die mittleren Wasserstände im Bodensee sinken.

Die gleichzeitige und hochfrequente Messung des Oberflächenwellenfeldes und des Unterwasser-Lichtklimas ermöglichte die Charakterisierung der Amplituden und zeitlichen Skalen der Fluktuationen der Lichtintensität. Sie können durch den Linseneffekt von Oberflächenwellen (wave focusing), der Auslenkung der Wasseroberfläche und der Resuspension von Partikeln hervorgerufen werden. Wave focusing wird vor allem durch sehr niedrige und kurze Windwellen erzeugt. Es verursacht sehr große und hochfrequente Fluktuationen der Lichtintensität im Wasser, die weit über denen liegen, die durch die Auslenkung der Wasseroberfläche erzeugt werden. Andererseits können die durch Oberflächenwellen resuspendierten Partikel die Lichtintensität in der Flachwasserzone erheblich verringern und somit die Verfügbarkeit von Licht für das Wachstum von Phytoplankton und Biofilmen.

Messungen des Oberflächenwellenfeldes und der damit verbundenen Strömungen wurden auch in einem Wellenmesokosmos durchgeführt. Der Mesokosmos wird für verschiedenste biologische Untersuchungen genutzt, die sich mit den Auswirkungen von Oberflächenwellen auf Organismen in der Flachwasserzone beschäftigen. Der Vergleich einer typischen Oberflächenwelle im Mesokosmos mit den Wellen im Bodensee zeigte die Einschränkungen und Vorteile von Mesokosmos- gegenüber Freilandexperimenten. Die Messungen ergaben, dass sowohl die Höhen und Perioden der Oberflächenwellen als auch die Werte anderer wellenbezogener Parameter im Mesokosmos wesentlich unter denen im Freiland liegen. Deswegen werden wahrscheinlich die Auswirkungen von Oberflächenwellen auf Organismen, die in Mesokosmosexperimenten bestimmt werden, gegenüber denen im Freiland unterschätzt.

Diese Dissertation ist die erste, zeitlich hochaufgelöste und detaillierte Langzeituntersuchung zu den Charakteristika von Oberflächenwellen in einem limnischen Ökosystem. Im Bodensee bestimmen sowohl Wind- als auch Schiffswellen das Wellenfeld, wobei Schiffswellen das Wellenfeld im Sommer sogar dominieren können. Das zeitliche Auftreten und die spezifischen Eigenschaften von Wind- und Schiffswellen erzeugen unterschiedliche zeitliche Muster und haben verschiedene Auswirkungen auf die Resuspension von Partikeln und das Unterwasser-Lichtklima, die wiederum biotische Prozesse im Ökosystem des Litorals beeinflussen. Die Ergebnisse dieser Arbeit haben gezeigt, wie eng die Kopplung zwischen physikalischen Prozessen und biologischen Bedingungen ist. Das verdeutlicht die Notwendigkeit von ganzheitlichen Ansätzen in der Forschung.

General introduction

Surface gravity waves are an ubiquitous feature of lakes and oceans. These waves are initiated by an arbitrary, external disturbance of the water surface (e.g., by wind), where gravity is the restoring force. In natural environments surface gravity waves appear as a unsteady pattern of crests and troughs on the water surface because of the irregularity of wave shape and the variability in the direction and speed of propagation (Fig. I). This is particularly true when the waves are generated by wind. The friction of wind at the air-water interface sets the water surface in motion and generates traveling surface waves. Faster waves overtake and pass through slower ones from various directions. Thus, the observed shape of the water surface is the result of permanent superposition, where waves sometimes reinforce or cancel each other by this interaction (Fig. I).

Fig. I Typically occurring surface wave field generated by wind (Lake Constance).

The first mathematical approaches to describe the phenomenon of surface gravity waves theoretically were made by Airy (1845) and Stokes (1847). Whose theories are referred to as small-amplitude or linear wave theory that generally predicts wave behavior reasonably well as long as the ratio between wave amplitude and wave length as well as water depth are much smaller than one. This implies that the instantaneous depth does not differ significantly from the undisturbed depth. The motion beneath the waves is assumed to be irrotational, ignoring viscous effects of the fluid, the Coriolis force, and density stratification. Linear wave theory is of fundamental importance since it is not only easy to apply, but also reliable over a large segment of the whole wave regime.

The theories by Airy and Stokes were further refined in order to develop adequate and practical solutions for engineering problems, e.g., wave field prediction or coast and harbor protection. Many publications are available that fulfill this purpose by presenting the appropriate theory in accordance with its applications and limitations (e.g., Wiegel 1964; Kinsman 1965; Ippen 1966; CERC 2002). Especially during the last decades, oceanographers have focused on this topic with emphasis on various aspects (e.g., Pond and Pickard 1983; Kundu and Cohen 2002; Duxbury et al. 2003; Garrison 2005). Since linear wave theory provides a reliable description of surface waves in lakes and oceans under most circumstances it is commonly applied and also used throughout this study.

The description of a surface wave involves the waveform at the water surface and the fluid motion beneath the wave. Since the surface profile can be described by a combination of sine and cosine functions, these waves are called sinusoidal or simple harmonic waves. A wave is periodic when its surface profile or motion recurs in equal intervals of time, and is progressive (traveling) when it moves relative to a fixed point whereby the direction in which it moves is called the direction of wave propagation. Further, surface waves have the property to be dispersive, i.e., waves of different wave length or with different frequencies propagate at different velocities. Surface waves are considered oscillatory or nearly oscillatory when the motion of a particle in the water is described by orbits that are closed or nearly closed for each wave period. Taking this into account the wave propagates only energy and not mass.

The most fundamental properties to describe a sinusoidal, oscillatory wave are its length (λ, the horizontal distance between corresponding points on two successive waves), height (H, the vertical distance between its crest and the preceding trough), period (T, the time needed by a wave to travel a distance of one wave length), phase velocity (c, the rate at which the phase of the wave propagates), direction of propagation, and energy (E, total wave energy in the water column per unit horizontal area) (Fig. II). Other more advanced wave parameters are defined by IAHR (1989).

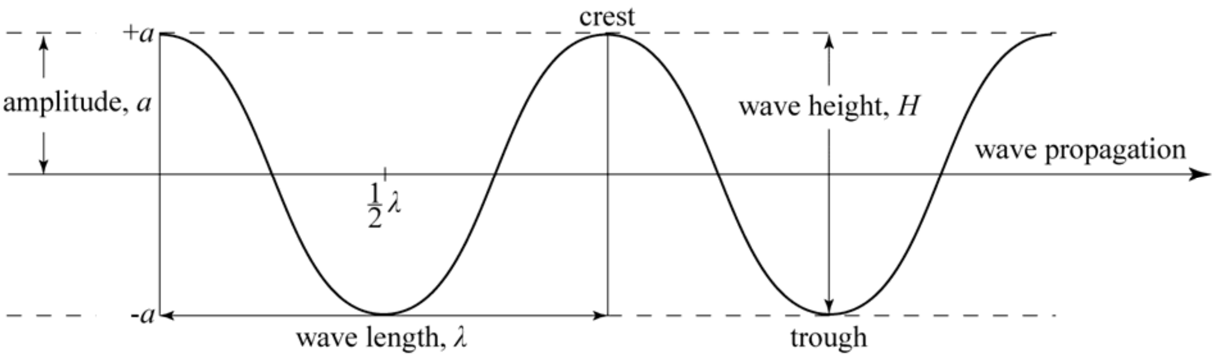

Fig. II Wave nomenclature. Idealized, sinusoidal, progressive wave oscillating around the mean water level.

These wave properties are strongly influenced by the source of forcing, whereby each force generates specific wave properties. The most common way to distinguish waves is by their period or the reciprocal of the wave period, the wave frequency (Fig. III).

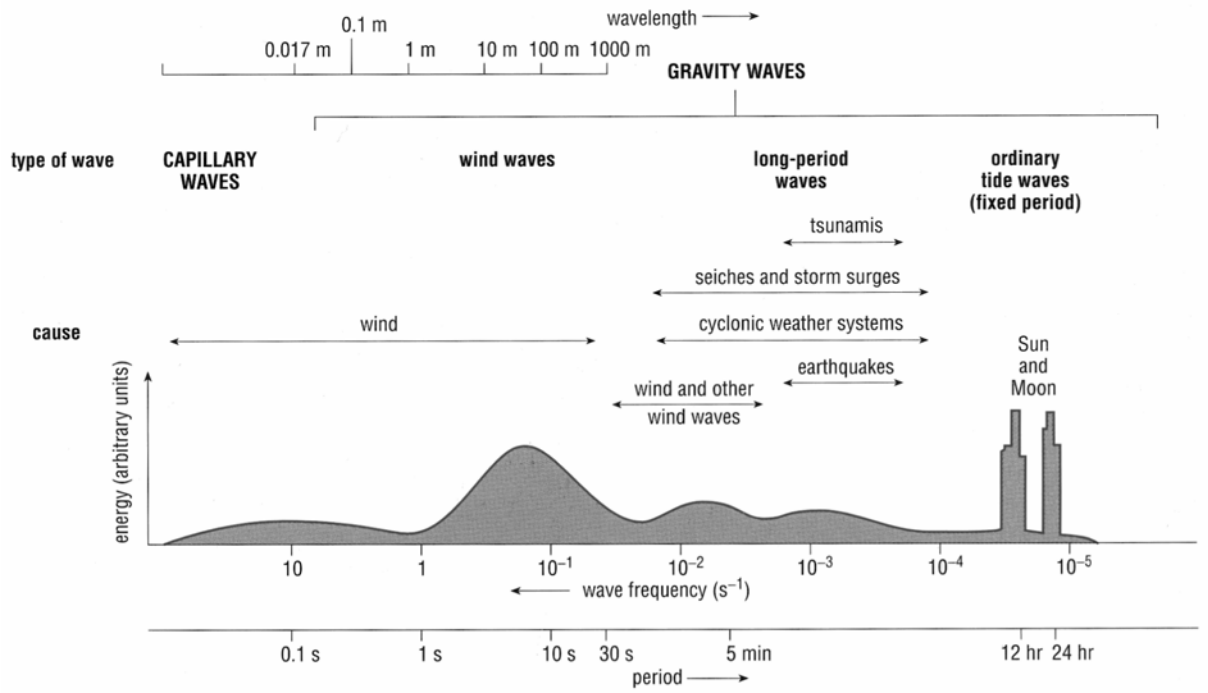

Fig. III Types of surface waves by showing the relationship between wave length, wave period (frequency), the nature of forces that cause them, and the wave energy in the ocean (Brown et al. 2005), after Kinsman (1965).

The illustration in Figure III provides a classification of waves by wave period and frequency ranging from milliseconds (capillary waves) to one day (tide waves). Wind waves have periods of about 1-30 s and form, apart from tide waves, the most energetic part of the wave spectrum.

When waves propagate from the open, deep water into the shallow water they undergo a transformation process due to the interaction with the bottom of the water body. According to the ratio of water depth (*h*) to wave length (λ), deep-water, transitional, and shallow-water waves are distinguished (Fig. IV).

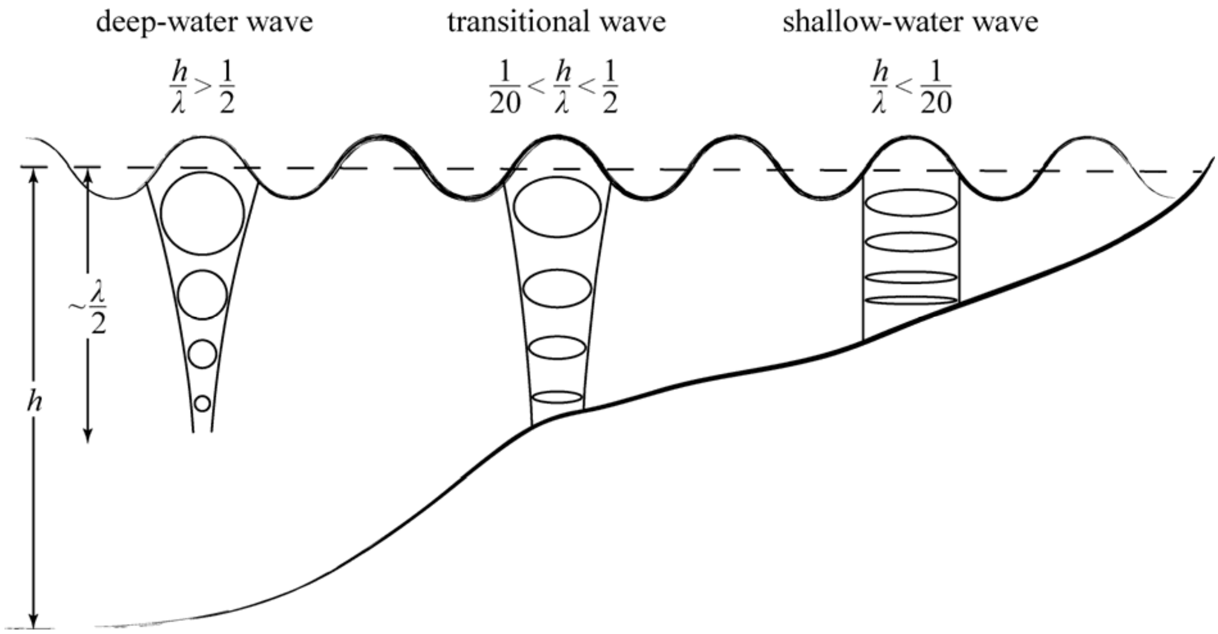

Fig. IV Classification of gravity waves according to the ratio between water depth (*h*) and wave length (λ) (adapted from Ippen (1966)). The wave transformation process from the deep into the shallow water alters the associated motion that is expressed in a change of the resulting particle orbits (circles and ellipses). In deep water the particles oscillate on circles (deep-water wave), but with decreasing water depth the wave reaches the point when it starts to feel the bottom (transitional wave). Thenceforward, the orbits flatten in the vertical and particle motion describes an ellipse. This process is further reinforcing, until the minor (vertical) axis of the ellipse vanishes near the bottom and the major (horizontal) axis becomes dominant (shallow-water wave). The cones represent the magnitude and extensions of the particle orbits beneath the wave.

During this transformation process the particle motion beneath the wave, which is in deep water characterized by circular orbits, shifts to elliptical orbits, which flatten further as they reach the bottom. The shallow-water wave is no longer energy dispersive, because their phase velocity is proportional to the square root of the water depth and independent of the wave length. Waves that propagate from deep to shallow waters experience a decrease in phase velocity and wave length with decreasing water depth. Since this study is conducted in the littoral zone, the general wave equations had to be considered that cover the whole range and are not simplified to the specific case (Komen et al. 1996; Kundu and Cohen 2002; Brown et al. 2005).

Many studies deal with the description and investigation of wind-generated waves, but most of these studies are based on investigations in oceans and ocean-shelf regions (e.g., Madsen 1976; Le Blond and Mysak 1978; Dean and Dalrymple 1998). In oceans, waves are generated by strong and frequent winds over long fetch lengths and propagate to the coast with large amplitudes. Typical wave heights vary between 0.5 m during calm sea and several meters during storm events, whereas characteristic wave periods vary between 5 and 10 s (e.g., Komen et al. 1996; CERC 2002; Donelan et al. 2005). On lakes, in contrast, the wind field is mostly characterized by infrequent winds, low wind speeds, and changing wind directions. In addition, the wind forcing at the water surface often varies on small spatial scales and the effective fetch length is restricted to a few kilometers. Hence, the wave field in most lakes is characterized by waves with small amplitudes and high frequencies (short periods) and thus differs considerably from the wave field in the ocean. Wind-generated waves in lacustrine environments have been investigated mainly in the Great Lakes (e.g., Lawrence and Davidson-Arnott 1997; Meadows et al. 1997; Hawley et al. 2004), where the dimensions are rather comparable with ocean-shelf regions. Only a few studies, however, investigated wind waves in smaller lakes (Jin and Wang 1998; Allan and Kirk 2000).

Apart from wind, surface waves can also be generated by ships. The forward motion of a ship disturbs the water around it, resulting in a set of waves with a characteristic pattern. This pattern was first studied and described by Froude (1877) and later by Lord Kelvin (William Thomson 1887). The wash pattern generated by ships in deep water (Fig. V) covers a range of waves in terms of length, phase velocity, and direction of travel. The longest and fastest waves propagate at the same velocity and in the same direction as the ship and are called transverse waves. The shorter, slower waves propagate at a nearly fixed angle of 19.47° to the track of the ship and are called the divergent waves. The transverse and divergent wave components interact at the cusp locus line and result in the so-called Kelvin wedge (Ursell 1960; Sorensen 1973).

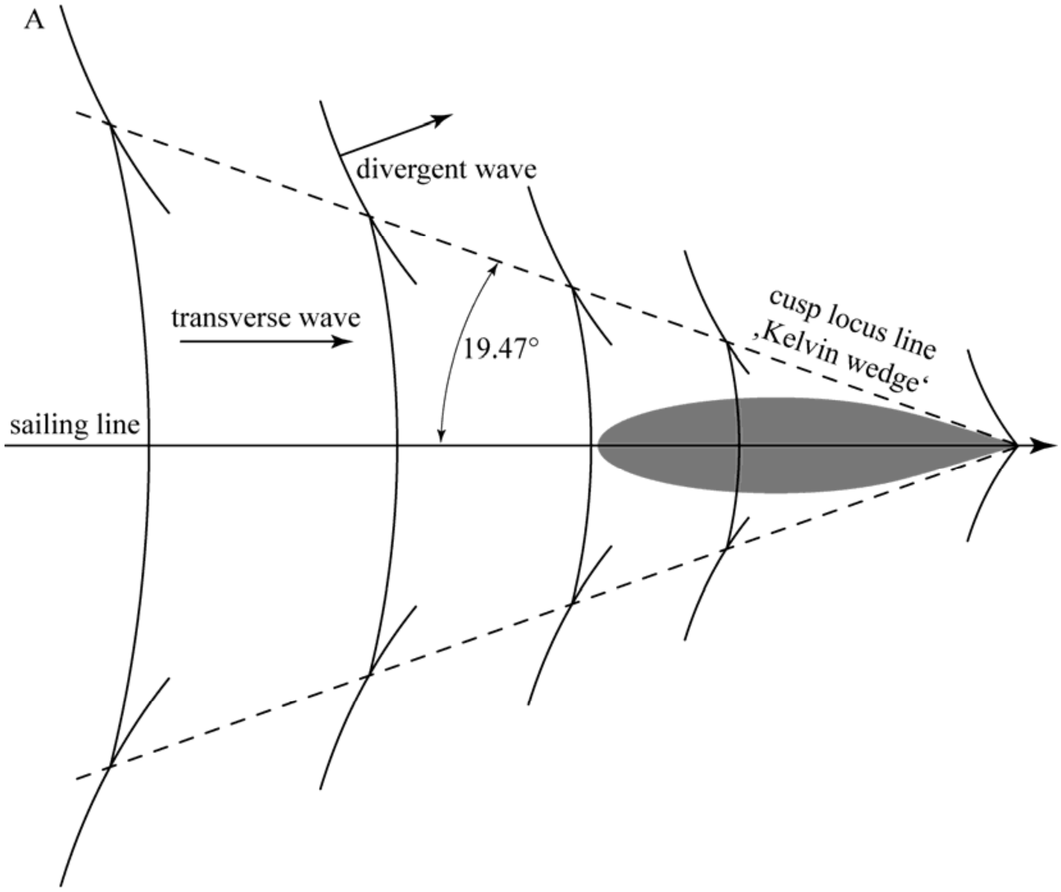

Fig. V Ship waves. (A) Wash pattern generated by ships in deep water (adapted from Sorensen (1973)). (B) Ship waves (divergent and transverse) propagating from their point of generation (sailing line of the car and passenger ferry on Lake Constance, open white circle) over the whole lake into the littoral zone (in the foreground).

During the last decades, many studies were conducted with the focus on a detailed description and simulation of ship waves (mainly carriers) for engineering purposes under consideration of the specific properties of the ships (e.g., length, width, displacement mass, velocity, and shape (e.g., Weggel and Sorensen 1986; Chen and Huang 2004). Several other studies investigated the properties and the importance of regular ship traffic in rivers and channels or ocean-shelf regions (e.g., Sorensen 1973; Stumbo 1999; Bauer et al. 2002), and the relevance of high-speed catamaran ferries in coastal environments (e.g., Parnell and Kofoed-Hansen 2001; Soomere 2005), but, as for wind-generated waves, only a few studies focused on ship waves in lakes (Bhowmik 1975; Maynord 2005).

However, it is particular important to understand and characterize the surface wave field in lacustrine ecosystems too, since surface waves (wind and ship waves) provide an important energy source and thus a hydrodynamic disturbance for the littoral zone, where most of the wave energy is eventually dissipated. Waves are associated with motion in terms of currents of the water column and directly interact with the sediment surface and the benthic biota. Thus, surface waves affect a huge range of abiotic and biotic processes in the littoral ecosystem, such as, resuspension, erosion, and transport of particles (Luettich et al. 1990; Hawley and Lesht 1992; Lee et al. 2007); the release of nutrients and methane (Søndergaard et al. 1992; Güde et al. 2000; Bussmann 2005); the oxygenation of the sediment-surface layer (Precht and Huettel 2003; Precht et al. 2004); the reallocation and stress on benthic invertebrates and their diversity (Rasmussen and Rowan 1997; James et al. 1998; Scheifhacken et al. 2007); the abrasion of periphyton from stones (Cattaneo 1990; Francoeur and Biggs 2006) and aquatic macrophytes (Keddy 1982; Wilson and Keddy 1985; Kawamata 2001); the damage of reed belts (Ostendorp et al. 2004; Schmieder et al. 2004); the light climate via the fluctuations in water level and light attenuation by suspended particles (Stramski et al. 1992; Pierson et al. 2003; Erm and Soomere 2006); and the growth and behavior of juvenile fishes (Stoll et al. 2008).

The central aspects of this thesis are therefore the characterization of the surface wave field in a lacustrine environment and to gain knowledge of its importance for the littoral ecosystem.

The study site is Lake Constance, a large lake, which is located in the southwest of Germany. It is the second-largest (by surface area) prealpine lake in Europe. Lake Constance is not regulated and experiences seasonal water level fluctuations of about 2-3 m (Luft and van den Eertwegh 1991; Jöhnk et al. 2004). The littoral zone covers about 10% of the total surface area (Braun and Schärpf 1990). The shores are mainly exposed to westerly and northeasterly winds, the most and second most frequent wind direction at Lake Constance (Bäuerle et al. 1998). In addition to wind-generated waves, the shores around Lake Constance are exposed to ship-generated waves. These waves stem from ferries with regular sailings throughout the year, passenger ships connecting cities and tourist sites all around Lake Constance, a newly introduced catamaran ferry, and leisure boats. The specific exposure to wind and ship waves of Lake Constance is comparable to many other prealpine and alpine lakes in Europe.

During the last decades intensive biological, chemical, and physical experiments were conducted at Lake Constance (e.g., Fischer and Eckmann 1997; Bäuerle et al. 1998; Scheifhacken et al. 2007). These studies were intensified since the Collaborative Research Center 'Littoral Zone of Lake Constance' was established in 1998. During these experiments the different shores were differentiated and characterized indirectly according to their exposure to wind and according to the resulting properties of the shore (e.g., sediment structure and distribution, slope, and occurrence of macrophytes), but not according to the characteristics of the actual wave field. Only one previous study is known, where measurements of the wave field in the bay of Friedrichshafen (Lake Constance) were conducted (Rosenthal 1993). However, technological limitations restricted correct measurements of surface waves to wave heights above 0.3 m, which represents wave heights during strong winds only. Additionally, predictions of the wave field, based on wind fetch and speed, were reasonable but limited by the strong temporal dynamics of the wind and the resulting unsteady wave field (Piroth and Plate 1993). Ship waves were not considered in these studies.

Recent improvements of instrumentation (e.g., pressure sensors) and data acquisition systems allow measuring the water surface elevation very precise, at high frequencies, and over long time periods. This enabled me to measure surface waves during different seasons, wind regimes, and water levels in the littoral zone and to provide a detailed characterization of the wave field including small-amplitude wind and ship waves. In combination with additional measurements I could also determine their implications on physical processes and biological conditions.

In this thesis, I first review different temporal scales of water level fluctuations from a physical perspective (**Chapter 1**). Hydrologically induced water level fluctuations range from days to centuries and are referred to as long-term water level fluctuations. Wind forcing and ship traffic affect the surface wave field and cause water level fluctuations on time scales from seconds to hours. Water level fluctuations are presented in an order of decreasing time scales, beginning with centuries and ending with seconds. This temporal range of water level fluctuations is exemplified using data from Lake Issyk-Kul (Kyrgyzstan) for century scales, the Caspian Sea for decadal scales, and Lake Constance for shorter time scales ranging from years to seconds. Long-term as well as short-term water level fluctuations have specific impacts on the lake littoral ecosystem that are discussed with special emphasis on the importance of the combined effects of both.

In **Chapter 2**, I present an one-year data set on surface wave parameters, which was obtained from the analysis of measurements with a pressure sensor. The data allow for resolving small-amplitude and high-frequency waves. Since the surface wave field in Lake Constance is characterized by wind-generated and ship-generated waves, the purpose of the current study was to analyze and compare their relative importance in terms of frequency of occurrence, wave energy flux to shore, and near-bottom current velocities. This analysis enabled me to identify temporal patterns in the frequency of occurrence of wind and ship waves that result in different patterns of disturbance of the littoral ecosystem.

After the detailed characterization of the wave field and its temporal patterns in Lake Constance, the next step was to investigate potential ecological implications. I concentrated hereby on two effects: the implication on the resuspension of particles and implications on the underwater light climate. To investigate the resuspension of particles (**Chapter 3**), which is highly related to the properties of the surface wave field, synchronized high-resolution measurements of the wave parameters, the near-bottom current velocities, and the suspended sediment concentrations and properties were conducted using a pressure sensor, an acoustic Doppler velocity meter, and sediment traps, respectively. These measurements were analyzed over a time period of one year. Whereas the relative importance of wind and ship waves in terms of the frequency of occurrence was presented in the previous chapter, this study is focused on the different temporal patterns of resuspension, the intensity of disturbance, and the dispersion and reallocation of particles caused by wind and ship waves.

In **Chapter 4**, I experimentally investigated the variability of the underwater light climate in the littoral zone using synchronized, high-frequency measurements of the photosynthetically active radiation and pressure. Fluctuations of the underwater irradiance are not only caused by the variation in the incoming light intensity but also by variations in the elevation and curvature of the water surface resulting from surface waves generated by wind and ships. Synchronized measurements were conducted with the intension of providing amplitudes and temporal scales of the fluctuations in light intensity resulting from wave focusing, the change in surface elevation, and resuspension.

Apart from the field experiments in Lake Constance, I conducted measurements of the surface wave field and the wave-generated currents in the wave mesocosm of the Limnological Institute at the University of Konstanz using a pressure sensor, an acoustic Doppler velocity meter, and a video camera imaging system (**Chapter 5**). These measurements were motivated and required for various biological experiments that focused on the implications of surface waves on biota in the shallow littoral during the last years and also very recently. Additionally, I compared the waves typically generated in the wave mesocosm with wind and ship waves occurring in the field (Lake Constance).

At the end of this thesis, I summarize and discuss the main results drawn from the preceding chapters. Thereafter, I highlight selected questions and perspectives for future research.

Chapter 1

Temporal scales of water level fluctuations in lakes and their ecological implications

HILMAR HOFMANN, ANDREAS LORKE AND FRANK PEETERS

Hydrobiologia 163 (1): 85-96

Abstract

Water level fluctuations (WLF) of lakes have temporal scales ranging from seconds to hundreds of years. Fluctuations in the lake level generated by an unbalanced water budget resulting from meteorological and hydrological processes, such as precipitation, evaporation and inflow and outflow conditions usually have long temporal scales (days to years) and are here classified as long-term WLF. In contrast, WLF generated by hydrodynamic processes, e.g., basin-scale oscillations and traveling surface waves, have periods in the order of seconds to hours and are classified as short-term WLF. The impact of WLF on abiotic and biotic conditions depends on the temporal scale under consideration and is exemplified using data from Lake Issyk-Kul, the Caspian Sea, and Lake Constance. Long-term WLF induce a slow shore line displacement of meters to kilometers, but immediate physical stress due to currents associated with long-term WLF is negligible. Large-scale shore line displacements change the habitat availability for organisms adapted to terrestrial and aquatic conditions over long time scales. Short-term WLF, in contrast, do not significantly displace the boundary between the aquatic and the terrestrial habitat, but impose short-term physical stress on organisms living in the littoral zone and on organic and inorganic particles deposited in the top sediment layers. The interaction of WLF acting on different time scales amplifies their overall impact on the ecosystem, because long-term WLF change the habitat exposed to the physical stress resulting from short-term WLF. Specifically, shore morphology and sediment grain size distribution are the result of a continuous interplay between short- and long-term WLF, the former providing the energy for erosion the latter determining the section of the shore exposed to the erosive power.

Introduction

Water level fluctuations (WLF) and their ecological and socio-economic consequences have been investigated in large lakes, e.g., Aral Sea (Usmanova 2003; Zavialov et al. 2003), Lake Chad (Guganesharajah and Shaw 1984; Coe and Foley 2001), Great Salt Lake (Stephens 1990) or Salton Sea (Bourne et al. 2005) and also in small lakes and reservoirs (e.g., Hunt and Jones 1972; Coops et al. 2003; McGowan et al. 2005; Naselli-Flores and Barone 2005). The reasons and causes of WLF can be various: Hydrologically induced WLF are connected to climatic changes, changes in the constellation of large atmospheric pressure systems (North Atlantic and Southern Oscillation), or, most frequently, to seasonal variations in meteorological conditions. They can also be the result of anthropogenic use of water resources, as in the case of the Aral Sea (Usmanova 2003). Hydrologically induced WLF are the result of a change in the water budget and therefore depend on the amounts of precipitation and evaporation, catchment size and characteristics, and on the discharge conditions (inflow vs. outflow) of the basin. Prominent examples are Lake Constance (Luft and van den Eertwegh 1991; Jöhnk et al. 2004) or Lake Issyk-Kul (Brennwald et al. 2004). The time scales of the hydrologically induced WLF range from days to centuries (and even up to geological time scales) and will be referred to as long-term WLF throughout this paper. Wind forcing and ship traffic affect the surface-wave field and cause WLF on time scales on the order of seconds to hours. These hydrodynamically driven WLF are classified throughout this paper as short-term WLF.

Here, we present examples for WLF at different temporal scales from a physical oriented perspective and discuss their implication on the lake ecosystem with specific emphasis on the littoral zone. WLF are presented in an order of decreasing time scales, beginning with a time scale of centuries and ending with a time scale of seconds. Examples are taken from different lakes: Lake Issyk-Kul (Kyrgyzstan) for century scales, the Caspian Sea for decadal scales, and Lake Constance for shorter time scales spanning years to seconds.

Long-term WLF and their ecological impacts are subject of a number of papers throughout this special issue. Here, we will put special emphasis on the discussion of short-term WLF. Often, the latter are not considered in the context of WLF, although they can have a major impact on the abiotic and biotic processes in the littoral zone. Several studies have investigated the impact of short-term WLF on coastal and shelf regions (Clark 1997; Eriksson et al. 2004; Soomere 2005; Erm and Soomere 2006). Only few investigations, however, have focused on lake-littoral zones (Luettich et al. 1990; Eggleton et al. 2004; Scheifhacken 2006). Information on short-term WLF are required for the understanding of shore formation, which is the result of the interaction between short- and long-term WLF. Furthermore, short-term WLF impose physical stress on aquatic and riparian plants and organisms. This stress varies with the properties of the substrate (e.g., sand or stones), which, in turn, is altered by long-term WLF moving the boundary of the aquatic habitat up or down the shore. Hence, short-term WLF are important for an understanding of the ecological consequences of long-term WLF for aquatic organisms living in the littoral zone.

In the following sections, we first provide information on the materials and the methods used in this study. Then we present data on long-term and on short-term WLF at the example of Lake Constance. The subsequent discussion is focused on the impact of long- and short-term WLF on the littoral ecosystem, and specifically emphasizes the importance of the combined effect of both. In the final section we summarize the main conclusions of the paper.

Materials and methods

Daily readings of water levels at gauge Konstanz for the time period 1817-2005 were provided by the State Institute for Environment, Measurements and Nature Conservation Baden-Württemberg (LUBW). The water levels are measured relative to the reference level of the gauge (391.89 m a.s.l., level Amsterdam). The water level time series was corrected for reading errors between 1817 and 1825 (Jöhnk et al. 2004). Note that between 1817 and 1876 the resolution of water level readings was only 3 cm, thereafter 1 cm.

Short-term WLF were measured using a pressure sensor with a resolution of 0.1 mbar, corresponding to about 1 mm water level. Measurements were carried out in the western part of Upper Lake Constance at a site called Littoral Garden (LG; 47°41’29’’N, 09°12’11’’E). The pressure sensor was deployed 1 m above the sediment at 2.0-2.5 m water depth and measured at a sampling frequency of 16 Hz throughout the entire year 2005. Pressure is a direct measure of water level only under hydrostatic conditions. However, the assumption of hydrostatic conditions is valid only if the wave length of the WLF exceeds a critical wave length of about 20 times the local water depth. WLF generated by surface gravity waves usually have a wave length that is significantly shorter than this critical wave length. Hence, the calculation of water level and WLF from pressure measurements requires a correction for pressure attenuation that depends on the water depth, the depth of the sensor, and the wave length (Kundu and Cohen 2002; Hofmann et al. 2008a). In the procedure wave length was calculated from wave frequency using the approximation to the dispersion relation of surface gravity waves by Fenton and McKee (1990).

Maximum near-bottom current velocities generated by surface waves, u_{max} (m s^{-1}), were estimated using (Brown et al. 2005):

$$u_{\max} = \frac{\pi \cdot H}{T \cdot \sinh \frac{2 \cdot \pi \cdot h}{\lambda}} \qquad (\mathrm{m\ s^{-1}}) \qquad (1.1)$$

where H denotes the wave height (m), h the water depth (m), λ the wave length (m), and T the wave period (s). The remobilization of particles is related to u_{max} and can be determined from empirical equations. For non-cohesive sediments with a mean grain size d_{50} between 0.063 and 2 mm (sand fraction) the formulation by Hallermeier (1980) was used to estimate the remobilization of particles at 1 m water depth in the littoral zone of Lake Constance.

An Acoustic Doppler Velocity Meter (ADV) was deployed close to the pressure sensor at the site LG throughout the entire year 2005. The instrument measured the 3-dimensional current velocity 0.05 m above the sediment (at 1-2 m water depth) with a sampling frequency of 8 Hz. Current velocities associated with distinct frequencies (e.g., 54.6 min for the first-mode surface seiche in Lake Constance; see Table 1.1) were estimated using spectral analysis (Emery and Thomson 2001).

Results

Long-term WLF

In the following we analyze long-term WLF from Lake Constance, the second largest prealpine lake in Europe with a surface area of 536 km^2 and a maximum water depth of 254 m (Braun and Schärpf 1990). Lake Constance and its main tributary, the river Rhine, are almost unregulated and the lake level shows a strong seasonal cycle. The level declines during winter and typically reaches the annual minimum at the end of February, when precipitation in the catchment area is, to a large extent, stored as snow. The lake level typically reaches an annual maximum in June/July due to increased snow melt in spring (Luft and van den Eertwegh 1991; Jöhnk et al. 2004). Long and intense precipitation in the catchment area in combination with snow melt can result in extreme floods with rapidly increasing water levels. Some examples of major flood events are marked in Figure 1.1A. The relative height in the figure indicates the importance of the events (Luft and van den Eertwegh 1991; Jöhnk et al. 2004). The greatest flood within the time period considered here was observed in 1817 with 623 cm above reference level. Other floods between 525 and 575 cm occur more frequently with an average recurrence time period of about 12 yr. Maximum water levels between 400 and 500 cm seem to be a regular range within the gauge Konstanz time series (Fig. 1.1A).

Linear regression reveals that the annual mean water level shows a significant long-term trend and declined by about 21 cm between 1817 and 2005 (slope: -0.11 ± 0.03 cm yr^{-1}, $p < 0.01$; Fig. 1.1B). From 1817-1940 the annual mean water level shows no significant trend (slope: -0.008 ± 0.05 cm yr^{-1}, $p = 0.87$), but from 1941-1980 the level started to decrease (slope: -0.12 ± 0.14 cm yr^{-1}, $p = 0.40$). This decrease is even more pronounced during the last two and a half decades (slope: -0.41 ± 0.57 cm yr^{-1}, $p = 0.48$) and is mainly caused by decreasing maximum water levels in summer. The reasons for the obvious break point around 1940 and the ongoing decline in water level has been widely discussed and was explained by changes in hydraulic discharge conditions and climatic changes in the catchment area (Luft and Vieser 1990; Jöhnk et al. 2004).

Inter-annual WLF, determined from the difference between the annual mean water levels of consecutive years (Fig. 1.1B), are about 20 cm ± 17 cm (SD) on average. The maximum of the inter-annual WLF was 75 cm between 1921 and 1922.

Seasonal WLF can be quantified by the difference of the minimum and maximum water level with respect to the mean water level of the particular year (Fig. 1.1C). Extreme seasonal WLF reach up to more than 300 cm and occur in years with unusually high maximum water levels. The linear regressions of the annual maximum (slope: -0.17 ± 0.06 cm yr^{-1}, $p < 0.01$, ±45 cm yr^{-1} SD) and minimum (slope: -0.02 ± 0.02 cm yr^{-1}, $p = 0.33$, ±14 cm yr^{-1} SD) water level indicate a significant decline in the seasonal WLF from about 215 cm at the beginning of the 19th century to about 185 cm at the beginning of the 21st century (Fig. 1.1C). The long-term decline is caused by the decrease in the annual maximum water level, where in contrast the annual minimum water level remained constant. This also explains the observed trend of the annual deviation from the mean of the seasonal WLF (slope: -0.15 ± 0.06 cm yr^{-1}, $p < 0.01$, ±42 cm yr^{-1} SD; Fig. 1.1C), which is mainly stated by the deviation of the annual maximum water level and thus shows the same significant decline. The decrease in the seasonal WLF especially during the last decades can be partly explained by the construction of hydropower reservoirs in the catchment (Luft and van den Eertwegh 1991; Jöhnk et al. 2004).

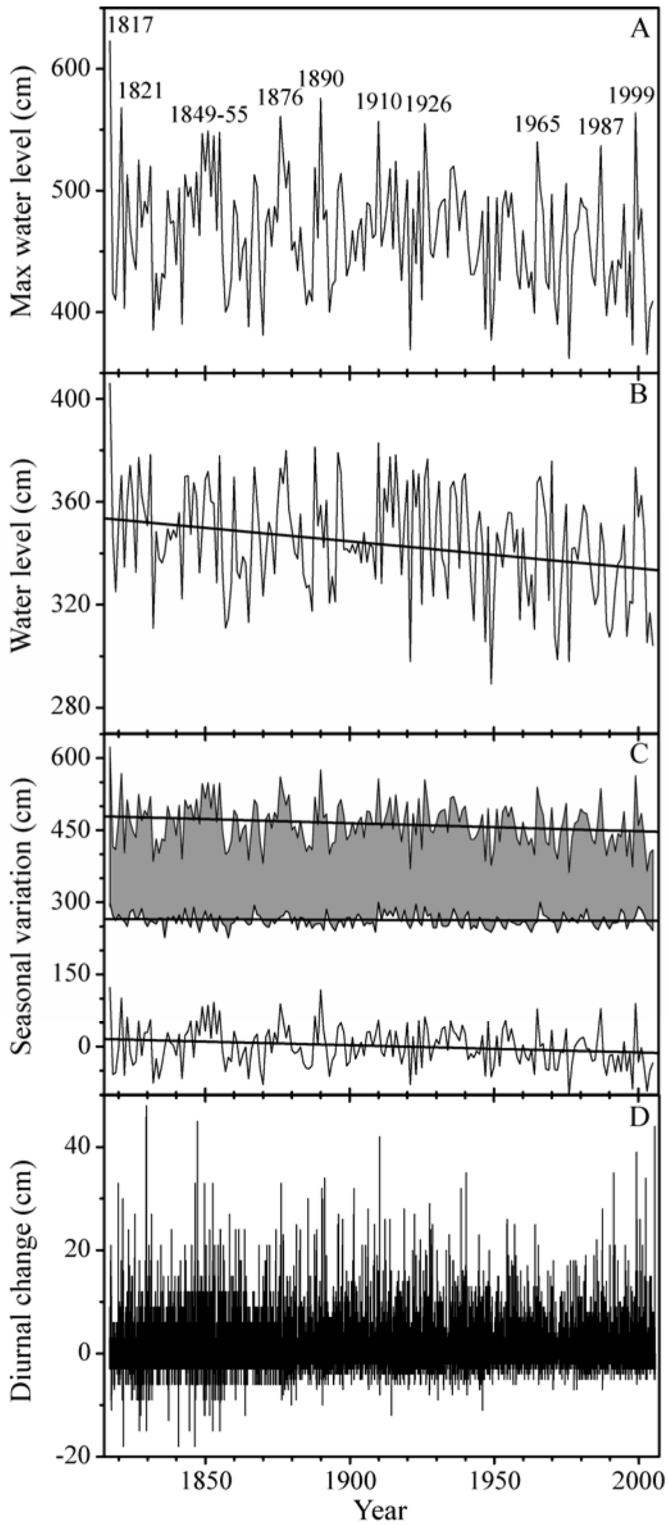

Fig. 1.1 Lake-level time series at gauge Konstanz (Lake Constance) based on daily measurements from 1817-2005. (A) Annual course of the maximum water levels. Major floods are marked by the individual year or period, whereas the height corresponds to the importance of the flood. (B) Mean annual water levels with linear regression line. (C) Seasonal variations within a single year (filled gray surface) determined as the difference between the maximum and minimum water level of the respective year. Linear regression lines emphasize the trend of the maximum and minimum water levels. The solid line fluctuating around zero shows the annual deviation from the mean of the seasonal WLF (over the whole time series) with its linear regression line. (D) Diurnal change of the water level shown as the difference between the daily mean values.

Over a single day, the water level can change by up to 40 cm (Fig. 1.1D). Such rapid increases in water level are always caused by extreme discharge events of the river Rhine resulting from intense precipitation in the catchment. Large water level increases continuing over several consecutive days can lead to major flood events (Luft and van den Eertwegh 1991). However, the typical daily decrease or increase in water level is much smaller than the extreme case mentioned above and typically ranges only from -5 to 10 cm (Figs. 1.1D, 1.2A).

Short-term WLF

Short-term WLF, at scales from seconds to hours, are mainly caused by hydrodynamic processes. In the following section we analyze high-frequency and high-resolution data of surface water level (estimated from pressure measurements) and current velocity from the littoral zone of Lake Constance. Single-day time series were chosen to explain the temporal variability of hydrodynamic processes on 17 and 26 January 2005 (Fig. 1.2). Both days differ considerably due to different surface forcing generated by strong on-shore wind on 26 January 2005 and no wind on 17 January 2005.

A very prominent feature of enclosed water bodies are basin-wide oscillations of the surface level, often referred to as surface seiching (Mortimer 1974; Lerman et al. 1995). The periods of such basin wide oscillations, called ‘modes’, are determined by the morphology of the basin. The first-mode surface seiche in Lake Constance has a period of 54.6 min and can be seen in the running average applied to the surface level time series shown in Figure 1.2, although the period may differ slightly depending on the actual water level of the lake (Hollan et al. 1980). The vertical displacements of the water surface associated with the first-mode surface seiche are only a few centimeters and were measured to be about 2 cm at the measuring site LG (Fig. 1.2). These lake level oscillations are excited by wind forcing at the water surface or due to atmospheric pressure gradients. Power spectra of high-frequency pressure time series show several spectral peaks with periods between minutes and one hour. Numerical calculations suggest that these peaks correspond to level fluctuations due to second-, third- or even higher-order modes of basin-scale surface oscillations of Lake Constance (Bäuerle, pers. comm.).

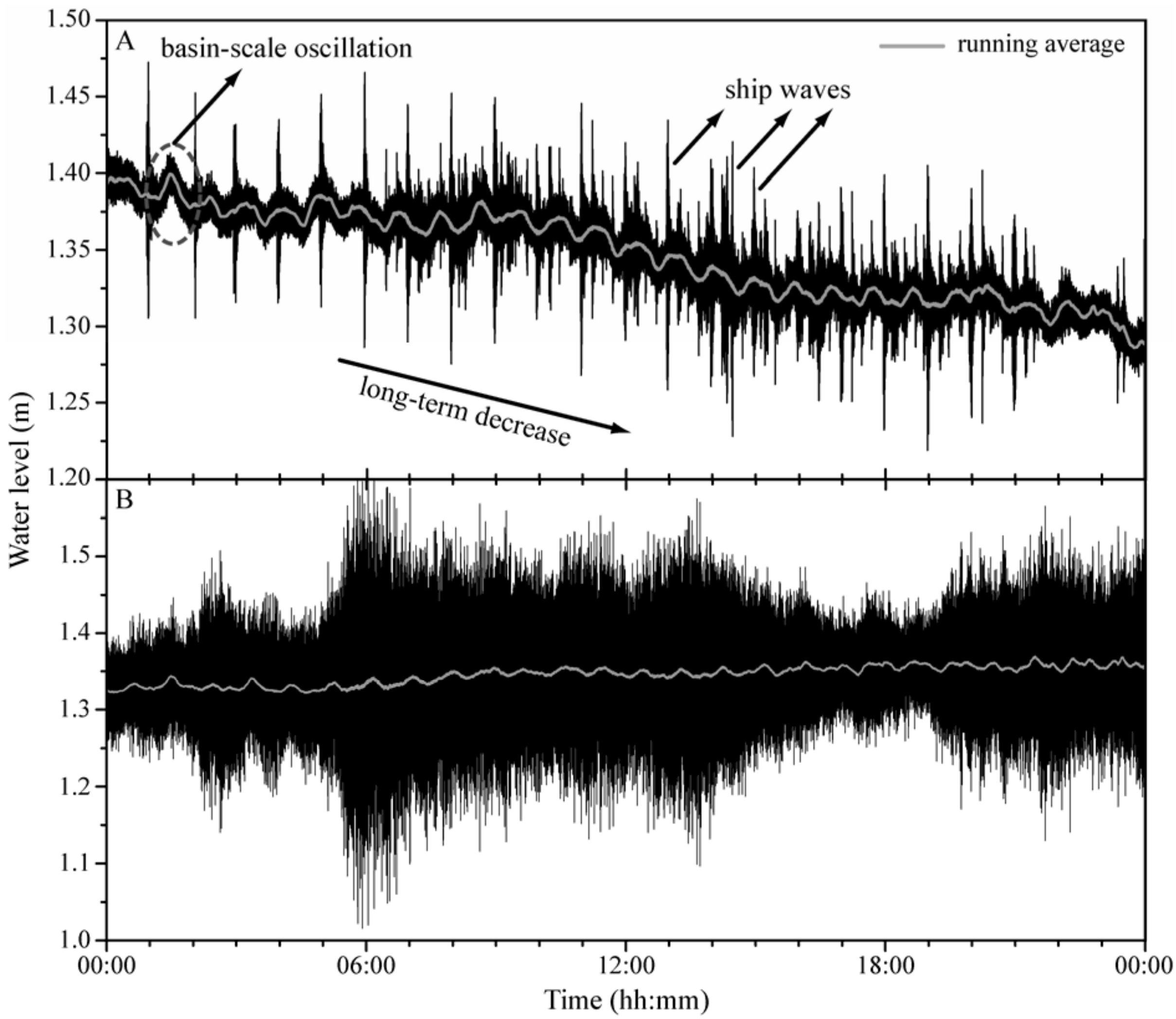

Fig. 1.2 High-frequency (16 Hz) and high-resolution (1 mm) measurements of the water level over a single day. (A) On 17 January 2005 under a no wind situation. (B) On 26 January 2005 under a strong (wind speed was about 9-10 m s^{-1}) on-shore wind. The different arrows point out examples of different temporal scales of WLF, e.g., long-term decrease in water level (diurnal change), basin-scale oscillation, and short-term WLF generated by ship waves. The 1 min running average highlights the basin-scale oscillation with a magnitude of about 2 cm (emphasized by the dashed gray ellipse with arrow).

From an ecological perspective, traveling surface gravity waves are probably the most important short-term WLF. Such waves are generated by wind or by ships and are usually classified as wind waves and ship waves. Both types of waves were measured, characterized, and analyzed at Lake Constance (Fig. 1.2; Hofmann et al. 2008a). Ship waves cause very harmonic and regular surface oscillation and their periods are determined by their excitation, which is characteristic for each individual ship. The frequency of occurrence and the wave heights of ship waves are highly predictable in time for Lake Constance. They are controlled by the regular sailings of various ferry lines throughout the year with each individual wave group identified as a distinct signal (Fig. 1.2A; Hofmann et al. 2008a). Wind waves in contrast are irregular and are determined by the length of the effective wind fetch and the wind speed, which changes from site to site. Ship waves generated by ferries, passenger ships, or by the recently introduced fast catamaran ferries have wave periods of 2.9-6.3 s, characteristic wave heights of 0.04-0.5 m, and wave lengths of 13-50 m (assuming deep-water waves); whereas the wave periods, heights, and lengths of wind waves are 1.5-2.3 s, up to 0.8 m, and 2-8 m, respectively (Fig. 1.2; Hofmann et al. 2008a). If no wind is present, the wave field is dominated by ship waves (Fig. 1.2A), which are masked by the higher wind waves during periods of strong on-shore wind (Fig. 1.2B). Depending on the duration of wind forcing, wind waves can dominate the wave field for hours or even days (Fig. 1.2B).

Discussion

Impacts of long-term WLF

Since long-term WLF are associated with large shore line displacements, the major impact of long-term WLF on lake ecosystems is a change in habitat. Long-term WLF flood formerly dry shore areas or expose submerged sediment surfaces to the atmosphere. Thus, long-term WLF play a role in the selection of sessile species adapted to dry or wet conditions. In addition, long-term WLF result in a change of the properties of the sediment surface in the littoral zone, because the grain sizes in the shore region are not homogeneously distributed but change from large to small towards deeper regions of the lake. In the following we provide examples for the range and consequences of long-term WLF.

Based on noble gas concentrations in sediment pore water Brennwald et al. (2004) concluded that the water level of Lake Issyk-Kul, one of the largest and deepest lakes in the world (volume: 1,740 km^3, max. depth: 668 m) located in Kyrgyzstan, has been at least 250 m lower during the mid-Holocene than today. As Lake Issyk-Kul is a closed basin lake, its water level is very sensitive to changes in the meteorological conditions. The drop in water level by 250 m during the mid-Holocene implies a shore line displacement of 20-60 km and a reduction of water volume by more than 40%. During low water level the salinity was more than twice its present value of 6‰ as indicated by noble gas data from the pore water (Brennwald et al. 2004). WLF induced salinity changes between 6‰ and above 12‰ can be expected to have had severe effects on the species composition, because most freshwater animals cannot survive in waters with salinities of more than 10‰ (Wetzel 2001). This long-term WLF had clearly visible consequences for the basin morphology. During low water level, rivers caused large gully erosion especially in the eastern shallow region, which was dry at this time, resulting in channels of 100 m depth (Tsigelnaya 1995). Today, these ancient shallow regions are 20 m below water level and the flooded channels play an important role in the renewal and the oxygenation of the deep water in Lake Issyk-Kul (Peeters et al. 2003). Hence, today's high oxygen levels in the deep water can be considered as an indirect consequence of the long-term WLF.

Long-term WLF on decadal time scales have been recorded for the Caspian Sea, the largest inland water body (with respect to surface area and volume) on earth. Between 1880 and 1978 the level of the Caspian Sea decreased by 4 m and then rose again by 2.5 m within 20 yr. According to Rodionov (1994) the sea level fluctuations of the Caspian Sea are caused by variations in the inflow, which resulted from natural fluctuations of the North Atlantic Oscillation (NAO) and, to a minor extend, by anthropogenic influences, e.g., the use of Volga water for irrigation (Klige and Myagkov 1992). The vertical amplitudes of the WLF of the Caspian Sea are small compared to those mentioned above for Lake Issyk-Kul, but the associated change in surface area is much higher with about 50,000 km^2. The inflow of freshwater related to the water level increase during the 1980s and 1990s caused a significant reduction in vertical mixing, which resulted in nearly anoxic conditions in the deep water (Peeters et al. 2000). The consequence of a long-term increase in water level for internal mixing processes is particularly important in saline lakes, e.g., Mono Lake (Romero and Melack 1996) or Caspian Sea (Peeters et al. 2000), because a change in water level is usually associated with freshwater inflow that leads to an increase in water column stability, and thus, hinders convective mixing processes. In freshwater lakes and reservoirs long-term WLF have an impact on vertical mixing only if the level is altered substantially, e.g. if the level is reduced sufficiently that wind forcing or nocturnal convection reaches down to the lake bottom of a formerly dimictic or monomictic lake.

The examples above demonstrate that long-term WLF can influence the oxic state of saline lakes, which in turn affects sediment-water exchange and the chemical composition of the deep-water. Long-term WLF have also implications on socio-economic circumstances. The Aral Sea is a very drastic example (Usmanova 2003). However, in the Caspian Sea the comparatively small decline until 1978 caused rapidly decreasing ground water levels, which resulted in a drastic reduction of agricultural production (Kosarev and Yablonskaya 1994). The rising sea level in the 1980s and 1990s destroyed infrastructure built along the shore line during the period of low water level (Dumont 1995). Furthermore, the strong decline in the abundance of sturgeon in the Caspian Sea during the last decades has been explained by the reduction of appropriate spawning grounds (Khodorevskaya and Krasikov 1999). Impacts of long-term WLF on fish reproduction have been demonstrated in Lake Constance as well as in other lakes. The temporal variability of seasonal WLF affects the fish specific substrate availability for spawning, and hence determines egg mortality and breading success (Gafny et al. 1992). Also water birds are affected by long-term WLF at Lake Constance (Werner, pers. comm.). Especially low water levels in spring reduce the availability of appropriate breeding-sites, and hence increase the mortality due to predation. Seasonal or even longer-lasting WLF also cause shifts and variations of the riparian plant community, e.g., diversity, abundance, and structure (Kotowski and Piořkowski 2005). In contrast, flood events as specifically drastic long-term WLF can have severe effects on a former established plant community. Schmieder et al. (2004) has documented the degradation of reed belts after early spring floods at Lake Constance.

Impacts of short-term WLF

Since short-term WLF do not induce large horizontal shore-line displacements but are accompanied by high current velocities near the sediment (Table 1.1), their major impact on the lake ecosystem is the imposition of hydrodynamic stress on organisms living in the shore region and on the sediment surface. The hydrodynamic stress affects ecological processes such as competition between individual organisms, short-term production and losses in biofilms and erosion of sediments. The impact of the short-term WLF is, however, variable in strength and time.

Wind and ship waves can be observed throughout the entire year and at any lake shore as long as no ice cover exists. However, wave heights and frequencies can vary substantially due to the different exposure to wind or ship traffic (see section 'Short-term WLF'). Particularly affected by short-term WLF are the shallow littoral zones of lakes, even if wave heights are small. Note that the littoral zone is of specific importance to the entire ecosystem because they are characterized by high species diversities and abundances and are important for the reproduction and the life cycle of many fish species.

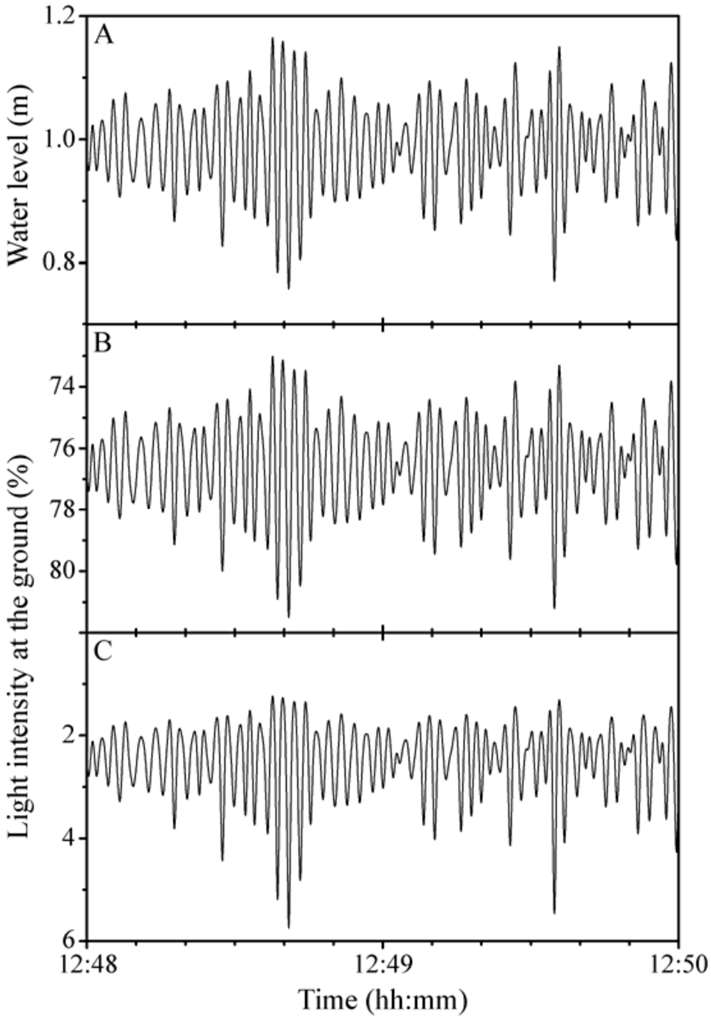

Fig. 1.3 Wave-generated high-frequency water level and light fluctuations. (A) Water level fluctuations measured in Lake Constance on 18 September 2005 during a period of strong on-shore wind. Light intensity fluctuations at the ground are given as percents of the incoming light intensity at the water surface. (B) For clear water. The light intensity was calculated for an exponential decay of light with depth using an average extinction coefficient (K_d) of 0.27 m^{-1} representative for pelagic waters (IGKB 2002). (C) Considering the additional shading effect due to resuspended particles in the shallow littoral ($K_{dss} = 0.27 + 0.025 * C_{ss}$) (van Duin et al. 2001). The particle concentration C_{ss} was measured to 140 mg L^{-1} during the time of measurement.

The availability and intensity of light, as an indispensable resource for primary production of phytoplankton in the water column or of periphyton on stones and on the sediment surface, is affected by short-term WLF. Fluctuations of the underwater light intensity associated with short-term WLF due to wind waves are exemplified in Figure 1.3. During on-shore wind on 18 September 2005, short-term WLF (wind waves) with a period of about 2 s and wave heights between 0.1 and 0.4 m were observed (Fig. 1.3A) and caused light intensity fluctuations at the ground of 2-8%, based on exponential light decay with an average extinction coefficient (K_d) of 0.27 m^{-1} representative for pelagic waters (Fig. 1.3B; IGKB 2002). The remaining mean light intensity at 1 m water depth is then about 77% of the incoming light at the water surface. Fluctuations of the underwater light intensity can be further amplified by wave focusing which increases the light intensity within milliseconds up to five times of the mean value (Dera and Gordon 1968; Stramski and Legendre 1992; Schubert et al. 2001; Hofmann et al. 2008a). In the shallow littoral the observed surface waves induce resuspension of particles with grain sizes up to 1 mm at 1 m water depth (Fig. 1.4B). The increased backscatter of light due to suspended particles leads to intense shading and reduces dramatically the light intensity at the sediment surface down to 2-3% of the incoming light at the water surface (Fig. 1.3C; van Duin et al. 2001). During an individual wind event, which can last for more than one day, primary production can be reduced or even inhibited (van Duin et al. 2001). In the aftermath of such events the remobilized and suspended particles settle down and cover biofilms and periphyton on stones. The frequency of occurrence of strong wind events determines the density and appearance of periphyton in the shallow littoral, and hence indicates the habitat exposure to hydrodynamic disturbances (Cattaneo 1990; Airoldi and Cinelli 1997; Francoeur and Biggs 2006).

Also higher developed organisms are influenced by hydrodynamic stress due to waves. The comparison of zoobenthos and fish communities at surface wave exposed and non-exposed shores revealed the different sensitivity, selectivity, and species composition of these communities in many studies (Clark 1997; Abdallah and Barton 2003; Eggleton et al. 2004).

The high productivity of the shallow littoral zone results in intense microbial decomposition rates of organic material (Wetzel 2001). The sequence of production and decomposition is forced by boundary conditions as nutrient availability or the renewal of diffusive gradients for deoxidization of organic material to carbon dioxide and methane. High current velocities and strong turbulence associated with shoaling surface waves enhance solute diffusion across the sediment-water interface (Lorke et al. 2003), lead to remobilization of particles and reallocation of sediment layers (Fig. 1.4B), and hence reset the adjusted gradients due to increased pore-water exchange (Precht and Huettel 2003; Precht et al. 2004). An important implication is the rapid release of recycled nutrients and methane (Li et al. 1997; Asmus et al. 1998; Heyer and Berger 2000; Schulz et al. 2001).

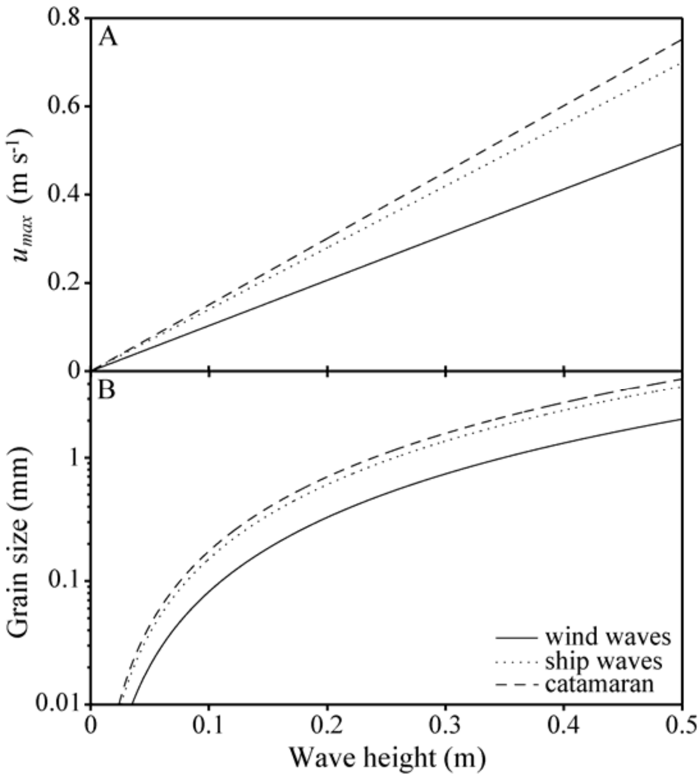

Fig. 1.4 Potential forcing of short-term WLF in the littoral zone. (A) Maximum wave-generated near-bottom current velocity (u_{max}) at 1 m water depth as a function of wave height and wave period (T) for wind-generated ($T = 2$ s) and ship-generated ($T = 3.3$ and $T = 6.3$ s) waves, respectively. (B) Minimum wave heights required for the remobilization of particles of different grain sizes as a function of wave period (as under (A)) at the water depth of 1 m.

Interacting long- and short-term WLF

The discussion above exemplifies the impacts of WLF on abiotic or biotic processes at very different temporal scales. In the following we demonstrate that the interaction between different time scales, i.e., the interaction between long-term and short-term WLF, has important ecological consequences.

With respect to WLF, Lake Constance can be considered to represent natural conditions typical for prealpine lakes before their regulation. The seasonal change in water level is about 2 m. During summer, the entire shore region up to the very shallow littoral is covered with water, whereas in winter the littoral is reduced to a very narrow zone along the steep slope of the lake (Fig. 1.5). At low water levels the shallow littoral is not submersed, and hence widely exposed to atmospheric decomposition, weathering, and deflation. These processes change the former sediment composition, where rock will break up and fine particles will be blown away or deposited.

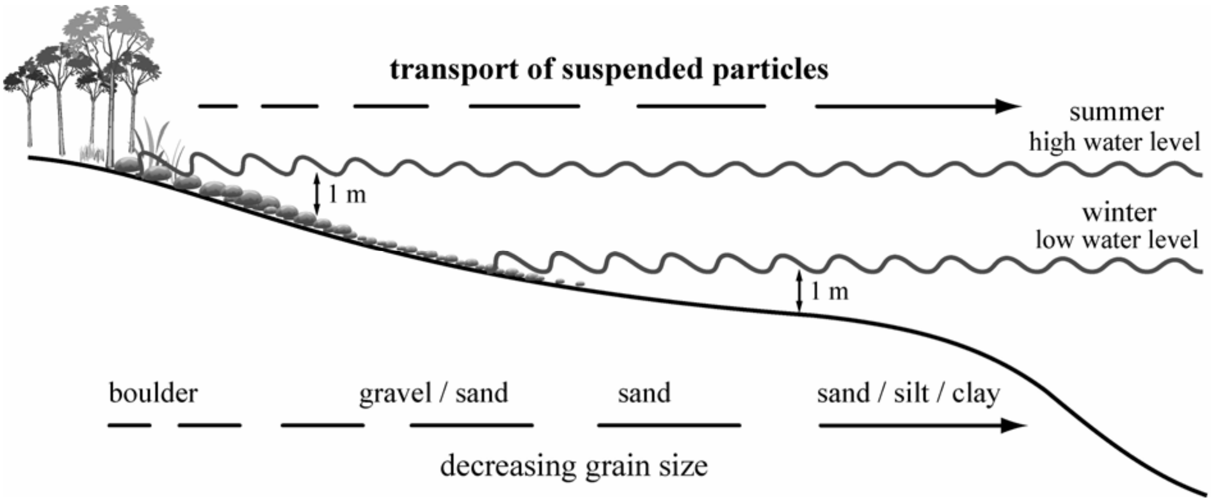

Fig. 1.5 Sketch of a typical prealpine shore line for different water levels. The sketch indicates the interactions and impacts of long-term versus short-term WLF on remobilization, resuspension, transport, and distribution of particles in the littoral zone.

Waves impose hydrodynamic shear stress on the lake bottom and initiate sediment remobilization, resuspension, and transport due to background currents in cross- or along-shore direction. Remobilization of particles at the sediment surface depends on water depth, grain size, wave height, and wave period. The maximum near-bottom wave-generated current velocity u_{max} at the sediment surface at 1 m water depth was estimated for wave heights of 0-0.5 m and for wave periods of 2, 3.3 and 6.3 s (Eq. 1.1; Fig. 1.4A). These represent typical values at Lake Constance for wind waves, for ship waves generated by permanent ferries or passenger ships, and for ship waves generated by fast catamaran ferries, respectively (Hofmann et al. 2008a). Long-periodic ship waves induce much higher velocities at the ground and remobilize much larger particles in comparison to wind waves with the same height (Fig. 1.4). For example, with a wave height of 0.2 m, wind waves remobilize particles of grain sizes up to 0.3 mm, whereas ship waves are able to remobilize particles with grain sizes up to 0.6 mm. This demonstrates the importance of ship waves for sediment remobilization at exposed shores. Although wind and ship waves occur throughout the whole year, they develop their main impact at different sections of the littoral zone due to seasonal, long-term WLF (Fig. 1.5). Due to the shore line displacement by seasonal WLF the substrate at the ground at shallow depths varies substantially over the year. During summer, when the water level is high, the substrate consists mainly of boulders, cobbles, gravel, and sand. In winter, the substrate at low water levels is formed by much smaller particles like fine sand, silt, and clay (Fig. 1.5). Therefore, the same wind and ship waves result in much higher rates of remobilization, resuspension, and transport into the pelagic zone during winter than during summer (Figs. 1.4B, 1.5). The interaction between seasonal WLF (long-term WLF) and waves (short-term WLF) is a permanent process leading to a continuously decreasing grain size distribution from boulders to clay in off-shore direction (Fig. 1.5). Over decades, small particles that can be remobilized by waves, are transported to deeper zones. At the site LG the lake floor falls off gently from the shore line towards the open water. At a water depth of about 1-2 m below the average annual minimum water level, the slope of the lake floor increases significantly, thus, forming the so-called 'Haldenkante'. The location of the 'Haldenkante' and the presence of the fine-grained sediments at this location reflect the combined action of long- and short-term WLF in Lake Constance.

The export of fine particles from the littoral zone to the pelagic, and thus, erosion is expected to increase with the decreasing mean water levels observed during the recent past. In combination with the increasing exposure of the shore region to ship waves due to increasing ship traffic on Lake Constance, i.e., due to passenger ships and the recently introduced fast catamaran ferries, erosion of the shore region may be even more dramatic. Observations of divers investigating oak poles in the context of maritime archaeology suggest that many historic and archaeologically important underwater heritages like pile dwellings are more and more threatened by the interaction between surface waves and long-term WLF, i.e., previously sand covered sites became uncovered by erosion and are now directly exposed to oxygen rich water, and thus, faster biological decomposition (Bürgi and Schlichterle 1986; Körninger 2005).

Conclusions

WLF in lakes exist on temporal scales from seconds to even hundreds of years (Table 1.1). The ecological impact of WLF depends on the time scale of the level fluctuation and can be amplified by the combined action of long- and short-term WLF. In this paper, WLF are classified as long- and short-term WLF based on the generation mechanism of the WLF with long-term WLF being the consequence of changes in the hydrologic conditions and short-term WLF being the result of hydrodynamic processes, namely waves and basin-scale oscillations.

Table 1.1 Temporal scales of WLF with the corresponding amplitudes and estimated maximum near-bottom current velocities. Whereas long-term WLF are generated by meteorological and hydrological processes, short-term WLF are generated by hydrodynamic processes: '*' surface seiching and '+' surface waves generated by fast catamaran ferries (6.3 s), passenger ships or ferries (3.3 s), and wind (2 s) measured at Lake Constance.

Example		Temporal scale		Amplitude (m)	Near-bottom velocity (m s^{-1})
Issyk-Kul	*Long-term WLF*	~2,000	yr	~250	<<10^{-3}
Caspian Sea	*Long-term WLF*	20 - 100	yr	~2.5 - 4	<<10^{-3}
Lake Constance	*Long-term WLF*	1 - 10	yr	1 - 3	<<10^{-3}
	Long-term WLF	1	yr	0.5	<<10^{-3}
	Long-term WLF	0.5	yr	1 - 4	<<10^{-3}
	Long-term WLF	1	day	0 - 0.5	<<10^{-3}
	Short-term WLF	54.6 *	min	0.02 - 0.05	10^{-3}
	Short-term WLF	6.3 +	s	~0.04	10^{-2}
	Short-term WLF	3.3 +	s	0.1 - 0.5	10^{-1}
	Short-term WLF	2 +	s	0 - 0.8	10^{-1}

Long-term WLF can have large amplitudes and induce a slow shore-line displacement of meters or even kilometers, whereas the immediate physical forcing due to currents is negligible. Although the physical forcing of long-term WLF is low, the impacts on the entire ecosystem can be versatile: long-lasting changes in habitat availability for organisms adapted to terrestrial and aquatic conditions, lake salinity, vertical mixing, deep water renewal, or oxygen supply to the deep water. In the case of Lake Constance, the annual mean water level has changed only very little over the last 189 yr and also the inter-annual variation of the annual mean water level did never exceed 0.75 m. However, seasonal changes in water level can reach up to more than 3 m, and thus, cause shore-line displacements of up to hundreds of meters. Hence, seasonal WLF are probably the most important component of long-term WLF affecting competition and survival of species in the littoral zone.

Compared to the seasonal WLF, short-term WLF have much smaller amplitudes and do not significantly displace the boundary between the terrestrial and aquatic habitat but provide high amounts of mechanical energy to abiotic processes, e.g., remobilization and resuspension of particles, sediment transport, release of nutrients and methane, and abrasion of biofilms. The change in abiotic habitat conditions is often followed by changed biotic processes, e.g., resuspended and settled particles reduce the availability of light for photosynthesis, which then result in a decreased growth of phytoplankton and biofilms.

Although the forcing of long- and short-term WLF is different the interaction of both can cause additional consequences to those resulting from the individual process themselves. Long-term WLF change the habitat exposed to the physical stress provided by short-term WLF. Specifically, shore morphology and sediment grain size distribution are the result of a continuous interplay between short- and long-term WLF, the former providing the energy for erosion the latter determining the section of the shore exposed to the erosive power.

Acknowledgments

We thank Georg Heine and his colleagues from the electronic and mechanical workshop at the University of Konstanz for technical assistance and the development of the pressure sensors. We gratefully acknowledge the help of the technical staff at the Limnological Institute and many students during fieldwork and data analysis. We thank the two anonymous referees whose valuable comments improved the manuscript. The gauge Konstanz water level time series between 1817 and 2005 was provided by the State Institute for Environment, Measurements and Nature Conservation Baden-Württemberg (LUBW). This work was supported by the German Research Foundation (DFG) within the framework of the Collaborative Research Center 454 'Littoral Zone of Lake Constance'.

Chapter 2

The relative importance of wind and ship waves in the littoral zone of a large lake

HILMAR HOFMANN, ANDREAS LORKE AND FRANK PEETERS

Limnology and Oceanography 53 (1): 368-380

Abstract

Surface waves and their interactions with sediments and benthic organisms are the main hydrodynamic process affecting littoral ecosystems. Here, we present a long-term data set on surface-wave parameters, which was obtained from the analysis of measurements with a pressure sensor. The data set covers a time period of a year and allows for resolving waves with heights down to less than a centimeter and frequencies up to 0.8 Hz. Wind waves and three different types of ship waves were distinguished by their spectral properties. In Lake Constance, ship-generated waves are as important as wind-generated waves and contribute about 41% of the annual mean wave energy flux to shore. In summer, during the most productive time period, ship waves dominate the wave field in terms of the energy flux to shore and also in their frequency of occurrence. Ship waves cause a diurnal and a seasonal pattern in the frequency of occurrence and in the heights of surface waves, whereas in the case of wind waves these parameters do not vary significantly with season or between nighttime and daytime. In contrast to wind waves that occur only sporadically, ship waves propagate into the littoral zone very frequently at regular time intervals. The different pattern of occurrence of ship and wind waves results in a different pattern of disturbance in the littoral ecosystem.

Introduction

One of the most prominent differences between the littoral and the pelagic zone is the role of surface waves. In the littoral zone, waves interact directly with the sediment surface and biota and thus cause, for example, resuspension, erosion, and transport of particles (Luettich et al. 1990; Hawley and Lee 1999; Håkanson 2005); release of nutrients and methane (Güde et al. 2000; Bussmann 2005); reallocation and stress on zoobenthos affecting zoobenthos diversity (Scheifhacken 2006); abrasion of biofilms from stones (Cattaneo 1990; Peters 2005; Francoeur and Biggs 2006) and aquatic macrophytes (Eriksson et al. 2004); and damage of reed belts (Schmieder et al. 2004). Surface waves also influence the growth and behavior of fish that cannot escape from the fluctuating currents by vertical migration (Stoll, pers. comm.), the light regime via the fluctuations in water level and light attenuation by resuspended particles (Stramski et al. 1992; Erm and Soomere 2006), and the riparian plant community (Ostendorp et al. 2004; Kotowski and Piorkowski 2005).

Nevertheless, most descriptions of surface waves are based on studies in marine environments or shelf regions (e.g., Madsen 1976; Le Blond and Mysak 1978; Donelan et al. 2005). In oceans, waves are generated by strong and frequent winds over long fetch lengths and propagate to the coast with large amplitudes. Typical wave heights vary between 0.5 m during calm sea and several meters during storm events, whereas wave periods vary between 5 and 10 s (e.g., Komen et al. 1996; CERC 2002; Brown et al. 2005). In most lakes, winds are infrequent and wind speeds are low. In addition, wind forcing at the water surface often varies on small spatial scales, and the effective fetch length is restricted to a few kilometers. Hence, the wave field in most lakes is characterized by waves with small amplitudes and high frequencies and thus differs considerably from the wave field in the ocean.

The ecological effect of wind-generated surface waves in lacustrine environments has been investigated mainly in the Great Lakes (Lawrence and Davidson-Arnott 1997; Meadows et al. 1997; Hawley and Lee 1999). Only a few studies specifically investigated wind waves in smaller lakes (Jin and Wang 1998; Allan and Kirk 2000).

Apart from the wind, commercial and tourist ship traffic causes surface waves. Several studies investigated the properties and the importance of regular ship traffic in rivers and channels or shelf regions (e.g., Sorensen 1973; Stumbo 1999; Bauer et al. 2002) and the relevance of high-speed catamaran ferries in coastal environments (Parnell and Kofoed-Hansen 2001; Soomere 2005), but only few studies focused on ship waves in lakes (Bhowmik 1975; Maynord 2005). Because of their specific generation, ship and wind waves have considerably different properties (e.g., wave form, period, and length) and thus potentially have a different ecological effect in the littoral zone (Bauer et al. 2002; Soomere 2005; Erm and Soomere 2006). However, the hydrodynamic forcing in the littoral zone due to ship waves is often underestimated or even neglected (Bhowmik 1975; Maynord 2005). The purpose of the current study is, therefore, to fill this gap by comparing the relative importance of wind- and ship-generated surface waves in a large lake over a year.

Materials and methods

Study sites

Lake Constance is located in the southwest of Germany and borders Switzerland and Austria. It is the second largest (by surface area) prealpine lake in Europe with a surface area of 536 km^2 and a maximum depth of 254 m (Braun and Schärpf 1990). Lake Constance is not regulated and experiences seasonal water level fluctuations of about 2-3 m (Luft and van den Eertwegh 1991; Jöhnk et al. 2004). The littoral zone, where most of the disturbances due to surface waves occur, covers about 10% of the total surface area (Braun and Schärpf 1990).

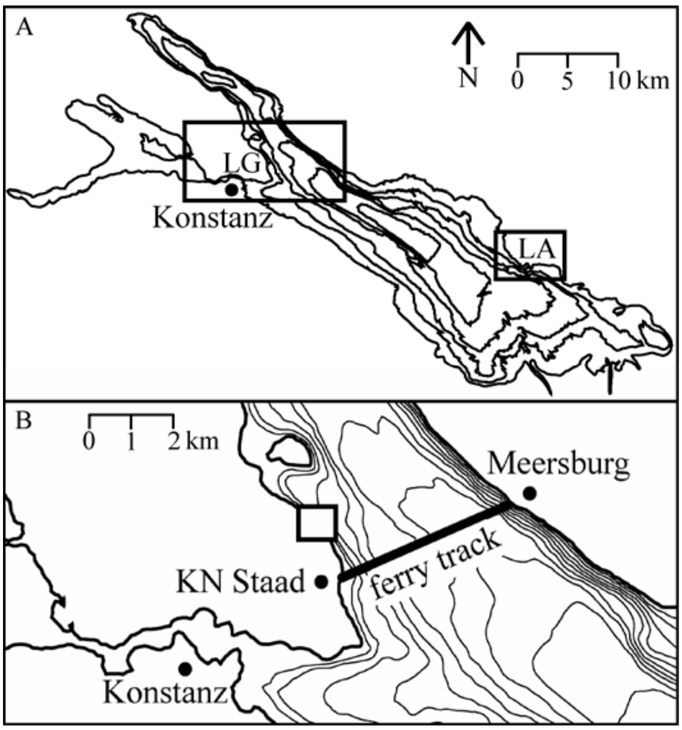

Fig. 2.1 Study sites. (A) Map of Lake Constance. The upper box shows the section of the main study site Littoral Garden (LG) and the lower box the site near the city of Langenargen (LA). (B) Zoom to the study site LG (indicated by the square), which is situated at Upper Lake Constance close by the ferry crossing from Meersburg to Konstanz-Staad.

Measurements were carried out in the western part of Upper Lake Constance at a site called Littoral Garden (LG; 47°41’29’’N, 09°12’11’’E) (Fig. 2.1), where intensive biological, chemical, and physical experiments were performed in earlier years (Fischer and Eckmann 1997; Bäuerle et al. 1998; Baumgärtner and Rothhaupt 2005).

The shore is sheltered against westerly winds and exposed to northeasterly winds with a fetch of about 3.5 km (Fig. 2.1A). The study site is close to the ferry crossing from Meersburg to Konstanz-Staad with regular sailings throughout the year (Fig. 2.1). Additionally, during the tourist season (middle of March to middle of October), large passenger ships travel parallel to the shore line and increase the frequency of occurrence of ship-generated waves.

In addition to the long-term measurements at LG, short-term measurements were carried out in the eastern part of Upper Lake Constance at a site next to the city Langenargen (LA; 47°35’42’’N, 09°31’59’’E) (Fig. 2.1A). This shore is exposed to westerly winds with a fetch of about 20 km. Ferries as well as passenger ships pass the study site nearby.

Instrumentation

Meteorological data

A meteorological station 1 km to the west of the study site provided wind speed and wind direction averaged over 20 min during 2005. The anemometer was deployed directly at the shore at 6 m height. The data are corrected to the reference height of 10 m using a parameterized drag coefficient derived for lakes with low wind speeds (Wüest and Lorke 2003; Guan and Xie 2004).

Wave measurements

Wave characteristics and their temporal changes were studied using a pressure sensor (PS) and a NORTEK Vector - Acoustic Doppler Velocity Meter (ADV) during the year 2005. Both devices were deployed close to each other at the study site LG at water depths of about 2 m (PS) and 1-3 m (ADV).

The custom-made PS has a full-scale range of 7 m, an accuracy of 0.1 mbar, and a maximum stand-alone deployment time of 45 d. The sensor was always positioned 1 m above the bottom and about 1 m below the surface (the water height above the sensor did not vary by more than 0.3 m during individual deployment periods). To compensate for the seasonal water level fluctuations (Jöhnk et al. 2004), the sensor was moved to shallower or deeper water depths. Pressure measurements were made at 16 Hz throughout 2005 with some gaps resulting from battery replacements or malfunction. Wave parameters were calculated for burst intervals of 1,024 (~1.1 min) and 4,096 (~4.3 min) samples. The measured time series of subsurface pressure in each burst interval was converted to a time series of surface elevation using the following procedure: In each burst interval, the mean value and linear trend was subtracted from the pressure data before a fast Fourier transform with a Hanning window was applied. The spectral density of the subsurface pressure was transformed to the spectral density of surface elevation by applying the pressure attenuation coefficient calculated for the given sensor position, water depth and wave frequency using the dispersion relation of surface waves (Krogstad and Arntsen 2000; Tucker and Pitt 2001; Kundu and Cohen 2002). All frequencies in the range between 0.05 and 0.8 Hz were considered, which covers the frequencies expected to be relevant in the field. The inverse Fourier transform of the spectrum of surface elevation and later addition of the mean water depth, and the linear trend in water elevation provided an estimate of the water surface elevation as a function of time (Fig. 2.2A). Note that the technique is based on linear wave theory and assumes sinusoidal waves, which may not be exactly fulfilled for ship waves (Soomere et al. 2005). The accuracy of the sensor and the technique allows for resolving fluctuations of water surface elevation within 1 cm.

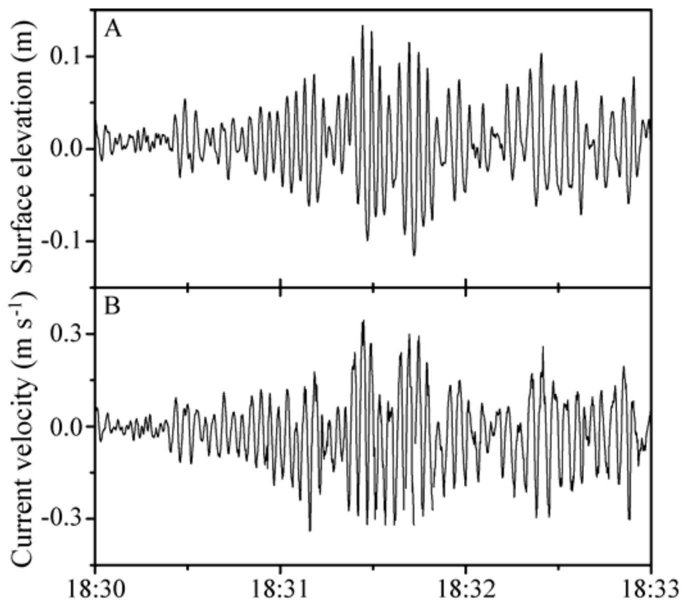

Fig. 2.2 Train of characteristic ship waves measured simultaneously by pressure sensor (PS) and Acoustic Doppler Velocity Meter (ADV) at ~1 m water depth on 04 August 2005. (A) Surface elevation (wave height) corrected for pressure attenuation. (B) Near-bottom horizontal current velocity (cross-shore velocity).

Maximum and significant wave heights (H_{max}, H_s) and significant period (T_s) were calculated by using the zero-upcrossing method (IAHR 1989). Within each burst, the wave amplitude was calculated separately for each time period between two consecutive zero upcrossings. The difference between the maximum elevation in this time period and the mean elevation in the burst interval was used as a measure of wave amplitude. Twice the maximum of all wave amplitudes in the burst interval gave H_{max}. H_s is two times the average of the highest one-third of all amplitudes in the burst interval. The significant wave period T_s is defined as the average of the periods of the highest one-third of wave heights (H_s) in the burst interval (IAHR 1989).

The wind-wave field is usually characterized by the significant wave height H_s. Because of the transient nature of ship waves (Fig. 2.2), short burst intervals (~1.1 min) were chosen to calculate H_s. However, the maximum current velocity at the sediment surface u_{max} during these short burst intervals is one of the most important consequences of surface waves affecting the ecological conditions in the littoral zone. Because u_{max} is directly related to H_{max} rather than to H_s, H_{max} was used for the comparison between ship and wind waves.

The ADV was attached to a bottom-resting tripod that also supported the data acquisition system. Current velocities were measured within a range of ±0.3 m s^{-1} with an accuracy of 10^{-3} m s^{-1} and a sampling frequency of 8 Hz. The ADV measurements of the near-bottom current velocities were performed simultaneously to the pressure measurements with the PS (Fig. 2.2B).

Turbidity measurements

Turbidity measurements were carried out using an optical backscatter sensor (Driesen & Kern) deployed during distinct time periods in 2005. Turbidity was measured with an accuracy of 0.01 FTU and a sampling frequency of 0.1 Hz. The sensor was attached to the tripod of the ADV next to the PS 0.2 m above the bottom at ~1 m water depth.

Wave statistics, energy flux, and wave-generated current velocities

Wind and ship waves can be distinguished by their respective periods. As we will show below, wind-generated waves are characterized by wave periods below 2.5 s, whereas ship-generated waves have periods above 2.5 s.

In the statistical analysis of the wave field, we investigate the frequency of occurrence of ship and wind waves and distinguish between daytime (09:00-21:00 h) and nighttime (21:00-09:00 h) on monthly scales. Waves with heights below 0.05 m are excluded from the statistical analysis because they represent mainly ripples with small periods and have a negligible effect on the shallow littoral.

The comparison of wind and ship waves solely by frequency of occurrence, however, does not take into account the different properties of ship and wind waves (e.g., wave length or wave energy) and thus does not adequately consider their different potential for disturbance in the shallow littoral. A more appropriate measure of the ecological relevance of waves is the energy flux to shore associated with the wave motion per unit length of wave crest E_F (W m^{-1}). E_F can be estimated as the product of the group velocity and the wave energy. The latter is solely determined by the wave amplitude. E_F implicitly accounts for the different wave periods of ship and wind waves since the group velocity of surface waves depends on the wave period (Fenton and McKee 1990; Kundu and Cohen 2002):

$$E_F = E \cdot c_g \qquad (W\,m^{-1}) \qquad (2.1)$$

$$E = \frac{1}{2}(\rho \cdot g \cdot a^2) \qquad (Ws\,m^{-2}) \qquad (2.2)$$

$$c_g = \frac{c}{2} \cdot \left(1 + \frac{2 \cdot k \cdot h}{\sinh(2 \cdot k \cdot h)}\right) \qquad (m\,s^{-1}) \qquad (2.3)$$

$$c = \sqrt{\frac{g}{k} \cdot \tanh(k \cdot h)} \qquad (m\,s^{-1}) \qquad (2.4)$$

$$k = \frac{2 \cdot \pi}{\lambda} \qquad (m^{-1}) \qquad (2.5)$$

$$\lambda = \frac{g \cdot T^2}{2 \cdot \pi} \cdot \left\{ \tanh \left[\frac{2 \cdot \pi \cdot \sqrt{\frac{h}{g}}}{T} \right]^{\frac{3}{2}} \right\}^{\frac{2}{3}} \qquad (m) \qquad (2.6)$$

where E is the wave energy (Ws m^{-2}), c_g the group velocity (m s^{-1}), a the wave amplitude (m), c the phase velocity (m s^{-1}), k the wave number (m^{-1}), λ the wave length (m), T the wave period (s), g the gravitational acceleration (m s^{-2}), and h the water depth (m). Note that Eq. 2.6

is an approximation for short and long waves in water of intermediate depth (Fenton and McKee 1990).

The calculation of the monthly mean wave energy flux to shore is performed at a water depth of 2 m, where the PS was deployed. The wave energy and its flux are calculated per individual wave basis, derived from the zero-upcrossing method. The mean wave energy flux for each burst interval (~1.1 min) is determined by weighting the energy flux of each wave by its wave period prior to averaging. Then the energy flux is classified as ship-wave or wind-wave generated, depending on the significant wave period (T_s) for the specific burst; that is, ship waves have periods above and wind waves periods below the threshold period of 2.5 s. Energy fluxes from individual bursts are averaged in order to obtain monthly mean values.

Another parameter that characterizes the impact of surface waves on the littoral zone in terms of bottom shear is the maximum near-bottom current velocity u_{max} (m s^{-1}) (Brown et al. 2005):

$$u_{\max} = \frac{\pi \cdot H}{T \cdot \sinh \frac{2 \cdot \pi \cdot h}{\lambda}} \qquad (m\, s^{-1}) \qquad (2.7)$$

where H denotes the wave height (m), T the wave period (s), h the water depth (m), and λ the wave length (m).

Here we considered u_{max} at a water depth of 1 m. In the calculation we used the appropriate dispersion relation and H_{max} and T_s measured with the PS. Thereby we assumed that H_{max} and T_s do not change significantly between 1 and 2 m water depth. The maximum near-bottom current velocity is calculated for each burst interval (~1.1 min) and classified as wind-wave or ship-wave generated following the same procedure as outlined for the wave energy flux. The relative monthly frequency distribution of u_{max} generated by wind or ship waves is obtained for a constant frequency distribution step size of 0.005 m s^{-1}, where the individual wind and ship wave distribution was normalized by the total number of burst intervals counted in the specific month. Values of u_{max} for waves of heights below 0.05 m are not considered in the statistics.

Results and discussion

Wind exposure

The wind field and hence the wind exposure of the study site changes at a seasonal time scale. Figure 2.3 shows wind speed and relative frequency of occurrence per degree direction for summer (May-October) and winter (November-April), respectively. Westerly winds are most frequent during the year, but the associated wind speeds at the study site are small. The second most frequent winds come from southeast during summer and northeast during winter. In general, wind speeds averaged per degree direction vary between 1 and 5 m s^{-1} (Fig. 2.3B), although maximum values can exceed 8 m s^{-1} (Figs. 2.5B, 2.6C). At the study site LG high wind speeds from northeast are most relevant for the generation of wind waves (Fig. 2.5). In 2005 several major wind events could be observed and were slightly more frequent during winter as compared to summer, where strong winds were nearly absent.

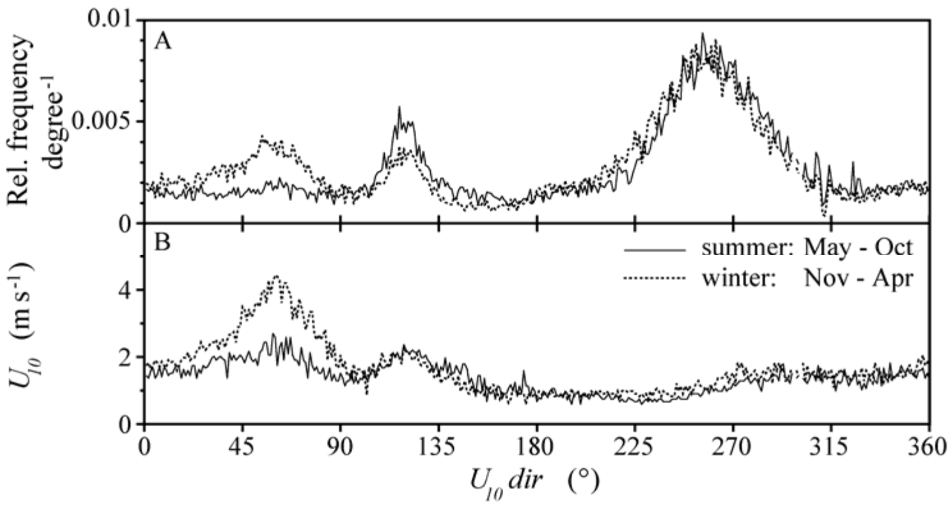

Fig. 2.3 Wind exposure of the study site Littoral Garden (LG). (A) Relative frequency and (B) wind speed (U_{10}) per degree wind direction (direction where the wind is blowing from) between 2001 and 2005 in summer (solid line) and winter (dotted line). Values are averaged per degree direction.

Wave spectral properties

The different spectral characteristics of wind and ship waves are exemplified in Fig. 1.4 for different wind conditions: Whereas the 28 February and 12 May were accompanied by strong on-shore winds (U_{10} = 6-8 m s^{-1}, $U_{10}\,dir$ = 40-60°), the 04 March, 15 May, and 04 August were characterized by nearly no wind (U_{10} = 0-2 m s^{-1}, $U_{10}\,dir$ = 180-270°). In the pressure spectra, four typical peak frequencies or frequency bands can be identified that are assigned to wind- and ship-generated waves (Fig. 2.4). On all five days the spectra have a clear peak at 0.27 Hz (T = 3.7 s). The occurrence of waves with this frequency correlates with the timetable of the ferry traffic from Meersburg to Konstanz-Staad (Figs. 2.1, 2.4, square). The spectral peak at 0.35 Hz (T = 2.9 s) visible in the spectra from 15 May and 04 August when winds were calm can be assigned to passenger ships (Fig. 2.4, triangle). The broad, wind-generated spectral band of frequencies masks this peak on 12 May (strong wind event). In winter under calm conditions (represented by 04 March), when passenger ships have stopped their service, their signal cannot be found. On 04 August the spectrum has an additional peak at 0.16 Hz (T = 6.3 s) that was not observed before (Fig. 2.4, circle). This peak can be assigned to the newly introduced catamaran ferry on Lake Constance. The identification of the three types of ship waves with their typical frequencies was validated by visual observations confirming the linkage between the passage of a specific ship and its typical wave signature (e.g., wave frequency).

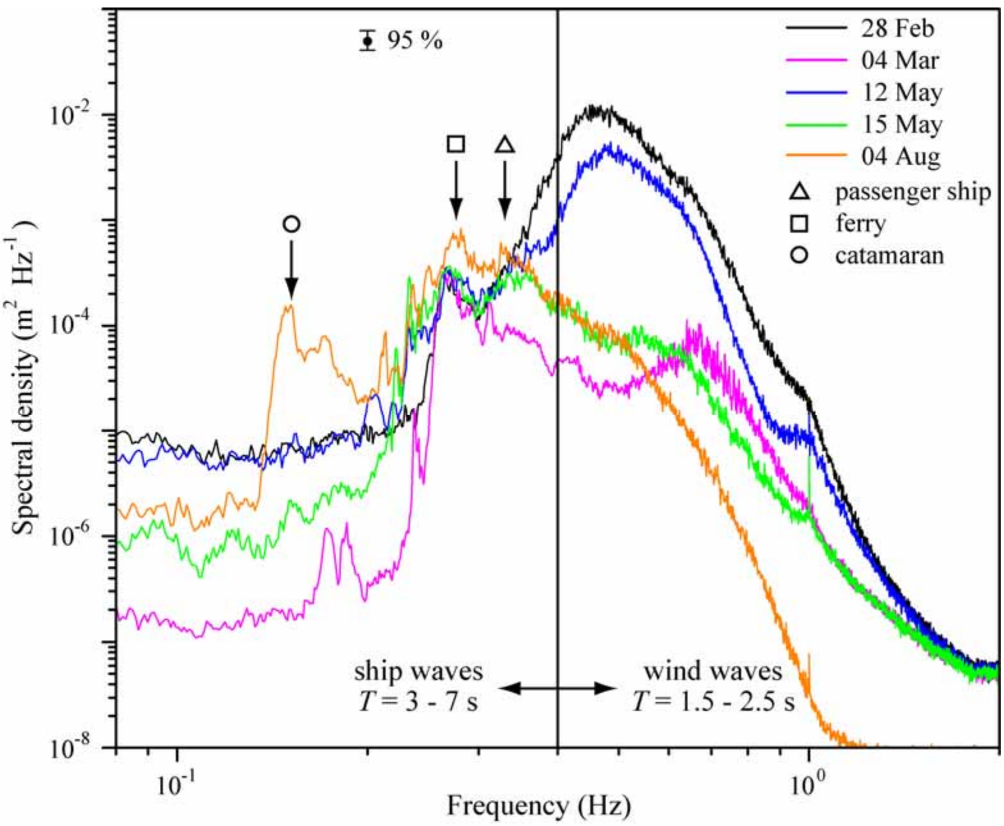

Fig. 2.4 Wave spectrum (surface elevation) of two wind-wave-dominated days (28 February and 12 May 2005, black and blue) and three ship-wave dominated days (04 March, 15 May, and 04 August 2005; magenta, green, and orange). The vertical line indicates the threshold frequency of 0.4 Hz (T = 2.5 s) where ship-generated (left-hand side) and wind-generated (right-hand side) waves can be discriminated. The most prominent ship types with their typical wave frequencies are noted by the triangle (passenger ship), square (ferry), and circle (catamaran). The spectrum was estimated from pressure sensor (PS) data on the respective days using 16,384 samples (~17 min), respectively. The spike at 1 Hz is an artifact of the PS.

As indicated above, the 28 February and 12 May were accompanied by wind-generated wave events that showed no distinct spectral peaks. Wind waves are characterized by a rather broad spectral peak between 0.4 and 0.7 Hz (T = 2.5-1.4 s) (Fig. 2.4). The spectral density and peak frequency of wind waves is related to the effective fetch length, the wind speed, and the duration of the wind. Although Figure 2.4 is not a variance-preserving plot, spectral densities are higher for the data from 28 February than for the data from 12 May at all frequencies. This indicates that the wind-generated wave event on 28 February was slightly stronger than that on 12 May, which fits with the measured wave heights (Fig. 2.6A,D). Weak and short-lasting winds are typical especially during summer (e.g., mountain vent and local thunderstorms) and cause small-amplitude waves with short periods and wave lengths. A good example for such waves was observed on 04 March between 00:00 and 01:00 h, where a short wind event occurred (Fig. 2.6A-C). The maximum wave height was slightly above 0.1 m, and the frequency ranged between 0.6 and 0.7 Hz. In comparison, higher wind speeds with longer duration on 28 February and 12 May resulted in significant lower frequencies between 0.4 and 0.5 Hz (Figs. 2.4, 2.7).

The characteristic spectral properties of wind and ship waves are used to discriminate between wind and ship waves at the threshold frequency of 0.4 Hz (T = 2.5 s). Waves with frequencies above 0.4 Hz are classified as wind waves, below as ship waves. Additionally, the expected significant wave period T_s can be estimated following (CERC 2002) by considering an effective fetch length of 3.5 km for winds from northeast and a maximum wind speed of 10 m s^{-1}, resulting in T_s = 2.0 s. This period is significantly lower than the threshold period of 2.5 s. Both spectral analysis and the calculation of the empirical wave properties confirm that the chosen threshold period of 2.5 s is reasonable.

The wind-wave field

The maximum wave heights observed during 2005 are shown in Figure 2.5C. In general, wave heights range from about 0.01 to nearly 0.8 m. Wave heights between 0.4 and 0.8 m mainly occur in combination with strong and long-lasting (at least 2 h) northeastern winds (Fig. 2.5). Maximum wave heights of 0.7-0.8 m seem to be the upper limit at the study site LG and are in agreement with empirical estimations under the given effective fetch length and wind speed (CERC 2002). Such wind-wave events, however, are rare and unevenly distributed over the year. In 2005 about 10 major wind-wave events with maximum heights above 0.4 m could be observed. The relative frequency of occurrence of these events increased slightly during spring, autumn, and winter compared to a single event during summer or even none from June to the end of August, when southeastern and western winds with low wind speeds are dominant (Figs. 2.3, 2.5).

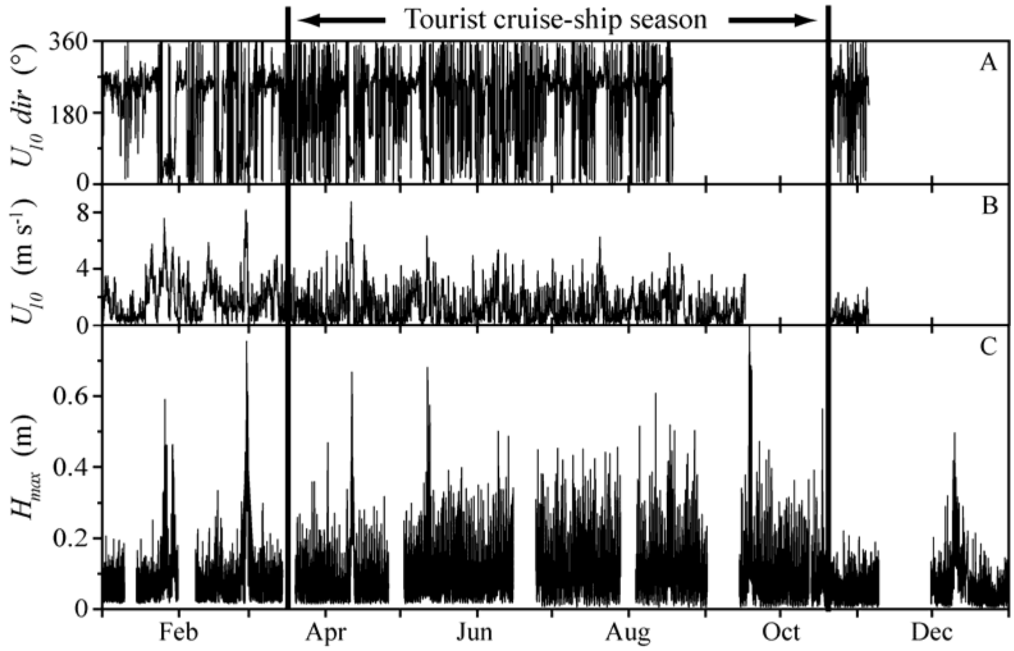

Fig. 2.5 Wind and wave exposure of the study site Littoral Garden (LG) in 2005. (A) Wind direction (U_{10} *dir*, direction where the wind is blowing from) and (B) wind speed (U_{10}) averaged over 3 hours. (C) Time series of maximum wave height (H_{max}) measured by pressure sensor (PS; burst interval (~4.3 min)). Data gaps are due to battery replacement, malfunction, and nondeployment periods, respectively.

The observation of wind waves at the study site LG reflects its specific shelter against western winds (the main wind direction at Lake Constance), and its exposure to northeastern winds (the second most frequent wind direction) with relatively low wind speeds and a short effective fetch, because wind waves are only generated in combination with northeastern winds. The wind-wave events around 28 February (winter season) and 12 May (early summer season) illustrate this relation (Fig. 2.6). Even strong western winds, observed on 14 and 15 May (Fig. 2.6E,F), did not generate increased wave heights compared to those observed on 12 May (Fig. 2.6D). Typical wind-wave events last between several hours and more than a day. The wave growth and their subsequent decline last only between 1 and 2 h (Fig. 2.6A,D; e.g., wind-wave events from 28 February and 12 May). The rapid formation of the wave field is mainly caused by the relatively short effective fetch. This also explains the extremely dynamic wave heights measured during a single event, which follow closely the temporal dynamics of the wind speed (Fig. 2.6A,C,D,F; e.g., wind-wave events from 28 February and 12 May). Also the wind-wave period follows this behavior. On 28 February during increased wave heights (until 19:00 h), the significant wave period fluctuated between 1.8 and 2.3 s (Fig. 2.7A,B). In general, the measured wind-generated significant wave periods are between 1.5 and 2.3 s. The upper limit is determined by fetch length and the maximum wind speed (Fig. 2.7B). The observed wind waves have 'deep-water wave lengths', defined here as the wave length obtained from the dispersion relation for deep-water waves and by assuming that the wave period at the measuring site is the same as in deep water, ranging between 2 and 8 m.

The ship-wave field

As indicated above, in addition to the wind-generated wave field a variety of ship-generated waves could be measured. Spectral analysis of the PS time series shows that ferry, passenger, and catamaran waves can be distinguished by their frequencies (Fig. 2.4). The individual ship-wave types could be assigned to the distinct peaks in the spectra by considering the time of observation (during a single day or the whole year) in combination with their wave properties (e.g., wave height or length). The high temporal resolution of wave properties enabled the identification of individual ships by comparing the time of occurrence of certain spectral peaks in the data with the schedule of the ship traffic and visual observation.

Ship waves generated by the regular car and passenger ferry crossing from Meersburg to Konstanz-Staad are present throughout the whole year. The ferry waves have typical maximum heights of 0.04-0.15 m, periods of about 3.7 s and deep-water wave lengths of about 20 m (Figs. 2.4, 2.5C, 2.6A,D, 2.7C,D). These comparatively small-amplitude ship waves become a prominent and important feature of the wave field especially when wind speed is low. The occurrence of ferry waves follows the timetable of the ferries, four to five wakes per hour during daytime (09:00-21:00 h) and once per hour during nighttime (21:00-09:00 h) (Fig. 2.7C,D). The relative frequency of occurrence of ferry waves does not change throughout the year, but it follows a strong diurnal pattern with many waves during day time and a few at night (Figs. 2.5C, 2.6A,D, 2.7C,D).

Passenger-ship waves are even more pronounced than ferry waves. These tourist ships cruise all around Lake Constance from the middle of March to the middle of October ('tourist cruise-ship season'; Fig. 2.5). The passenger-ship waves have typical maximum heights of

0.1-0.5 m, periods of about 2.9 s and deep-water wave lengths of about 13 m (Figs. 2.4, 2.5C, 2.6A,D, 2.7C,D). The course of the maximum wave height in Fig. 2.5C shows a seasonal pattern, which is related to the 'tourist cruise-ship season'. In the middle of March, maximum wave heights start to increase, develop at a plateau from the middle of May to the middle of September with maximum values between 0.2 and 0.5 m, and finally decrease until the middle of October to characteristic wave heights generated by ferries. In addition to wave height, the relative frequency of occurrence of ship-generated waves increases significantly during this time period, which is confirmed by statistical analysis (see below). The comparison of two selected time periods when wind waves were absent (01-04 March and 13-16 May), illustrates the seasonal change of the ship-wave field (Fig. 2.6A,D). Passenger ships further intensify the diurnal pattern in the occurrence of surface waves (as described for ferry waves) by cruising only at daytime (Figs. 2.6A,D, 2.7C,D).

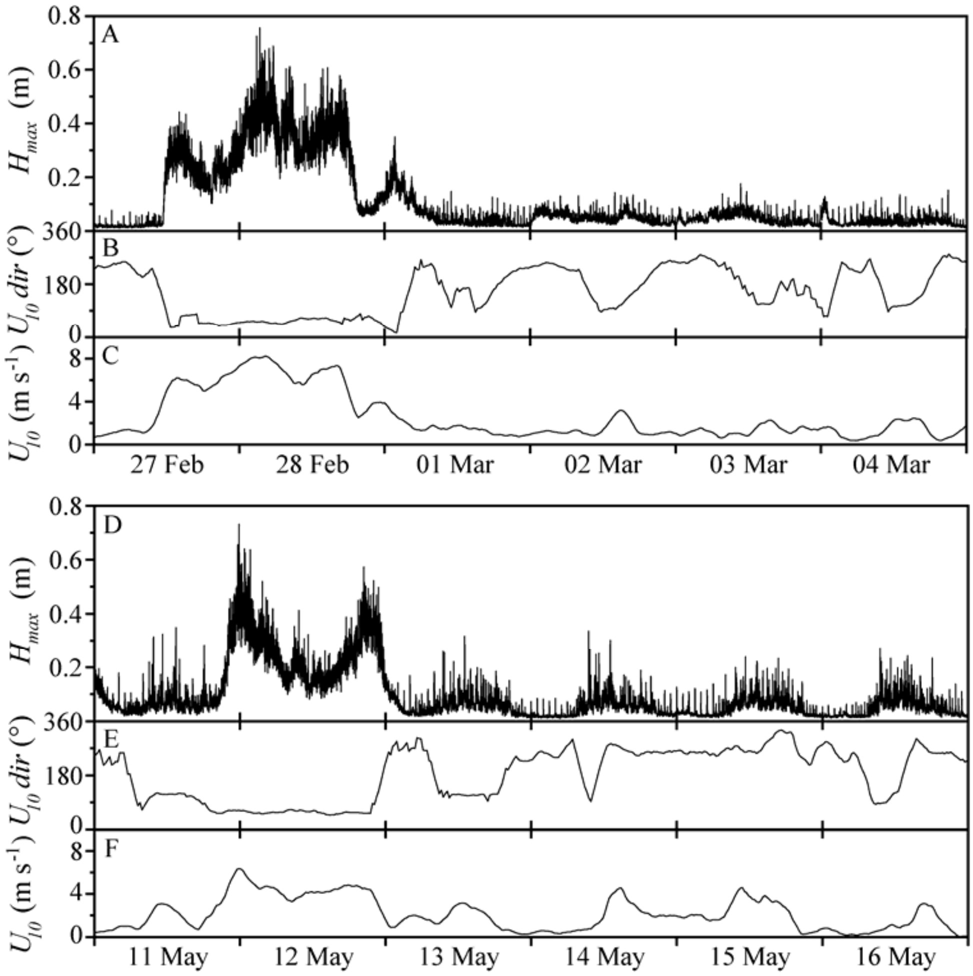

Fig. 2.6 Maximum wave height (H_{max}) and related wind direction (U_{10} *dir*) and speed (U_{10}). (A-C) In winter (27 February to 04 March 2005). (D-F) In summer (11-16 May 2005). Both periods include one major wind event and several windless, ship-wave-dominated days.

A new catamaran passenger ferry was introduced at Lake Constance for fast connection between Friedrichshafen (10 km to the north of site LA; Fig. 2.1A) and Konstanz in July 2005. Between 06:00 and 21:00 h, the catamaran ferry cruises hourly between the two cities during the whole year. Although the catamaran track is more than 10 km away from the study site, catamaran waves can be distinguished from the other wave types by spectral analysis (Fig. 2.4). The catamaran waves typically have heights of a few centimeters at site LG. The wave periods and deep-water wave lengths of the catamaran waves are about 6.3 s and up to 50 m, respectively. The much longer wave lengths generated by the catamaran compared to the other two ship types implies that shoaling of the catamaran waves has a larger impact on the nearshore region than that of other ship waves with the same wave height. However, this effect is more important at other sites in Lake Constance, where the catamaran waves have larger wave heights than at the site LG.

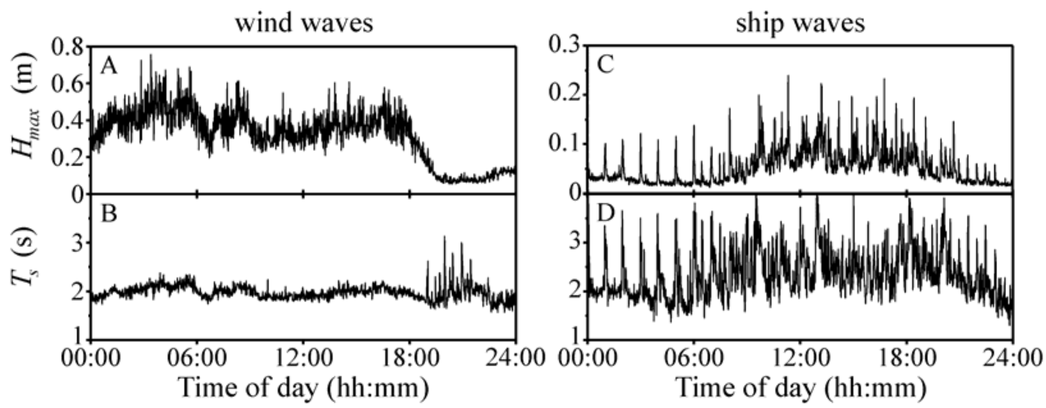

Fig. 2.7 Course of the maximum wave height (H_{max}) and significant period (T_s) during a single day. (A,B) Wind-wave-dominated day in winter on 28 February 2005. (C-D) Ship-wave-dominated day in summer on 15 May 2005.

The observed characteristic wave periods, lengths, and heights are related to the specific properties of the three dominating ship types at Lake Constance (e.g., length, width, displacement mass, speed, shape or the distance of the sailing line to the shore). Most of these properties are summarized in Table 2.1. Empirical relations describe and approximate wave characteristics (e.g., wave period and height) from ship properties (Sorensen 1973; Stumbo 1999; Maynord 2005). Ferries and passenger ships at Lake Constance do not differ significantly in their properties compared to the catamaran. The main differences between the ferries, passenger ships, and the catamaran on Lake Constance are not primarily the shape but the traveling speed (Table 2.1) and the distance to shore at which they pass the site LG. The wave period of the catamaran waves is about twice the period of the waves generated by the ferries or the passenger ships. The height of ship-generated waves decreases with distance from the sailing line (Sorensen 1973; Bhowmik 1975; Stumbo 1999). This effect contributes to the differences in the wave heights between passenger-ship, ferry, and catamaran waves observed at LG because the distance of the sailing lines of these ships from LG are 1-2 km, 2-3 km, and about 10 km, respectively.

Table 2.1 Characteristics of commercial ships operating regularly on Lake Constance.

Ship type	Length (m)	Width (m)	Displacement mass x 10^3 (kg)	Speed (km h^{-1})	Passengers	No. of ships
Ferries	55 - 72	12 - 13	340 - 900	22 - 24	500 - 700	9
Passenger ships	20 - 62	4 - 13	50 - 510	20 - 28	50 - 1,200	~60
Catamaran	33.6	7.6	60	40	182	3

Wave statistics: The relative importance of wind and ship waves

Since wind and ship waves can be distinguished by frequency (period) their relative importance can be quantified in terms of monthly wave distribution and wave energy flux to shore during the whole year 2005 (Fig. 2.8). To express not only the seasonal but also the diurnal pattern of the wave distribution, daytime and nighttime are considered separately (Fig. 2.8A,B).

During daytime, the overall proportion of the number of waves greater than 0.05 m is significantly higher in summer (March-October) than in winter (November-February), ranging from 44-89% and 23-40%, respectively (Fig. 2.8A). This increase in the number of waves ≥0.05 m from winter to summer is caused by ship waves. Whereas the proportion of wind waves remains almost constant throughout the whole year and accounts for 11-37% of the total number of waves during the day, the proportion of ship waves increases significantly in summer and amounts from 24% in March to 58% in August of the total number of waves. The seasonal pattern of ship waves from March to October follows the 'tourist cruise-ship season' of passenger ships. In winter, the proportion of ship waves accounts only for 9-14% of the total number of waves.

The total number of waves ≥0.05 m during nighttime (10-31%) is much lower than during daytime (Fig. 2.8B) and does not show a seasonal pattern. This is mainly due to the near absence of ship waves during nighttime, when ship waves contribute only 4-12% of the total number of waves. Passenger ships do not cruise at night. The remaining ship waves stem from the ferry crossing from Meersburg to Konstanz-Staad and occasional leisure boats.

The large difference in the number of ship waves between daytime and nighttime causes the pronounced diurnal pattern. The missing percentage to 100% in Figure 2.8A,B represents waves below 0.05 m. These small waves are dominant especially during winter and at night, when they contribute between 60-77% and 69-90% of the total number of waves, respectively.

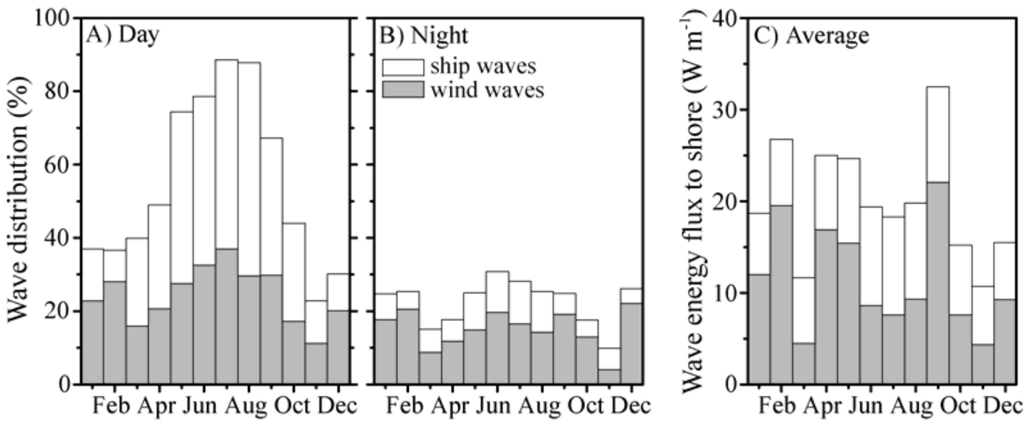

Fig. 2.8 Wave statistics. Relative wave distribution according to origin: wind-generated (gray bars) or ship-generated (open bars) and time (day: 09:00-21:00 h and night: 21:00-09:00 h) in 2005. (A) At day. (B) At night. (C) Average monthly wave energy flux to shore (E_F) of wind and ship waves in 2005. Wave heights below 0.05 m were excluded from the data sets (A-C), and are expressed by the missing percentage to 100% (A,B).

The wave energy flux to shore follows the seasonal pattern caused by passenger ships with highest energy fluxes between June and September, although both daytime and nighttime are considered together (Fig. 2.8C). In summer, the monthly mean wave energy flux was about 9 W m^{-1} (minimum of about 7 W m^{-1} in March and maximum of about 11 W m^{-1} between June and September), compared to about 6 W m^{-1} in winter (Fig. 2.8C). Note that the mean wave energy flux of ship and wind waves does not exactly reflect the pattern of their number of occurrence (Fig. 2.8) because the energy flux depends on wave height as a measure of wave energy and also on wave length affecting the group velocity. Note also that the wave energy flux due to ship waves is larger than that due to wind waves of the same height because at site LG ship waves have a larger wave length than wind waves.

The proportion of the annual mean wave energy flux caused by wind waves is about 50%, compared to 41% of ship waves (Fig. 2.8C), and only about 9% account for waves with heights below 0.05 m. During the main navigation period in summer, ship waves contribute about 50%, and in winter about 35% to the total wave energy flux to shore.

Apart from the seasonal pattern caused by ship waves, the monthly wave energy flux to shore is highly variable, which can be explained mainly by the irregular occurrence of wind-wave events. High wind events are responsible for the high values in February and September, and the absence of high winds explain the low values in March, October, and November (Fig. 2.8C).

Another measure of the wave forcing in the littoral zone is the maximum near-bottom current velocity (u_{max}) generated by the waves. Figure 2.9 shows a comparison of the relative monthly frequency distributions of u_{max} generated by wind and ship waves, respectively. The distributions reveal a clear difference between winter (January and February; Fig. 2.9A,B) and summer months (July and August; Fig. 2.9C,D). In winter, especially for u_{max} values exceeding 0.1 m s^{-1}, wind waves are dominant. In summer, the situation is the opposite, and ship waves are dominant even at high u_{max} values. Turbidity measurements suggest that at the study site LG near-bottom current velocities above 0.1 m s^{-1} are required to cause resuspension. Considering a water depth of 1 m the threshold of $u_{max} > 0.1$ m s^{-1} is exceeded by ship waves, especially in summer (Figs. 2.2B, 2.9C,D).

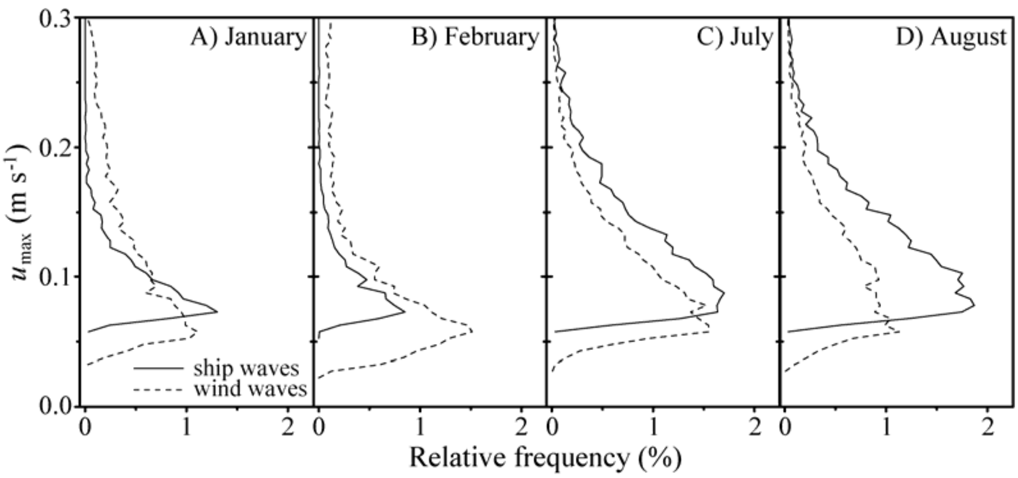

Fig. 2.9 Relative monthly frequency distribution of the maximum near-bottom current velocity at 1 m water depth generated by wind waves (dashed line) and ship waves (solid line) at the study site Littoral Garden (LG). (A,B) In January and February, representative of the winter months. (C,D) In July and August, representative of the summer months. Wave heights below 0.05 m were excluded from the data sets. The frequency distribution step size of u_{max} is 0.005 m s^{-1} throughout all data sets. The relative frequency distributions of wind and ship waves are normalized by the total number of burst intervals (~1.1 min) counted in the specific month.

Comparison to other sites and lakes

The wave field at site LG can be regarded as characteristic and representative for most of the southern and southwestern shores at Lake Constance. Along these shores the exposure to wind waves can be expected to be similar. However, the wave heights of the wind waves, which are also determined by the effective fetch lengths, can change slightly from site to site. The exposure to ship waves is similar at all shores because passenger ships travel all around Lake Constance, and ferries travel not only at the ferry crossing Meersburg to Konstanz-Staad but also across the center of Upper Lake Constance between Friedrichshafen (northern shore, Germany) and Romanshorn (southern shore, Switzerland). The ferries are of similar type and have similar timetables (Table 2.1). Hence, a large proportion of the shores at Lake Constance are highly influenced by a ship-wave-dominated wave field.

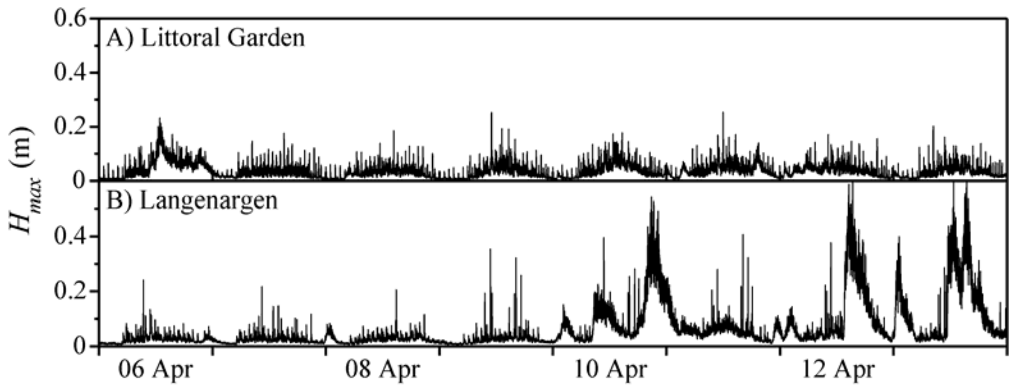

Fig. 2.10 Course of the maximum wave height (H_{max}) at two different sites between 06 and 13 April 2006. (A) At the study site Littoral Garden (LG), exposed to northern and northeastern winds. (B) At the study site Langenargen (LA), exposed to western winds.

To compare the wave conditions at the southern shore of Lake Constance with shores that are exposed to western winds, an additional PS was deployed at a site next to LA (Fig. 2.1A). Between 06 and 13 April 2006, pressure data were collected simultaneously at the stations LG and LA. Figure 2.10 compares the maximum wave heights during this period at both sites. The main difference between the two time series is due to the exposure to wind. When wind waves occur at site LG (e.g., 06 April; Fig. 2.10A), no wind-wave event can be observed at site LA (Fig. 2.10B) and vice versa. Wind-wave events at site LA seem to be stronger and more frequent than at site LG. When no wind is present, the wave field is dominated by ship waves, and the characteristic diurnal cycle can be observed at both sites. At site LA, which is typical for shores exposed to western winds at Lake Constance, the importance of ship waves in terms of frequency of occurrence and wave height appears to be somewhat lower than at site LG. However, ship waves play still an indisputable role for the overall wave field and the wave energy flux to shore.

The situation at Lake Constance, where ship waves contribute to a large extent to the wave field and hence the wave energy flux to shore, is representative for many prealpine and alpine lakes in Germany and Switzerland. Because of their morphometric characteristics and geographical exposure (e.g., high length-to-width ratio and shelter of the lake surface from high wind speeds by steep mountain slopes), these lakes have rather short effective fetch lengths and are typically exposed to low wind speeds limiting the wind-generated wave field. On the other hand, these lakes are typically located in highly populated areas with diverse recreational and commercial activities that lead to intensive ship traffic on the lakes. Examples for lakes that have a similar characteristic as Lake Constance are e.g., Lake Ammer, Lake Starnberg, and Chiemsee in Germany and Lake Zurich and Lake Lucerne in Switzerland. The types and characteristic properties of passenger ships cruising on these lakes are comparable to those operating on Lake Constance (Table 2.1, except the catamaran). Hence, it can be expected that on these lakes, ship waves significantly contribute to the overall wave field. However, detailed measurements are still required to confirm this hypothesis.

Forcing and disturbances by ship waves in the littoral zone

The littoral zone of a lake is a highly productive and diverse habitat the abiotic conditions of which are determined by, for example, the substrate structure and distribution, the light climate, the nutrient availability, and the prevailing temperature regime. These factors and mechanisms are influenced by hydrodynamic processes. The strongest forcing and main disturbances are generated by surface waves. Since ship waves can amount to nearly half of the annual mean wave energy flux to shore at Lake Constance, the overall hydrodynamic forcing in the littoral zone is significantly enhanced by ship traffic. In addition, ship waves affect the ecosystem at much larger depths than wind waves of the same amplitude because of the differences in wave length. For a given wave height and water depth, the maximum wave-generated near-bottom current velocity is determined by the wave length (Eqs. 2.6 and 2.7; Kundu and Cohen 2002). Hence, ship waves having longer wave lengths than wind waves potentially affect a much wider part of the littoral zone. Seasonal water level fluctuations amplify the wave-generated resuspension by exposing different sections of the littoral zone to wave forcing.

Whereas wind waves occur rather sporadically, ship waves can be considered as a frequent hydrodynamic forcing in the littoral zone, at least during daytime in summer (Figs. 2.6D, 2.7C, 2.8A, 2.10, 2.11A). Hence, ship and wind waves generate a considerably different pattern of disturbance that may have different consequences for the littoral ecosystem.

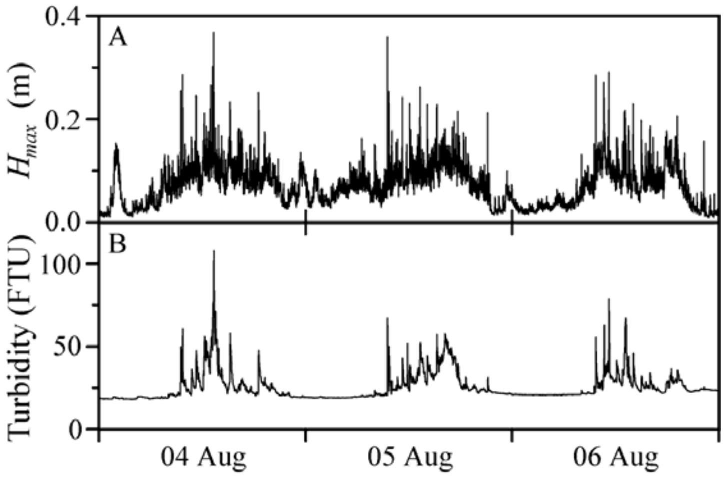

Fig. 2.11 Wave-generated resuspension. Time series of (A) maximum wave height (H_{max}) and (B) turbidity (optical backscatter strength in FTU) at the study site Littoral Garden (LG) on three consecutive days (04-06 August 2005). The turbidity was measured 0.2 m above the bottom at ~1 m water depth.

A major effect of hydrodynamic disturbances in the littoral zone is sediment resuspension and transport. Our analysis revealed that ship waves dominate the frequency distribution of u_{max} in summer (Fig. 2.9C,D), which indicates their potential for resuspension. The direct relation between the occurrence of ship waves and suspended particle concentration measured in terms of optical backscatter strength (turbidity) is exemplified in Figure 2.11. At daytime, distinct peaks in H_{max} generated by ship waves are correlated with peaks in turbidity, which makes it evident that the occurrence of ship waves cause resuspension. Further, ship waves cause an overall increase in turbidity at day time, which creates a diurnal cycle with high values at daytime and low at night (Fig. 2.11B). The periodic and regular occurrence of ship waves possibly prevents sediment consolidation and the development of a cohesive upper sediment layer (Dyer 1986; Schoellhamer 1996). The absence of a cohesive upper sediment layer increases the probability of resuspension and leads to strong impulse loads of suspended sediment in the water column mediated by ship waves (Schoellhamer 1996; Lindholm et al. 2001) and hence reduces water transparency (van Duin et al. 2001) and increases turbidity (Fig. 2.11B). Because ship waves are most frequent during daytime, they particularly affect the availability of light for primary production of phytoplankton and biofilms in the littoral zone. Utne-Palm (2004) showed that turbid water during daytime affects hunting success of fish and may even contribute to a competitive advantage of non-visually compared to visually orientated predators (Schleuter and Eckmann 2006). There is evidence that the specific wave exposure influences the community structure of benthic organisms and fishes (Scheifhacken 2006; Schleuter 2006). Furthermore, ship waves limit or even suppress the growth of macrophytes and biofilms (Eriksson et al. 2004; Francoeur and Biggs 2006). These effects are enhanced by their frequent occurrence, especially during summer.

The interactions between surface waves, the abiotic conditions, and the biota in the littoral zone are difficult to assess in the field. The regular and 'scheduled' occurrence of ship-generated waves, however, provides an ideal natural environment to study the ecological effect of surface waves on the littoral ecosystem in greater detail.

Acknowledgments

We thank Georg Heine and his colleagues from the electronic and mechanical workshop at the University of Konstanz for technical assistance and for the development of the pressure sensors. We gratefully acknowledge the help of the technical staff at the Limnological Institute and the ISF Langenargen. Helpful and valuable comments of the two anonymous referees improved the manuscript. This work was supported by the German Research Foundation (DFG) within the framework of the Collaborative Research Center 454 'Littoral Zone of Lake Constance'.

Chapter 3

Wave-induced resuspension in the littoral zone of a large lake

HILMAR HOFMANN, ANDREAS LORKE AND FRANK PEETERS

Water Resources Research **in revision**

Abstract

Sediment resuspension in lake littoral zones is strongly related to the properties of the surface wave field. Synchronized, high-resolution measurements of wave parameters, near-bottom current velocities, and suspended sediment concentrations were analyzed over a time period of a year. Wind and ship waves are distinguished based on their spectral properties, enabling a detailed investigation of their respective importance for sediment resuspension. In the littoral zone of Lake Constance, resuspension was observed during 33% of the entire observational period. Thereof, 58% is caused by ship waves, which are of similar importance as wind waves. Whereas resuspension induced by wind-generated waves occurs rather sporadically throughout the year, resuspension induced by ship waves occurs regularly during daytime in summer and is hence associated with pronounced diurnal and seasonal patterns in the suspended sediment concentration.

Introduction

Sediment resuspension on continental shelves (e.g., Dyer 1986; Nielson 1994; Lou et al. 1999), in estuaries (e.g., Roman and Tenore 1978; Hamblin 1989; Rolinski 1999), rivers (e.g., Garrad and Hey 1987; El Ganaoui et al. 2004), and lakes (e.g., Luettich et al. 1990; Hawley and Lesht 1992; Lesht and Hawley 2001; Håkanson 2005) and their corresponding driving forces (e.g., tidal currents, surface waves, and wave-current interactions) have been intensively studied.

Resuspension and re-allocation of particles primarily changes the sediment structure (consolidated/unconsolidated) but also causes varying abiotic and biotic habitat conditions for the growth of phytoplankton, biofilms, and macrophytes by, for example, nutrient release (Søndergaard et al. 1992; Güde et al. 2000), oxygenation of the sediment-surface layer (Precht and Huettel 2003; Precht et al. 2004), or a change in the light climate (Pierson et al. 2003; Erm and Soomere 2006).

In the littoral zone of small and large lakes, surface waves are the most important cause of resuspension. The characterization of surface waves, however, is mainly based on studies in marine and shelf regions (e.g., Madsen 1976; Le Blond and Mysak 1978; Komen et al. 1996), where waves are generated by strong and steady winds over long fetch lengths. In most lakes winds are infrequent and unsteady, wind speeds are low, and the effective fetch is limited to a few kilometers. Thus, wind-generated waves in lakes are characterized by small amplitudes, high frequencies, and short wave lengths (Hofmann et al. 2008a) and differ considerably from the waves in the ocean. Because of the short wave lengths of wind-generated waves in lakes their potential for resuspension is smaller than of wind-generated waves in the ocean.

In addition to wind-generated waves, commercial and tourist ship traffic causes ship-generated waves. The properties and importance of ship waves have been investigated in rivers and channels (e.g., Sorensen 1973; Garrad and Hey 1987; Bhowmik et al. 1991), in ocean shelf regions and harbors (e.g., Stumbo 1999; Parnell and Kofoed-Hansen 2001; Soomere and Engelbrecht 2005), and in lakes (e.g., Bhowmik 1975; Maynord 2005; Hofmann et al. 2008a). The specific generation of wind and ship waves results in considerably different wave frequencies and lengths, which allow to discriminate both types of waves in measurements (Hofmann et al. 2008a). The different properties of ship waves are associated with different implications for resuspension and ecological consequences in the littoral zone (e.g., Bauer et al. 2002; Eriksson et al. 2004; Soomere 2005; Erm and Soomere 2006).

Wind- and ship-wave induced sediment resuspension is solely considered separately: wind-wave induced resuspension by e.g., Hawley and Lesht (1992), Kristensen et al. (1992), Luettich et al. (1990), and Vittori (2003) and ship-wave induced resuspension by e.g., Lindholm et al. (2001), Parchure et al. (2001), and Schoellhamer (1996). The purpose of the present study is to fill this gap by analyzing a one-year long record of continuously and simultaneously measured surface wave properties and suspended sediment concentrations in the littoral zone of a lake where both types of waves are equally important.

First we provide a short introduction to the study site, which is followed by a description of the experimental setting, the sediment properties, the calibration of the optical and acoustical backscatter strength, and the data analysis methods. Thereafter, the data and observed patterns of wind- and ship-wave induced resuspension with their relative importance are presented in the results section. Then, the experimental results are discussed with special emphasis on the potential for resuspension of ship and wind waves and the consequences of the wave-induced disturbances for the ecosystem littoral zone. The conclusion section summarizes the main results of this study.

Materials and methods

Study site

Lake Constance, the second largest (by surface area, 536 km^2) prealpine lake in Europe, is located in the southwest of Germany. The littoral zone, where most of the energy of the surface waves is dissipated, covers about 10% of the total surface area (Braun and Schärpf 1990).

Measurements were carried out in the western part of Upper Lake Constance at a site called Littoral Garden (LG; 47°41’29’’N, 09°12’11’’E) (Fig. 3.1A). The study site is exposed to a highly variable surface wave field that is characterized by wind and ship waves (Hofmann et al. 2008a). Ship waves stem from a close by ferry track with regular sailings throughout the year, from passenger ships traveling parallel to the shore between middle of March and middle of October, and from a catamaran ferry. The littoral zone is shelf-like structured and slopes gently over a length of about 60 m before it drops rapidly. The shallow part (0-1 m water depth) of this cross-section is characterized by gravel-cobble like stones, sand and silt, and the deeper part (1-2 m water depth) by sand, silt and clay.

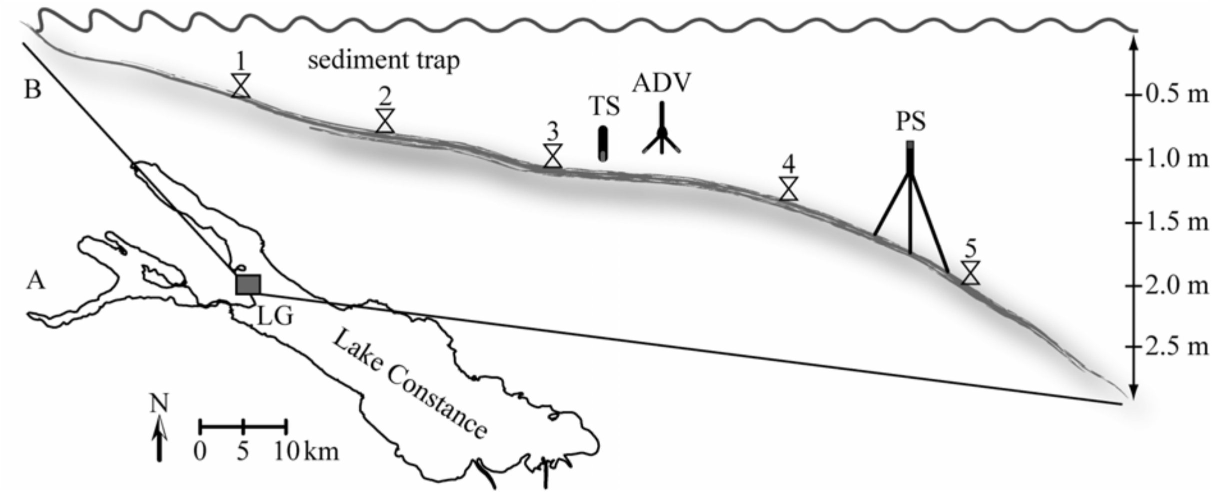

Fig. 3.1 Study site and instrumentation. (A) Map of Lake Constance. The square indicates the section of the study site Littoral Garden (LG). (B) Cross-section of the study site LG with all instruments: Pressure sensor (PS), acoustic Doppler velocity meter (ADV), turbidity sensor (TS), and sediment traps (ST 1-5).

Wave and current velocity measurements

The surface wave field and wave-generated near-bottom current velocities were studied using a pressure sensor (PS) and a NORTEK Vector Acoustic Doppler Velocity Meter (ADV). Both instruments were deployed between August 2005 and July 2006 along a cross-shore transect at water depths of about 2 m (PS) and 1-3 m (ADV), respectively (Fig. 3.1B). The position of both instruments was adjusted to compensate for seasonal water level fluctuations of about 2-3 m (Jöhnk et al. 2004; Hofmann et al. 2008a).

The custom made PS has a full-scale range of 7 m, an accuracy of 0.1 mbar, and a maximum stand-alone deployment time of 45 d. The sensor was always positioned 1 m above the bottom and about 1 m below the surface. Pressure measurements were made at a sampling frequency of 16 Hz during the entire deployment period. Sensor malfunction caused a data gap in February 2006. The measured time series of subsurface pressure was converted to a time series of surface elevation following the procedure described by Hofmann et al. (2008a). Maximum and significant wave heights (H_{max}, H_s) and significant period (T_s) were estimated for segments of 1,024 (~1.1 min) samples by using the zero-upcrossing method (IAHR 1989; Hofmann et al. 2008a).

The ADV and the data acquisition system were attached to a bottom-resting tripod. The sensor head was looking downward with its sampling volume located 0.05 m above the bottom. The near-bottom current velocities were measured within a range of ±0.3 m s^{-1} with an accuracy of 10^{-3} m s^{-1} and a sampling frequency of 8 Hz. The two measured horizontal components of the current velocity were rotated into a cross-shore and along-shore component, where the cross-shore component was used for all subsequent calculations and statistical analyses.

Suspended sediment measurements

Measurements of the suspended particles were carried out using an optical backscatter sensor (turbidity sensor (TS), Driesen & Kern) and by evaluating the acoustical backscatter strength recorded by the ADV. The TS was attached to the tripod at a height of 0.2 m above the bottom (Fig. 3.1B) between August and October 2005. Turbidity was measured with an accuracy of 0.01 FTU and at a sampling frequency of 0.1 Hz. Measurements of the acoustical backscatter strength (ADV) are available for the entire deployment period of the ADV (see above). The received echo intensity is recorded by the ADV in terms of counts, which are linearly related to acoustic power measured in dB (logarithmic scale).

The suspended sediment concentrations (SSC) can be measured by optical as well as by acoustical sensors in terms of backscatter strength. The calibration, application, and limitations of these methods are extensively discussed (Lynch et al. 1994; Holdaway et al. 1999; Fugate and Friedrichs 2002; Voulgaris and Meyers 2004). Here, the optical and acoustical backscatter strengths were calibrated against SSC measured in water samples (5 L) collected near the TS and the ADV sampling volume. Samples were collected on the 03 and 16 August 2005, when the wave field was dominated by ship waves, and on the 18 September 2005 during a strong on-shore wind. The samples were vacuum pumped using 0.45 µm GF 6 Schleicher & Schuell glass fiber filters and then dried at 105°C for 24 h. Mass difference between the packed and the empty filter was used to calculate the suspended sediment concentration SSC (mg L^{-1}). The set of samples covers varying forcing conditions for resuspension (wind and ship waves), and thus compensates for possible uncertainties of the optical and acoustical backscatter measurements arising from changing size distributions and flocculation of the particles (Thevenot and Kraus 1993; Lynch et al. 1994; Fugate and Friedrichs 2002; Voulgaris and Meyers 2004). The calibration equations were established by fitting a linear model to the optical backscatter strength and an exponential model (ADV) to the acoustical backscatter strength and the SSC (Fig. 3.2). Afterwards the measured optical and acoustical backscatter strengths were converted into SSC based on the calibration equations shown in Figure 3.2.

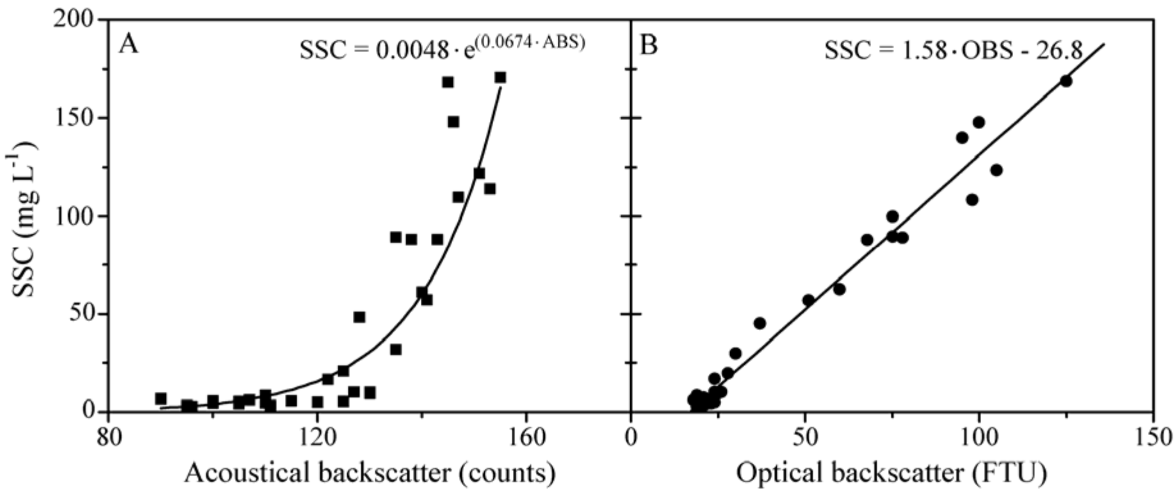

Fig. 3.2 Calibration experiment. Relation of the acoustical (ABS) (A) measured by an ADV and the optical backscatter strength (OBS) (B) measured by a turbidity sensor (TS) to the sampled suspended sediment concentration (SSC).

Characterization of the sediment

Sediment traps

Sedimentation rates of organic and inorganic material were measured by 5 cylindrical sediment traps deployed evenly distributed along a transect perpendicular to shore in the shallow littoral (water depths: 0.5-2.2 m) at the study site LG between August 2005 and July 2006 (Fig. 3.1). The specific deployment periods varied between 5 d and 6 weeks. The sediment traps had a diameter of 0.05 m and the opening of the cylinder was 0.25 m above the bottom. Sediment samples were dried at 105°C for 24 h and the dry weight and the resulting sedimentation rate per day and square meter were calculated. The amount of organic material (fraction) in the sediment samples was estimated as the ignition loss after the exposure in a muffle furnace (HERAEUS) at 550°C over 8 h. The mass of sediment remaining after exposure in the furnace is considered as inorganic material (fraction) (Ball 1964; Guy 1969).

Grain size distribution

The grain size distribution in water samples, sediment traps, and surface sediments was measured by the high-resolution laser particle size analyzer Saturn DigiSizer 5200, providing size distributions in the range between 0.001-1 mm with an accuracy of 3%. Note that only inorganic particles, which aggregate much less than organic particles, can be measured accurately with this technique. Therefore, all samples were ignited in a muffle furnace (see above) so that only the inorganic fraction was analyzed.

Figure 3.3 shows typical particle size distributions measured in water samples and in samples from the sediment traps. The mean grain size (d_{50}) of particles in the sediment traps and suspended in water samples at the study LG was estimated from the measured grain size distributions following Dyer (1986) to $d_{50} = 0.06$ mm.

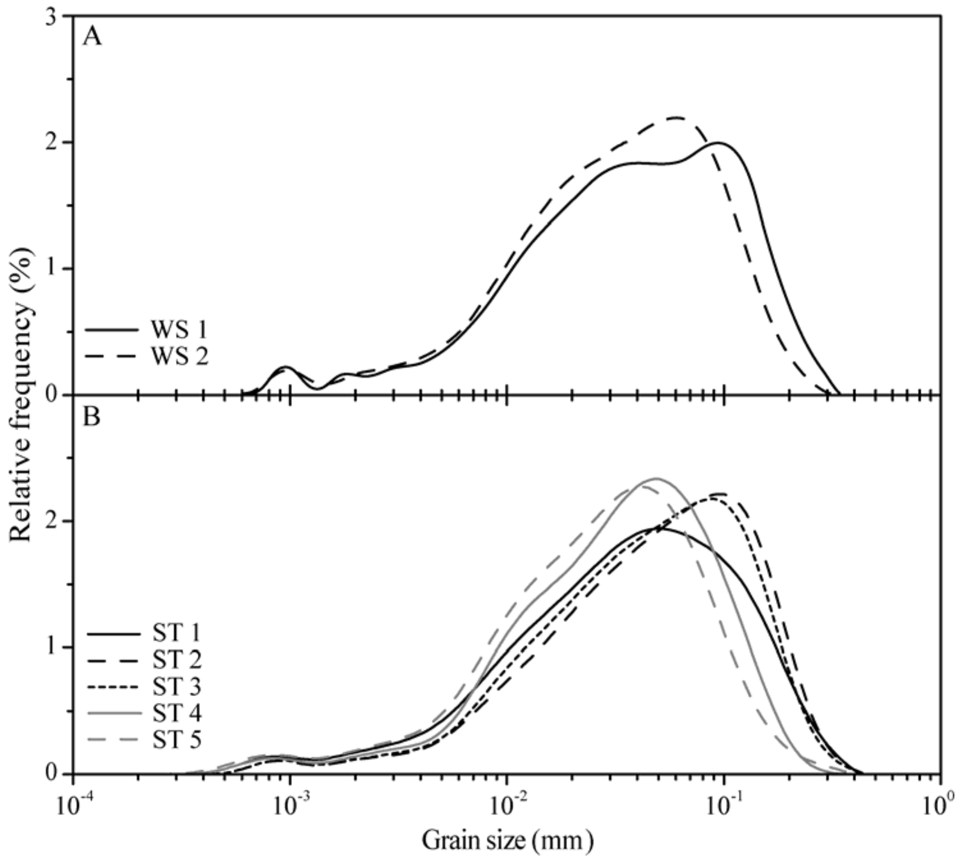

Fig. 3.3 Typical grain size distributions of suspended particles in the shallow littoral. (A) Water samples (WS) collected during the passage of a single ship-wave group at 1 m water depth. The solid line (WS 1) gives the grain size distribution at the maximum of the wave-generated current velocity, and the dashed line (WS 2) 30 s afterwards. (B) Sediment traps deployed 0.25 m above bottom at 0.5 m (ST 1, solid black line), 0.7 m (ST 2, dashed black line), 0.9 m (ST 3, short dashed black line), 1.2 (ST 4, solid gray line), and 1.9 m (ST 5, dashed gray line) water depth.

Sediment density

The sediment density ρ_s (kg m^{-3}) was experimentally determined with a pycnometer as described in (IFM-GEOMAR 2005). For this purpose, sediment samples were taken from the sediment top layer (1-2 cm) and from the sediments collected in sediment traps. The samples were dried at 105°C for 24 h, disaggregated, homogenized, and weighted. The sediment density was calculated from the ratio between the mass of the sediment sample and the displaced volume in the pycnometer.

The particles in the top layer of the sediments, collected near the sediment traps, TS, and ADV had a density between 2,500 and 2,600 kg m^{-3}. These particles are potentially available for resuspension. The particles collected in the sediment traps, however, had a density between 2,000 and 2,200 kg m^{-3}.

Statistics on wave-generated current velocities and suspended particles

The wave-generated maximum near-bottom current velocity $u_{max,\,ADV}$ and SSC measured by the ADV was calculated for burst intervals of 1 min and 30 min. Within each burst, $u_{max,\,ADV}$ is defined as the mean of the 1% largest current velocities and SSC as the mean of all samples.

The sediment resuspension potential of wind and ship waves was estimated from the distribution of their associated maximum near-bottom current velocity $u_{max,\,PS}$ calculated from the wave parameters of the PS (Brown et al. 2005):

$$u_{\max,\,PS} = \frac{\pi \cdot H}{T \cdot \sinh \frac{2 \cdot \pi \cdot h}{\lambda}} \qquad (\mathrm{m\ s^{-1}}) \qquad (3.1)$$

where H denotes the wave height (m), T the wave period (s), h the water depth (m), and λ the wave length (m). H_{max} and T_s are estimated from the PS and λ is calculated as a function of T_s using the dispersion relation provided by Fenton and McKee (1990). Here, $u_{max,\,PS}$ is considered at a water depth of 1 m. Thereby we assumed that H_{max} and T_s do not change significantly between 1 and 2 m water depth. $u_{max,\,PS}$ is calculated for each wave-burst interval (~1.1 min) and classified as wind-wave or ship-wave generated using the procedure outlined in Hofmann et al. (2008a), where wind and ship waves are distinguished by their respective periods. Wind-generated waves are characterized by wave periods below 2.5 s, whereas ship-generated waves have periods above 2.5 s. Further, we distinguished between daytime (09:00-21:00 h) and nighttime (21:00-09:00 h). Waves that generate $u_{max,\,PS}$ values below 0.08 m s^{-1} are excluded from the statistical analysis because these low $u_{max,\,PS}$ values are not able to cause significant resuspension at the study site LG (see below).

The usage of $u_{max,\,PS}$ for the statistical analysis is affirmed by the comparison of the measured (ADV) and calculated (PS) maximum near-bottom current velocity ($u_{max,\,ADV}$ and $u_{max,\,PS}$) at about 1 m water depth during August 2005 (Fig. 3.4). The scatter plot reveals a good correlation, although the estimates for $u_{max,\,PS}$ are slightly higher, especially for u_{max} values that are near the upper limit of the ADV measurement range (±0.3 m s^{-1}). Possible reasons for this difference are slightly incorrect wave parameters or water level fluctuations during the period of consideration.

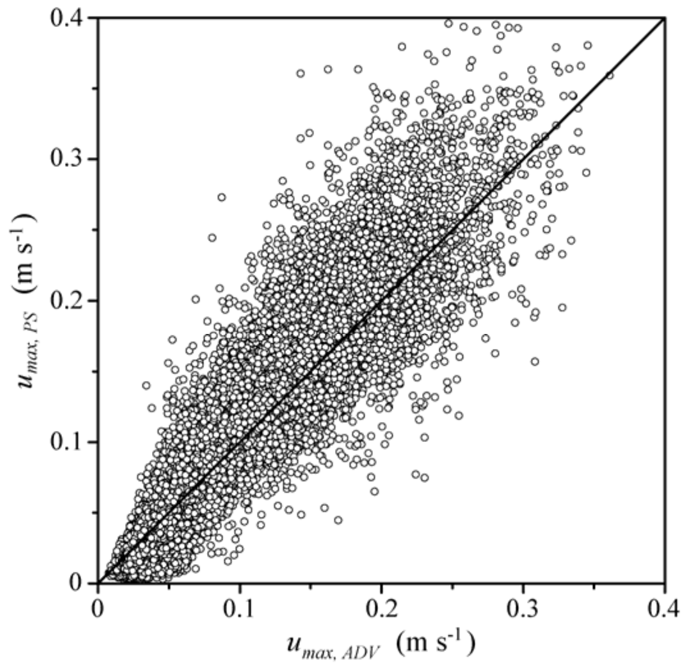

Fig. 3.4 Comparison of the measured ($u_{max,\,ADV}$) and calculated ($u_{max,\,PS}$) maximum near-bottom current velocities at about 1 m water depth during August 2005. Each open circle represents a 1 min time period. The black line indicates the 1:1 relation.

The remobilization of particles under oscillatory flow due to surface waves can be determined from empirical equations. For non-cohesive sediments with a mean grain size d_{50} between 0.063 and 2 mm (sand fraction) the appropriate threshold flow velocity $u_{max,\,res}$ is (Hallermeier 1980; CERC 2002):

$$u_{\max,\,res} = \sqrt{8 \cdot \left(\frac{\rho_s}{\rho_w} - 1 \right) \cdot g \cdot d_{50}} \qquad (\mathrm{m\ s^{-1}}) \qquad (3.2)$$

where d_{50} is the mean grain size (m), g the gravitational acceleration (m s^{-2}), ρ_s the sediment density (kg m^{-3}), and ρ_w the density of water (kg m^{-3}). At the study LG suspended sediment has a density ρ_s of ~2,200 kg m^{-3} and a mean grain size d_{50} of ~0.06 mm. Following Eq. 3.2 the appropriate threshold flow velocity at the study site LG to initiate the remobilization of particles is about 0.08 m s^{-1}.

Results

Patterns of wave-induced resuspension

Surface waves can cause near-bottom current velocities that are sufficient to induce resuspension and increase the load of suspended particles in the water column. At the study site LG, wind as well as ship waves could be observed (Hofmann et al. 2008a). Figure 3.5 exemplifies the dynamics of the near-bottom current velocity and the acoustical backscatter strength measured by the ADV during the passage of a ship-wave group on 13 August 2005 (Fig. 3.5A) and during a strong on-shore wind event on 16 August 2005 (Fig. 3.5B). Whereas the oscillating currents associated with the wind and ship waves have comparable amplitudes of about ±0.3 m s^{-1}, the acoustical backscatter strength shows a different pattern for wind and ship waves.

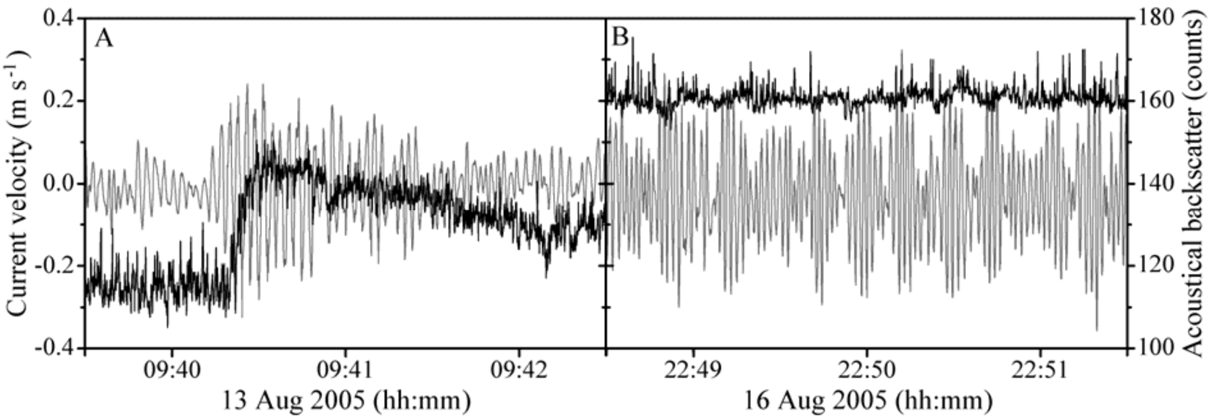

Fig. 3.5 Near-bottom current velocity in cross-shore direction (gray line) and the acoustical backscatter strength (black line) measured simultaneously by an ADV at about 1 m water depth. (A) During the passage of a ship-wave group on 13 August 2005. (B) During a strong on-shore wind event on 16 August 2005.

During the passage of ship waves, the acoustical backscatter strength increases drastically within seconds as soon as the current velocity exceeds the determined threshold velocity of about 0.08 m s^{-1}. After, the acoustical backscatter strength remains at a maximum value before it decreases slowly within minutes to its previous level (Fig. 3.5A) due to settling and horizontal transport. During the on-shore wind event on 16 August 2005, the acoustical backscatter strength remains at a very high level because continuously high current velocities prevent particle settling. The continuously high backscatter strength suggests that an equilibrium between resuspension, settling, and transport of particles is reached.

The times series of the maximum near-bottom current velocity measured by the ADV ($u_{max,\,ADV}$) and the SSC derived from the acoustical and the optical backscatter strengths are shown in Figure 3.6. These time series represent typical patterns of resuspension at the study site LG during a time period with no wind on 12 and 13 August 2005 (Fig. 3.6A-C), where ship waves dominated the wave field, and during a time period with strong on-shore wind on 16 and 17 August 2005 (Fig. 3.6D-F). During both time periods, the SSC derived from the acoustical and optical backscatter strengths agree very well, although short-term peak values of SSC derived from the optical backscatter strength are slightly lower than those derived from the acoustical backscatter strength because of the lower temporal resolution of the TS (0.1 Hz) compared to the ADV (8 Hz) (Fig. 3.6B,C, E,F). During the summer months, when on-shore wind events are rare, the SSC often shows a distinct diurnal cycle with low values (0-5 mg L^{-1}) during nighttime and high values (50-150 mg L^{-1}) during daytime (Fig. 3.6B,C). The diurnal cycle in SSC is highly correlated with the diurnal cycle in the magnitude of $u_{max,\,ADV}$ (Fig. 3.6A-C). The maximum values of $u_{max,\,ADV}$ during daytime (0.15-0.35 m s^{-1}) are mainly caused by waves from passenger ships that pass by the study site (Hofmann et al. 2008a). Since resuspension increases with increasing $u_{max,\,ADV}$, the passenger ships contribute to the elevated SSC during daytime. In addition, during daytime the more intense ship traffic causes frequent events of ship-wave induced resuspension such that particle settling between two consecutive events is too slow to remove the particles completely introduced by the previous event. Hence, during daytime resuspension of particles exceeds the loss due to settling and horizontal transport, leading to an increasing concentration of suspended particles in the water column.

During periods of moderate and strong on-shore wind, which occur rather infrequently at the study site LG (Hofmann et al. 2008a), $u_{max,\,ADV}$ and SSC do not show a distinct diurnal cycle as described for ship-wave dominated days (Fig. 3.6). Following the dynamics of the wind events $u_{max,\,ADV}$ and SSC are elevated over much longer time periods (several hours) compared to the passage of a single ship-wave group (several minutes) (Fig. 3.6). Especially during periods where $u_{max,\ ADV}$ is continuously high (~0.3 m s^{-1}) over at least one hour, SSC can be as high as 200-400 mg L^{-1} and exceed SSC observed on ship-wave dominated days (Fig. 3.6). During the same wind event, however, and at comparable values of $u_{max,\ ADV}$ (20:30-21:30 h and 22:30-23:30 h on 16 August 2005), the observed SSC can be considerably different (200 mg L^{-1} and 350 mg L^{-1}, respectively; Fig. 3.6D-F). A possible explanation is that during the first time period the sediment top layer was gradually eroded and spatially distributed in the whole water column and in the entire littoral zone, which lowered the measured SSC near the bottom. During the second time period, the previously and partially still resuspended particles were remobilized and added into the water column, which increased the SSC further and established a new equilibrium.

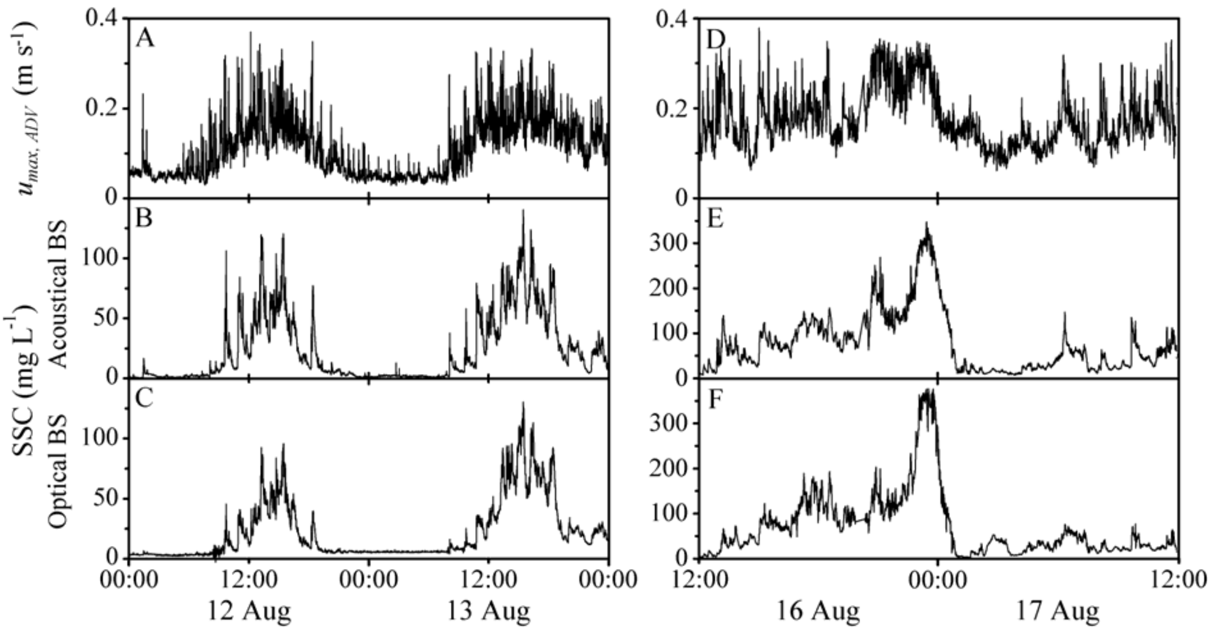

Fig. 3.6 Times series of the (A) maximum near-bottom current velocity ($u_{max,\ ADV}$), (B) suspended sediment concentration (SSC) estimated from the acoustical backscatter strength, and (C) SSC estimated from the optical backscatter strength for a ship-wave (12 and 13 August 2005), and (D), (E), and (F) for a wind-wave dominated time period (16 and 17 August 2005), respectively.

The relation between the maximum near-bottom current velocity and the suspended sediment concentration

The relation between $u_{max, ADV}$ and the SSC is exemplarily shown for August 2005 (Fig. 3.7), when the wave field was characterized by wind as well as ship waves. $u_{max, ADV}$ and the corresponding SSC are determined for 30 min time intervals. Figure 3.7 shows that the SSC remains rather constant for small $u_{max, ADV}$ and increases rapidly with increasing $u_{max, ADV}$ above a certain level of $u_{max, ADV}$. This supports the concept that a threshold value of u_{max}, $u_{max, res}$, is required for resuspension. We have estimated this threshold value by fitting the following model to our data:

$$\log SSC = \begin{pmatrix} A & ; u_{\max,\, ADV} \leq C \\ A + B \cdot \left(\log u_{\max,\, ADV} - \log C\right) & ; u_{\max,\, ADV} > C \end{pmatrix} \tag{3.3}$$

where the model parameter A corresponds to the log(SSC_{base}) and SSC_{base} is the mean background SSC. B is the slope of the curve above the point of intersection and C corresponds to the threshold velocity, $u_{max, res}$, above which wave-generated currents lead to resuspension. The parameter values were obtained by a least-squares fit providing $A = 0.41$, $B = 2.65$, and $C = 0.08$ m s^{-1}. Hence, the mean background SSC is about 2.6 mg L^{-1} (Fig. 3.7; Eq. 3.3) and the threshold flow velocity required for particle remobilization is 0.08 m s^{-1} (dashed black line). This threshold flow velocity for resuspension determined experimentally from SSC and velocity measurements agrees very well with the value obtained from the empirical relation (Eq. 3.2) in combination with the estimate of particle density and mean grain size of suspended sediments. Because the two independent methods provide the same threshold flow velocity for sediment resuspension $u_{max, res} = 0.08$ m s^{-1}, this value was used in the following statistical analysis.

The separation of the time series into daytime (red dots) and nighttime (gray dots) revealed that wave-induced resuspension indicated by high $u_{max, ADV}$ and SSC occurred mainly during daytime, where ship waves dominated the overall wave field (Fig. 3.7). During nighttime, $u_{max, ADV}$ and SSC are mostly very low (0.02-0.10 m s^{-1} and 1-10 mg L^{-1}) indicating a negligible importance for resuspension.

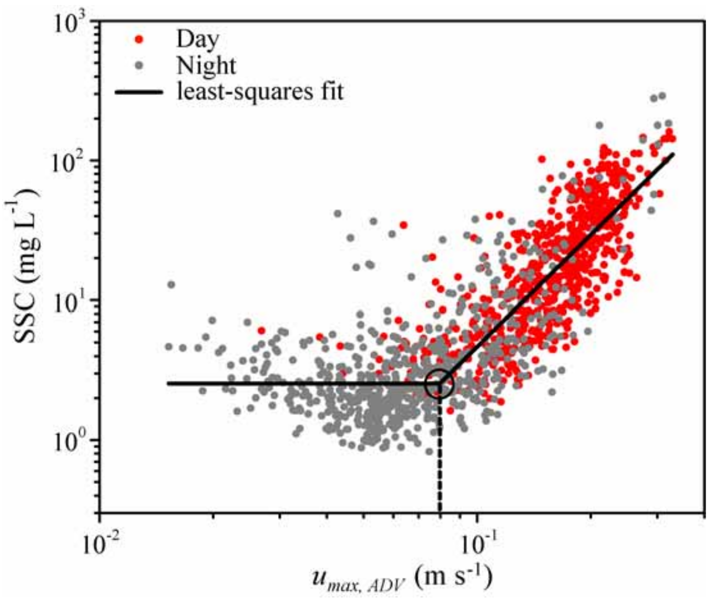

Fig. 3.7 Scatter plot of the maximum near-bottom current velocity ($u_{max, ADV}$) and the acoustically determined suspended sediment concentration (SSC) at about 1 m water depth during August 2005. Each dot represents the data for a 30 min time interval. The red dots indicate measurements from daytime (09:00-21:00 h) and the gray dots from nighttime (21:00-09:00 h). The black line represents the result from a least-squares fit of the model (Eq. 3.3). The point of intersection (open black circle) between the horizontal black line (mean background of the SSC) and the inclined black line (power law) marks the threshold of $u_{max, ADV}$ for resuspension (0.08 m s^{-1}, dashed black line).

The relative importance of wind and ship waves for resuspension

Experimental characterization of the surface wave field allows to distinguish between wind and ship waves by their corresponding frequencies (Hofmann et al. 2008a). The relative importance of wind and ship waves for resuspension can be quantified by the proportion of time where u_{max} exceeds $u_{max, res}$. This proportion is expressed in terms of the relative monthly distribution of $u_{max, res}$ between August 2005 and July 2006 (Fig. 3.8). Daytime and nighttime are considered separately to emphasize not only seasonal but also diurnal patterns (Fig. 3.8A,B).

During daytime, the overall proportion of waves that exceed the threshold flow velocity for resuspension of 0.08 m s^{-1} is significantly higher in summer (March-October) than in winter (November-February), ranging from 34-79% and 14-28%, respectively (Fig. 3.8A). This difference between summer and winter can be attributed to the strongly reduced ship traffic during winter. The proportion of wind waves that contribute to resuspension remains relatively constant throughout the whole year and accounts for 6-36%, whereas the proportion of ship waves increases significantly in summer and ranges from 9% in March to 55% in June. In winter, the proportion of ship waves that cause resuspension is reduced to 5-15%.

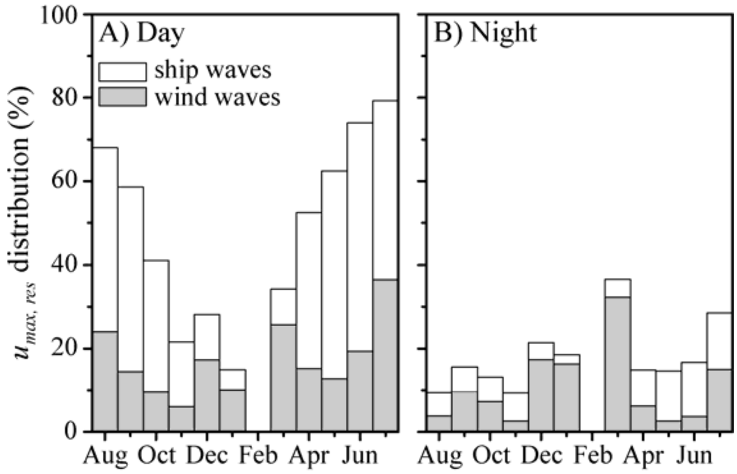

Fig. 3.8 Relative importance of wind and ship waves for resuspension expressed in terms of the relative monthly distribution of the maximum near-bottom current velocity that exceeds the calculated threshold for resuspension ($u_{max, res}$ = 0.08 m s^{-1}) at 1 m water depth. The statistics distinguishes between wind-generated (gray bars) and ship-generated (open bars) waves and is based on measurements between August 2005 and July 2006. (A) At daytime (09:00-21:00 h). (B) At nighttime (21:00-09:00 h). The maximum near-bottom current velocity $u_{max, PS}$ was calculated from wave parameters, which were derived from the pressure sensor (PS) time series. $u_{max, PS}$ values below the calculated threshold for resuspension were excluded from the data sets, and are expressed by the missing percentage to 100% (beside February where no data is available).

Apart from the seasonal pattern, ship waves cause, due to their dominant occurrence at daytime, a pronounced diurnal pattern in resuspension. During nighttime, the overall proportion of waves that exceed the threshold for resuspension (9-36%) is much lower than during daytime (Fig. 3.8B) and does not show a seasonal pattern. Also, this diurnal pattern can be attributed to reduced ship traffic during nighttime. The variability in the $u_{max, res}$ distribution of wind waves, in contrast, can be explained by their irregular occurrence. Strong on-shore wind events are responsible for the high values in August, September, March, and July, and the absence of on-shore wind events explains the low value in November (Fig. 3.8). Hence, the potential for resuspension is especially low during winter and nighttime, where 75-85% and 63-91% of the time the wave-generated near-bottom current velocities do not exceed the threshold velocity for resuspension.

On an annual mean, the proportion of the time at the study site LG when wave-induced resuspension can occur is about 33%. Thereof, 42% of the time when resuspension occurs is caused by wind waves and 58% by ship waves.

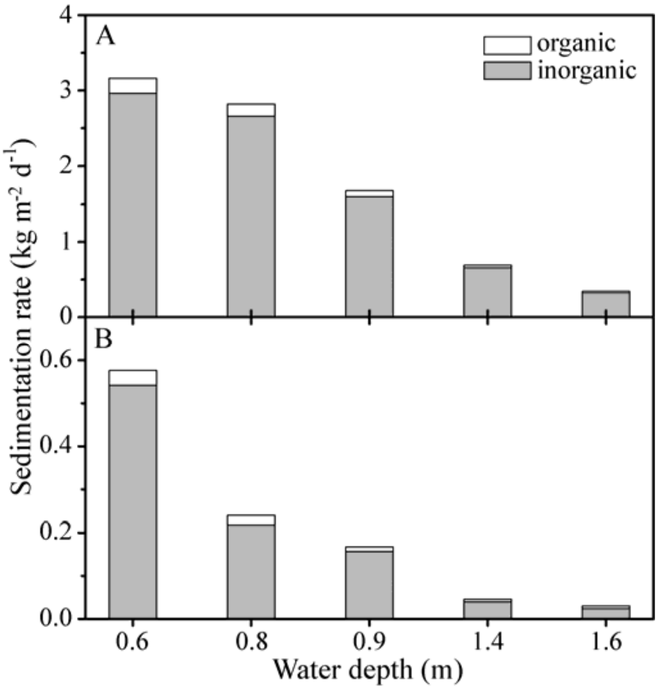

Fig. 3.9 Sedimentation rate of organic (open bars) and inorganic (gray bars) particles measured by sediment traps. (A) During a time period with strong on-shore wind (15-20 September 2005). (B) During a time period with no or calm wind (wave field was dominated by ship waves, 20-25 September 2005).

The sedimentation rates measured by the 5 shore-normal distributed sediment traps at the study site LG indicate the change in sediment resuspension with depth, time, and their relation to the wave field (wind or ship wave dominated). The comparison of two 5-days periods revealed that the sedimentation rate during a strong on-shore wind event (15-20 September 2005; Fig. 3.9A) is significantly larger than during a ship-wave dominated time period (20-25 September 2005; Fig. 3.9B). The sedimentation rate decreases with increasing water depths as the near-bottom current velocities do. Thus, the source of suspended particles in the water column is resuspension mainly in the shallow water followed by transport of these particles to the open water. Note that the large sedimentation rate (gross sedimentation) at shallower depths does not imply a large sediment accumulation rate, but is rather a consequence of the permanent interplay between resuspension and later deposition in the sediment traps. During the strong on-shore wind event, significant sedimentation not only occurred at 0.6 m but also at larger water depths. This may be caused by increased resuspension at the depths of the sediment traps because of the large amplitude wind waves generated by the strong on-shore wind and by an increased horizontal dispersion of particles resuspended at shallower depths. In the sediment traps the organic fraction (5-9%) is small compared to the inorganic fraction (91-95%) (Fig. 3.9). However, the organic fraction of particles showed a pronounced distribution towards increasing water depth, especially in summer.

Discussion

Especially the littoral zones of lakes are highly exposed to surface waves that generate near-bottom current velocities and shear. The surface wave field at the study site LG, Lake Constance, is dominated by wind waves in winter and ship waves in summer (Hofmann et al. 2008a). The wave field characteristics observed at Lake Constance can be expected to be comparable to many prealpine and alpine lakes in Germany and Switzerland. One important effect of wind as well as ship wave is resuspension of bottom sediment. But both wave types cause considerably different temporal and spatial patterns of resuspension.

Wind-wave induced sediment resuspension is infrequent and highly dependent on the wind direction, speed, and fetch length. At the study site LG only strong on-shore winds cause comparable or higher SSC as regularly occurring ship waves at the same water depth. During wind events the wind-wave generated maximum near-bottom current velocities and the SSC remain almost constant over hours (Figs. 3.5B, 3.6D-F). This can be explained by an equilibrium that is formed between the resuspension, settling, and transport of particles. During these specific time periods the concentration of suspended particles and the sedimentation rate is enhanced compared to an equal period of time when ship waves are dominant (Fig. 3.9).

The passage of a single ship increases the near-bottom current velocities drastically and causes a high and distinct peak in the SSC due to the resuspension of a wide range of grain sizes (Fig. 3.3A), where the coarser particles resettle quickly and finer particles remain in the water column for several minutes (Figs. 3.3A, 3.5A).

The relationship between near-bottom current velocities and SSC depicted in Figure 3.7 is a consistent pattern that was confirmed by long-term observations at the study site LG. Especially at daytime during summer, where ship waves dominate the wave field due to the occurrence of successive wave groups within minutes, the near-bottom current velocities remain above the threshold value for resuspension of about 0.08 m s^{-1} (Figs. 3.6A, 3.7). This threshold velocity was estimated from empirical relations based on the prevailing sediment properties at the study site and was confirmed by our measurements (Fig. 3.7). The regular ship traffic further reduces settling of suspended particles between subsequent wave groups. Thus, ship-wave induced resuspension causes a diurnal cycle in the measured SSC with high values at daytime and low values at nighttime (Fig. 3.6B,C). Also Garrad and Hey (1987) observed such periodicity in a river system caused by navigation. The 'tourist cruise-ship season' of passenger ships during summer and their near absence during winter (Hofmann et al. 2008a) causes further a seasonal pattern in sediment resuspension (Fig. 3.8).

At the study site, on 33% of the time the threshold for resuspension $u_{max,\ res}$ is exceeded, whereas ship-wave induced resuspension contributes 58% compared to 42% caused by wind waves. Here, the frequent occurrence of ship-wave induced resuspension of particles especially during summer is more pronounced than wind-wave induced resuspension due to sporadically occurring wind events. Thus, ship waves as an anthropogenic force dominate the process of resuspension.

The relative importance of ship waves for resuspension arises not only from the frequency of occurrence, but also due to the effect of wave length. For a given wave height and water depth, the wave-generated near-bottom current velocity is determined by the wave length (Eq. 3.1; Kundu and Cohen 2002). Since ship waves have much longer wave lengths (13-50 m) than wind waves (2-8 m) (Hofmann et al. 2008a), they induce much higher near-bottom current velocities than wind waves at the same water depth, and therefore affect the ecosystem (e.g., by resuspension of particles) at much larger depths than wind waves with the same wave height (Soomere 2005). Furthermore, the higher near-bottom current velocities of ship waves remobilize also particles with larger grain sizes, especially at daytime in summer, when ship waves dominate sediment resuspension. In contrast, wind waves need much higher wave heights compared to ship waves to remobilized particles of the same grain size, which is only the case during sporadically occurring on-shore wind events.

Regular resuspension events prevent sediment consolidation and the development of a cohesive sediment layer (Dyer 1986; Schoellhamer 1996). These newly deposited and unconsolidated sediments are more susceptible to resuspension and lead to strong impulse loads of suspended particles also due to previously ineffective wind waves or tidal currents (Garrad and Hey 1987; Schoellhamer 1996; Lindholm et al. 2001). Since we demonstrated that ship waves lead to regular resuspension events, which prevents the formation of cohesive sediments, the ship traffic may significantly contribute to erosion of sediments in the littoral zone.

The sediment traps provide indication to which extent wind- and ship-wave induced resuspension alters the sedimentation rate and sediment properties in cross-shore direction. The sedimentation rate as well as the grain size of settling particles decreases strongly with increasing water depth (Figs. 3.3B, 3.9). Both observations suggest that resuspension takes place mainly in the shallow littoral followed by transport of particles in off-shore direction, whereas the large particles resettle first. Since ship waves dominate the sediment resuspension at the study site LG, especially on daytime and during summer, they mainly contribute to the spatial distribution of sediments. In particular, we measured an increase of the organic and a decrease of the inorganic particle fraction with increasing water depth. This observation indicates that in contrast to inorganic particles only a reduced proportion of the organic particles mobilized by ship waves at shallow depths settle again within the littoral zone. Thus, the particulate organic material is exported to the pelagial.

Resuspension of particles has extensive ecological consequences, which are intensified by ship-induced resuspension. Ship waves cause strong impulse loads of suspended particles in the water column (Schoellhamer 1996; Lindholm et al. 2001) that alter the light climate in the littoral zone in terms of reduced water transparency and light penetration (van Duin et al. 2001; Erm and Soomere 2006; Hofmann et al. in press). Ship waves occur especially during daytime and in summer, and thus affect the availability of light for the growth of phytoplankton and biofilms in particular (Pierson et al. 2003). The re-allocation of particles alters the habitat structure on small scales in terms of reduced availability of cavities (interstitial) for benthic invertebrates and nematodes (Peters and Traunspurger 2005; Scheifhacken 2006; Scheifhacken et al. 2007), which make them more susceptible for predation (e.g., by fishes).

Conclusions

Sediment resuspension in lakes induced by surface waves is pronounced in the shallow littoral zone, where surface waves are the dominant hydrodynamic force. The process of sediment resuspension and the resulting increase in SSC in the littoral zone is highly related to the properties of the surface wave field. The different wave types: wind-generated and ship-generated waves cause different temporal and spatial patterns in resuspension and particle distribution.

Sediment resuspension induced by wind waves occurs sporadically and less frequent than ship-wave induced resuspension. The periodic and regular occurrence of ship waves, especially of passenger ships, during daytime and in summer cause a substantial increase in SSC in the shallow littoral. Thus, ship waves cause a diurnal cycle as well as a seasonal pattern in the SSC and resuspension. On an annual scale, the anthropogenic ship wave-induced resuspension is dominant over the natural wind-wave induced resuspension. Their importance is further pronounced since ship waves, having much longer wave lengths than wind waves, affect a much wider part of the littoral zone. The periodic and regular occurrence of ship waves suggests that the newly deposited, unconsolidated bottom sediments are more susceptible to resuspension. Ship-wave induced resuspension enhances the dispersion of particles by keeping the particles in suspension. Additionally, we assume that ship-wave induced resuspension increases the export of small-sized particles and organic material from the shallow to deep littoral and even to the pelagial of the lake in summer.

Acknowledgments

We thank Georg Heine and his colleagues from the electronic and mechanical workshop at the University of Konstanz for technical assistance and for the development of the pressure sensors. We gratefully acknowledge the help of the technical staff at the Limnological Institute and many students during fieldwork and data analysis. We further thank Dr. Martin Wessels and Karin Popp from the ISF Langenargen for providing the grain size analyzer and their help in the laboratory. This work was supported by the German Research Foundation (DFG) within the framework of the Collaborative Research Center 454 ‘Littoral Zone of Lake Constance’.

Chapter 4

Wave-induced variability of the underwater light climate in the littoral zone

HILMAR HOFMANN, ANDREAS LORKE AND FRANK PEETERS

Verhandlungen der Internationalen Vereinigung für Theoretische und Angewandte Limnologie **in press**

Introduction

Underwater irradiance, referred to as photosynthetically active radiation (PAR), undergoes strong temporal fluctuations. These fluctuations are not only caused by variations in the incoming light intensity but also by variations in the elevation and curvature of the water surface resulting from wave motion (Snyder and Dera 1970; Kirk 1994; Zaneveld et al. 2001). In addition, wave-induced resuspension of particles in the littoral zone can cause rapid changes of light attenuation within the water column. Thus, the variability of the light field is maximal at shallow depths (Dera and Gordon 1968; Rørslett et al. 1997; Schubert et al. 2001). Light intensity is important for the growth of phytoplankton (Finger et al. 2007), biofilms and macrophytes (Scheffer et al. 1993) and affects habitat choice, food uptake, and predation pressure of fishes (Utne-Palm 2004; Schleuter and Eckmann 2006). The biological relevance of fluctuating light is not only determined by the intensity of the fluctuations, but also by temporal scales (Walsh and Legendre 1983; Pahl-Wostl 1992).

We experimentally investigated the variability of the underwater light climate in the littoral zone with the intension of providing amplitudes and temporal scales of the intensity fluctuations resulting from wave focusing, the change in surface elevation, and resuspension.

Materials and methods

Study site

Lake Constance, the second-largest (in surface area, 536 km^2) prealpine lake in Europe, is located in the southwest of Germany and borders Switzerland and Austria. The littoral zone covers about 10% of the total surface area (Braun and Schärpf 1990). Measurements were carried out in the western part of Upper Lake Constance at a site called Littoral Garden (LG; 47°41'29''N, 09°12'11''E). The shore is exposed to a highly variable surface wave field, which is dominated by wind waves in winter and ship waves in summer (Hofmann et al. 2008a). Ship waves stem from a close by ferry track with regular sailings throughout the year, from passenger ships traveling parallel to the shore line during the tourist season (mid-March to mid-October), and from a newly introduced catamaran ferry.

Instrumentation

The underwater light climate was measured with a high temporal resolution (128 Hz) by a chain of 6 synchronized spherical PAR sensors (LI-193SA, LI-COR) combined with a pressure sensor (PS, PDCR 1730, DRUCK).

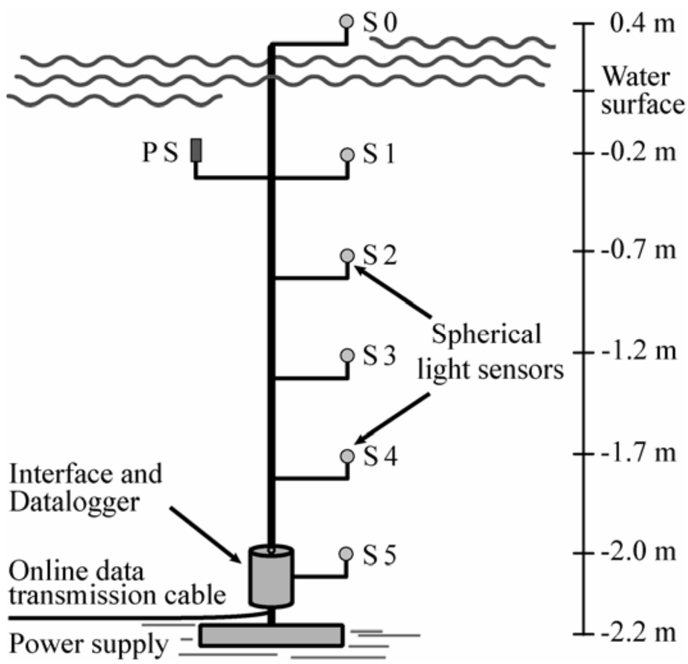

Fig. 4.1 Schematic sketch of the light chain deployed in the littoral zone of Lake Constance (PS: pressure sensor, S 0-S 5: PAR sensors).

The PS has an accuracy of 0.1 mbar, sufficient to resolve wave heights down to 0.01 m and wave frequencies up to 2 Hz corresponding to wave lengths down to 0.4 m, if the sensor is positioned 0.2 m below the water surface at 2 m water depth. The 6 spherical PAR sensors measure scalar irradiance with a response time of 10 µs.

Measurements were conducted between 18 April and 04 May 2007 at a water depth of 2.2 m. All sensors were attached to a bottom-resting pole. One of the light sensors (S 0) was placed 0.4 m above the water surface as a reference, measuring the incident light. The other 5 PAR sensors were mounted at 0.2 (S 1), 0.7 (S 2), 1.2 (S 3), 1.7 (S 4), and 2.0 m (S 5) below the water surface (Fig. 4.1). The pressure sensor was deployed next to S 1.

Analysis

The measured time series of subsurface pressure was converted to a time series of surface elevation using the procedure described in Hofmann et al. (2008a).

Power spectra of light intensity and surface elevation were estimated by calculating power spectra from segments of the time series consisting of 8,192 samples (~1.1 min) with 50% overlap and subsequent averaging of 56 consecutive spectra to reduce confidence intervals.

The amplitude of the fluctuations in the underwater light field as a function of depth was estimated from the 5 submerged light sensors by calculating the minimum and the maximum light intensities within 10 s time intervals. The mean and the standard deviation of the respective minima and maxima were calculated for one-hour time periods.

The effect of surface elevation on light intensity was estimated from Lambert-Beer's-Law. Assuming exponential decay of light with depth, hourly mean light intensities at two neighboring light sensors were used to determine the light attenuation coefficient (K_d) for the respective depth range. Then the surface elevation derived from the pressure sensor data was used together with the K_d values to calculate the fluctuations in light intensity due to fluctuations in surface elevation.

Results and discussion

Amplitudes of underwater light fluctuations

Data from the 19 April 2007 are chosen to elucidate the features of the underwater light climate on cloudless days with bright sunlight. Between 10:00 and 11:00 h, the measured incident light intensity did not fluctuate significantly, whereas the underwater irradiance showed fluctuations with high amplitudes and high frequencies at all depths. The highest amplitudes occurred near the surface. Between 10:31:30 and 10:32:00 h at 0.2 m below the surface (S 1), the light intensity fluctuated between +700 and -600 µmol quanta s^{-1} m^{-2} around its mean value of 1,684 µmol quanta s^{-1} m^{-2} (Fig. 4.2A), which indicates that the fluctuations are biased towards higher intensities due to non-linear refractive effects at the water surface (Stramski and Legendre 1992). During this time period the surface wave field was characterized by small-amplitude (0.01-0.05 m), high-frequency (1-2 Hz), short-length (0.4-1.6 m) wind waves (ripple waves) and a ship wave group with a maximum height of about 0.3 m (Fig. 4.2B). The ripple waves are known to induce wave focusing (Snyder and Dera 1970; Rørslett et al. 1997), whereas the ship waves with a period of 2.9 s and a wave length of 13 m essentially lead to an elevation of the water surface and not to a pronounced focusing effect of the incident light (Rørslett et al. 1997; Stramska and Dickey 1998).

The effect of the change in surface elevation on the near surface light climate was recorded (Fig. 4.2B). The 1 s running average of the S 1 time series shows a periodically fluctuating light intensity that is phase shifted by 180° relative to the oscillation of the surface elevation. The amplitude of the oscillating light intensity is about ±70 µmol quanta s^{-1} m^{-2}, which is small, compared to the total fluctuation of the light intensity. The difference between the total fluctuation in light intensity (Fig. 4.2A) and the light fluctuation due to the surface elevation (Fig. 4.2B) can be attributed to the effect of wave focusing and ranges between +40 and -35% of the mean light intensity. The effect of surface elevation contributes only about ±5% to the overall fluctuation in light intensity (Fig. 4.2C).

Clearly, extreme values of light intensity fluctuations are dominated by the effects of wave focusing. Schubert et al. (2001) and Rørslett et al. (1997) have demonstrated that wave focusing can cause light intensities significantly above the incident light intensity, reaching up to 5 times the mean. These extremely high light intensities were observed with small planar sensors that measure only downwelling irradiance and thus differ from the spherical sensors used in this study that integrate light from all directions.

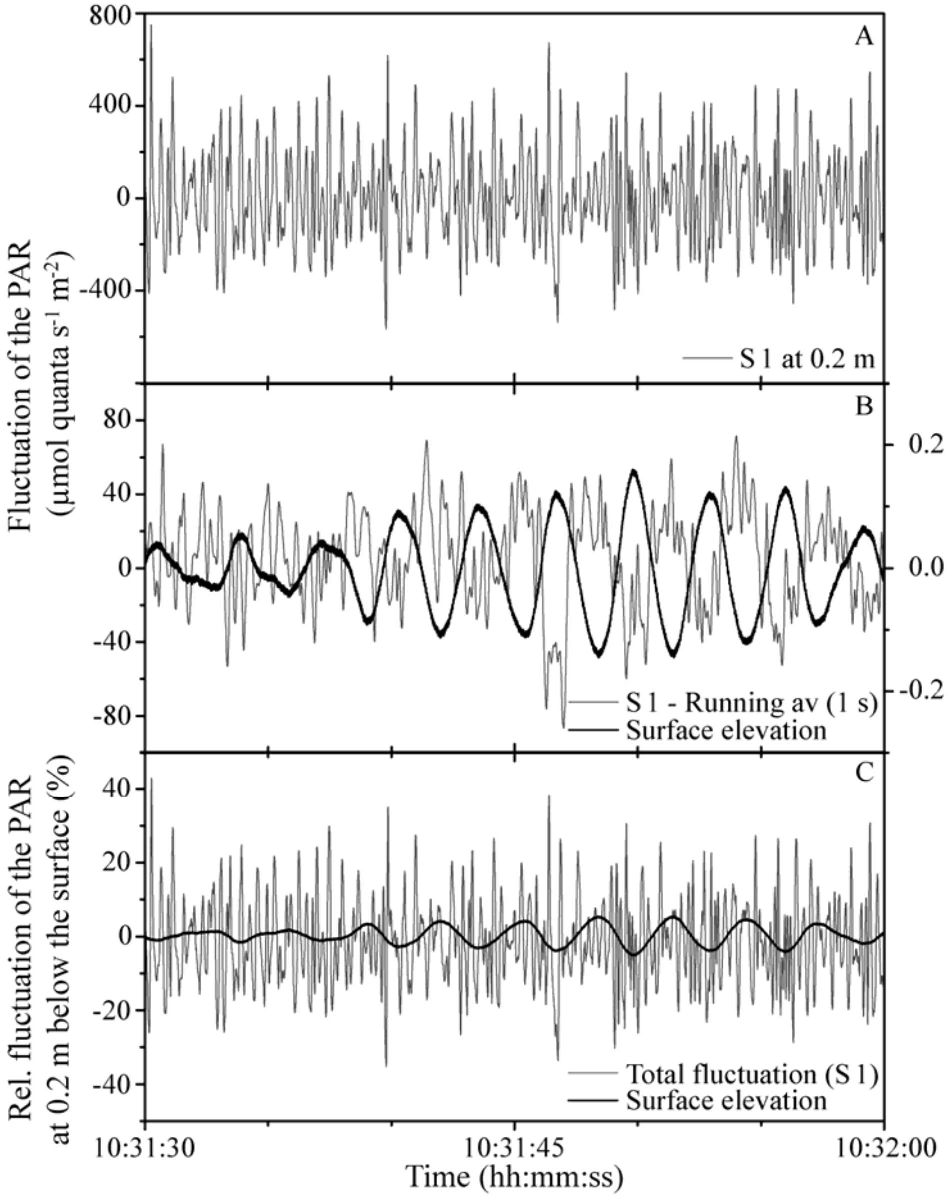

Fig. 4.2 Amplitudes of the near surface underwater light field and the simultaneously measured surface elevation on 19 April 2007 between 10:31:30 and 10:32:00 h. (A) Absolute fluctuations of the light intensity about its mean value at S 1 (0.2 m below the surface). The mean value was calculated for the time period specified above. (B) Surface elevation (generated by a ship wave, bold solid black line) and related absolute fluctuations of the light intensity (fine solid gray line) derived by applying a 1 s running average on the times series of S 1. (C) Relative fluctuations of the light intensity (fine solid gray line) and of the surface elevation (bold solid black line). The relative change of the light intensity caused by surface elevation at 0.2 m below the surface was calculated for an exponential decay of light with depth using the average attenuation coefficient (K_d) between S 1 and S 2 of 0.35 m^{-1}.

The vertical distribution of the range of the underwater fluctuations in the light intensities due to wave focusing and due to ship-wave induced surface elevation (Fig. 4.3) shows the minima and maxima of the light intensities at 0.2, 0.7, 1.2, 1.7, and 2.0 m below the surface measured on 19 April 2007 between 10:00 and 11:00 h.

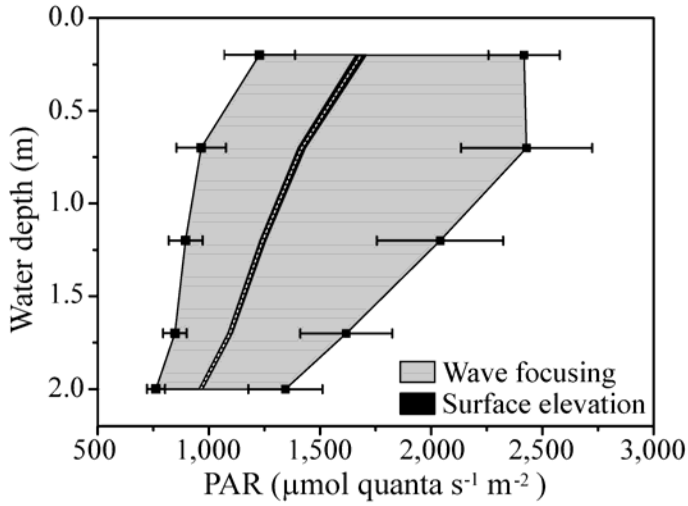

Fig. 4.3 Amplitudes of the fluctuations in the underwater light field as function of depth caused by the effect of wave focusing (gray area) and solely by the effect of surface elevation (black area) on 19 April 2007 between 10:00 and 11:00 h. Symbols (filled squares) show the mean values of the minimum and the maximum light intensities within 10 s time intervals with their standard deviation (not shown for the effect of surface elevation to keep graphical clarity). The overall mean of the measured light intensity is shown by the white dashed line. The effect of surface elevation on light intensity was estimated from Lambert-Beer's-Law. Assuming exponential decay of light with depth, hourly mean light intensities at neighboring light sensors were used to estimate the light attenuation coefficient (K_d) for the respective depth range. These attenuation coefficients in combination with surface elevation derived from the pressure sensor data were used to estimate the fluctuation in light intensity due to fluctuations in surface elevation as described above.

At all depths the amplitudes of light intensity fluctuations caused by wave focusing are much larger than those caused by the elevation of the surface alone. The mean light intensity, centered within the intensity range due to surface elevation, decreased monotonously with depth from about 1,680 µmol quanta s^{-1} m^{-2} at 0.2 m to about 960 µmol quanta s^{-1} m^{-2} at 2.0 m below the surface. In contrast, the maximum light intensities resulting from wave focusing did not monotonously decrease with depth: the maximum range (1,400 µmol quanta s^{-1} m^{-2}) and the highest maximum values in light intensity (2,750 µmol quanta s^{-1} m^{-2}) were observed at 0.7 m and not at 0.2 m depth. Further, the data indicate that the fluctuations of the light intensity are asymmetrical around the mean with positive deviations from the mean being larger than negative deviations at all depths (Fig. 4.3). Such a vertical distribution of the near surface underwater light field was also observed by Snyder and Dera (1970), but detailed measurements of the surface wave field were not available. Zaneveld et al. (2001) investigated the consequences of wave focusing on light intensities from a theoretical perspective. Assuming a modulated surface wave field consisting of low-frequency as well as high-frequency waves with different wave heights, they demonstrated that the maximum in light intensity is shifted from the surface to larger depths. This shift occurs because of the position of the first focal point owning to the lens effect of surface waves. The depth and the intensity of the maximum value in the light intensity are highly dependent on the composition of the surface wave field. Low-frequency waves shift the maximum in light intensity to larger depths, whereas high-frequency waves result in a maximum at shallower depths and cause higher maximal intensities. Our measurements can partly confirm these theoretical considerations, but detailed measurements with a higher spatial resolution near the water surface are needed to demonstrate the shift of the maximum in light intensity under changing properties of the surface wave field.

Temporal scales of underwater light fluctuations in relation to the surface wave field

Spectral analysis of the light intensity at S 1 and of the surface elevation (derived from the pressure sensor) time series on 19 April 2007 for the time periods between 10:00 and 11:00 h (first hour) and 13:00 and 14:00 h (second hour) reveals a clear linkage between the surface wave field and the underwater light field (Fig. 4.4). During both time periods, spectra of the light intensity show peaks at 0.27 Hz and between 0.5 and 0.6 Hz. Between 13:00 and 14:00 h the peaks are more pronounced, and an additional peak at 0.35 Hz appears in the spectrum of light intensity (Fig. 4.4A). The occurrence of these peaks is related to the low-frequency surface waves found also in the spectra of surface elevation (Fig. 4.4B). The peaks at 0.27, 0.35, and 0.5-0.6 Hz are due to surface waves generated by ferries, passenger ships, and wind, respectively (Hofmann et al. 2008a). During the two hours considered (Fig. 4.4), these wind and ship waves had wave heights between 0.05 and 0.3 m, which are sufficient to significantly affect the near surface underwater light climate. The peak at 0.16 Hz in the surface elevation spectrum (Fig. 4.4B) can be attributed to waves from the catamaran ferry. This peak is not resolved in the spectra of the light intensity (Fig. 4.4A) because the wave height resulting from the catamaran at site LG is too small (<0.05 m) to induce a substantial variance in the light intensity. In addition to the peaks described above, the spectrum of the light intensity from the first hour shows a broad peak between 1.2 and 4 Hz, which is narrower and less pronounced in the spectrum for the second hour. The latter spectrum has a small peak around 2.5 Hz with a spectral density, which is two orders of magnitude lower than that of the broad peak in the spectrum from the first hour (Fig. 4.4A). The variance of the light intensity at frequencies above 1 Hz can be most likely attributed to the effect of wave focusing.

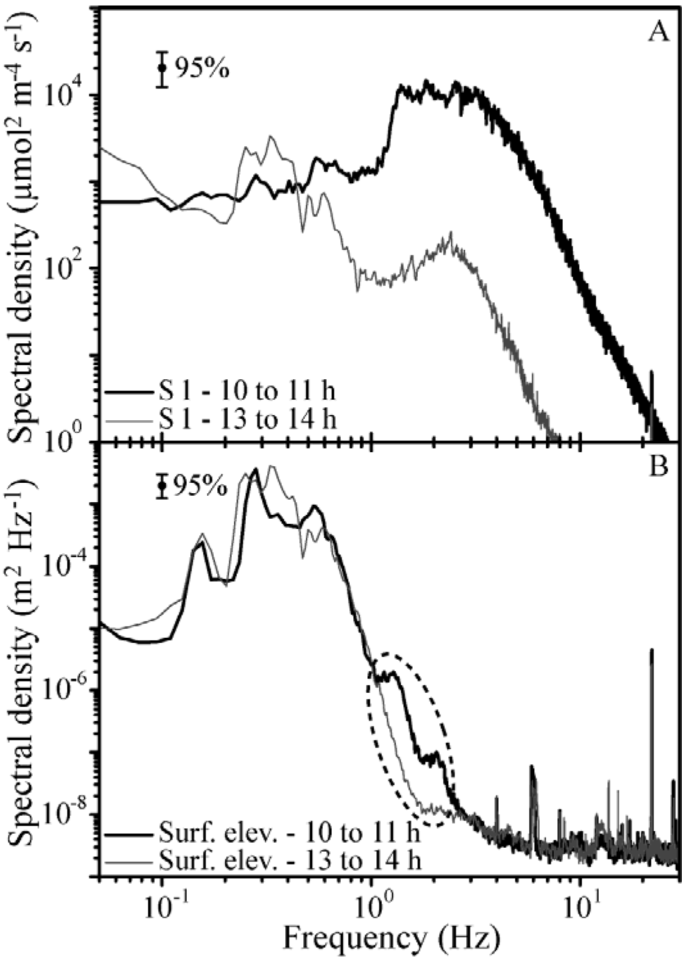

Fig. 4.4 Spectra of the light sensor S 1 (A) and the pressure sensor (PS, surface elevation) (B) at 0.2 m below the surface on 19 April 2007 between 10:00 and 11:00 h (bold solid black line), and 13:00 and 14:00 h (fine solid gray line). The spectra were estimated from the light and surface elevation time series over the respective hour using segments of 8,192 samples (~1.1 min) and subsequent averaging. The ellipse in the spectrum of the pressure sensor (panel B) emphasizes peaks around frequencies of 1.5 and 2 Hz, which were observed between 10:00 and 11:00 h but not between 13:00 and 14:00 h. These peaks can be attributed to the occurrence of ripple waves and correspond directly to the observed peaks in the spectrum of light intensity fluctuations (panel A). The spikes above 3 Hz in the spectra of surface elevation are artifacts of the PS.

As the spectra of light intensity, the spectra of surface elevation from the two hours also differ in the high-frequency range between 1 and 2 Hz. During the first hour, peaks were observed at 1.5 and 2.0 Hz, which are not visible in the spectrum from the second hour (Fig. 4.4B, dashed ellipse). These peaks can be attributed to ripple waves (described above). The coincidence of these ripple waves and the strong fluctuation in light intensity resulting from light focusing suggests that light focusing is predominantly connected to the occurrence of small ripple waves because wave focusing was pronounced during the first hour and was nearly absent during the second hour.

At frequencies above 2 Hz, the spectra of surface elevation do not show variance except for noise and instrumental resonance signals from the pressure sensor. At frequencies above 2 Hz surface waves have wave lengths <0.4 m. Pressure fluctuations from these waves attenuate rapidly with increasing depth and cannot be resolved by our pressure sensor.

In addition to fluctuations in light intensity (with periods below a few seconds due to wave-induced surface elevation and light focusing), light intensity in the littoral zone is affected by suspended particles resulting from wave-induced resuspension (Erm and Soomere 2006; Hofmann et al. 2008a) at time periods ranging from minutes to hours, and even up to seasonal fluctuations. During time periods with resuspension, the light intensities at 2 m depth decreased substantially by up to 70%, depending on the particle concentration in the water column. Light attenuation calculated from the PAR-sensor chain typically increased over the course of the day because ship-wave induced resuspension leads to an increase of the suspended particle load. Note that resuspension by ship waves is much more intense during daytime than at night because of increased ship traffic and larger wave heights during daytime (Hofmann et al. 2008a).

More important than the diurnal fluctuation in light attenuation is the daily cycle of incident light, which leads to a strong daily cycle in the underwater light intensity. On seasonal time scales, not only the seasonal variation in the incident light (about 25% between winter and summer at Lake Constance, latitude 47.7°), but also water level fluctuations, which are about 2-3 m at Lake Constance (Hofmann et al. 2008b), alter the underwater light climate for sessile organisms and biofilms. For a typical K_d for Lake Constance of 0.35 m^{-1}, the seasonal variation of the incident light would have the same effect as a change in water level of about 0.8 m. Thus the fluctuations of the light intensity induced by the water level fluctuations have larger amplitudes than seasonal variation of the incident light. Because of high water levels in summer and low in winter, where the incident light reaches its maximum and minimum, respectively, both processes counteract and reduce the amplitudes in the variation of the underwater light intensity for sessile organisms.

Conclusions

Fluctuations of the underwater light intensity caused by surface waves due to surface elevations were distinguished from those due to focusing and defocusing of the incident sunlight (wave focusing) by using synchronized high-frequency measurements of photosynthetically active radiation (PAR) and pressure. In general, PAR showed high-amplitude and high-frequency fluctuations near the surface (0.2-2.0 m depth). Strongest fluctuations were observed under bright sun when the surface wave field was dominated by small ripple waves. Under such conditions the amplitudes of the fluctuations in the light intensity due to wave focusing are much larger than that of the surface elevation caused by wind and ship waves. Further, wave focusing shifts the maximum of the underwater light intensity to greater depths, depending on the properties of the surface wave field.

The resuspension of particles induced by wind and ship waves can dramatically reduce the light intensity in the littoral zone on temporal scales ranging from minutes to hours and thus may contribute to light limitation of phytoplankton and biofilm growth.

Acknowledgments

We thank Georg Heine and his colleagues from the electronic and mechanical workshop at the University of Konstanz for technical assistance and for the development of the light chain. Special thanks to Dr. R. Kipfer for his support with the instrumentation. We gratefully acknowledge the help of the technical staff at the Limnological Institute, Tobias Merz, and Matthias Kohlndorfer during fieldwork and data analysis. We gratefully acknowledge the help of the technical staff at the Limnological Institute and many students during fieldwork and data analysis. This work was supported by the German Research Foundation (DFG) within the framework of the Collaborative Research Center 454 'Littoral Zone of Lake Constance' and by the European Science Foundation (ESF) with a travel grant.

Chapter 5

Wave field characteristics and currents in a wave mesocosm

HILMAR HOFMANN

Introduction

In lake littoral zones, surface waves are the hydrodynamically most important process in terms of shear stress. In shallow waters they interact directly with the lake bottom and thus alter abiotic and biotic habitat conditions. Typical processes are, for example, the resuspension and transport of particles (Luettich et al. 1990; Hawley and Lesht 1992; Lee et al. 2007) that cause a reduction of light in the water column available for the growth of phytoplankton, biofilms, and macrophytes, the release of nutrients (Søndergaard et al. 1992; Güde et al. 2000), the re-allocation and stress on benthic invertebrates (Rasmussen and Rowan 1997; James et al. 1998; Scheifhacken et al. 2007), the abrasion of biofilms (Cattaneo 1990; Francoeur and Biggs 2006) and macrophytes (Keddy 1982; Wilson and Keddy 1985; Kawamata 2001), and the hydrodynamic stress on juvenile fishes that suffer from higher energetic costs, and thus experience reduced growth rates (Stoll et al. 2008).

Surface waves can be generated by wind as well as by ships. In most lakes, on-shore winds occur infrequently, wind speeds are low, and the effective fetch is limited to a few kilometers. Thus, wind-generated waves in lakes are characterized by small amplitudes and short periods (Hofmann et al. 2008a). Apart from wind waves, commercial and tourist ship traffic cause ship-generated waves. The specific generation of wind and ship waves causes considerable different properties (e.g., wave period and length) with potentially different implications on the littoral zone (Eriksson et al. 2004; Erm and Soomere 2006; Hofmann et al.

2008a). Additionally, the temporal dynamics of wind and ship waves are different. Wind waves usually occur sporadically and infrequently, where in contrast ship waves can show a periodic and regular occurrence during the navigation periods (Soomere 2005; Hofmann et al. 2008a).

Wave mesocosms can be used to investigate the impact of surface waves with varying properties on habitat conditions and organisms. Mesocosm experiments help to understand how wave exposure affects the diversity and abundance of organisms apart from other effects, e.g., seasonality and biotic interactions such as competition. Many studies using a wave mesocosm were focused on marine habitats (e.g., Fonseca and Cahalan 1992; Gagnon et al. 2003; Precht and Huettel 2003), but only a few on lake littoral zones (Doyle 2001; Scheifhacken 2006; Droppo et al. 2007), where wave stress is less energetic as at marine shores.

To investigate the link between wave-generated hydrodynamic stress and ecological processes in lake littoral zones a wave mesocosm with a pneumatic wave machine was established at the Limnological Institute of the University of Konstanz. During the last years and also very recently, various experiments were conducted with special emphasis on the effect of waves on, e.g., the abrasion of periphyton (biofilms) (Scheifhacken 2006), the grazing activity of the herbivorous snail *Radix ovata* (Scheifhacken 2006), the distribution and activity of juvenile cyprinids (Klahold, pers. comm.), the hatching success of fish eggs (Probst and Stoll, pers. comm.), and energetic costs of juvenile cyprinids (Stoll, pers. comm.).

The purpose of the current study is to characterize and evaluate the wave field and wave-generated currents in this particular wave mesocosm by covering the different settings of the wave machine utilized during the biological experiments, and to compare the waves generated in the wave mesocosm with wind and ship waves typically occurring in Lake Constance.

Materials and methods

Wave mesocosm

The wave mesocosm is a 10 m long, 1 m wide, and 0.8 m deep concrete basin, of which one longitudinal side wall is made of glass. The mesocosm has a stepwise slope ranging between 1:6 and 1:10 that reflects the natural shore (littoral zone) of the prealpine Lake Constance (Fig. 5.1).

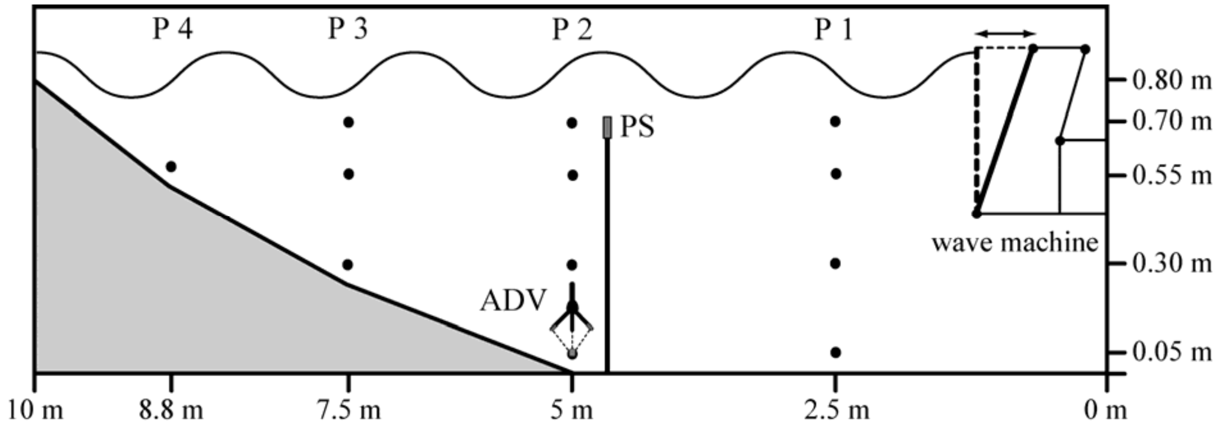

Fig. 5.1 Design of the wave mesocosm and experimental setup. The black dots mark the grid of the 12 measurement stations at the four sampling points (P 1-P 4). A piston-like wave machine generate the surface waves. Wave and current measurements were made by an Acoustic Doppler Velocity Meter (ADV), a pressure sensor (PS), and a video camera imaging system (VCIS, not shown).

Pneumatic wave machine

The pneumatic wave machine supports the generation of different wave heights and periods by adjusting pressure (intensity level, IL) and deflection (stroke length). In accordance with former biological studies the stroke length was kept constant (0.35 m) and the IL was varied in the range of 2-6 bar working pressure. The duration of the wave generation (permanent, periodic) can be regulated by a time switch. The working motion itself runs a double-acting piston activated by a compressor. The piston rod powers a flapping metal board (0.9 m x 0.5 m). To minimize counter currents and reduce the water impedance hinged lids close in the fast forward motion and re-open during the slow retraction (Scheifhacken, pers. comm.).

Wave and current measurements

Hydrodynamic measurements were carried out at four sampling points (P 1-P 4) in the mesocosm at distances of 2.5, 5.0, 7.5, and 8.8 m from the wave machine (Fig. 5.1). The sampling points correspond to different shore regions as follows: P 1 and 2 are located at the beginning of the shoaling region, where the wave already starts to feel the bottom, P 3 is further up in the transition zone, and P 4 in the surf zone where the wave begins to dissipate. At each sampling site, current velocities were measured at 0.05, 0.30, 0.55, and 0.70 m above the bottom, respectively, resulting in a grid of 12 measurement stations in total.

Wave properties were measured and derived at P 2 by three methodically independent techniques: a NORTEK Vector Acoustic Doppler Velocity Meter (ADV), a pressure sensor (PS), and a video camera imaging system (VCIS) with a sampling frequency of 8, 16, and 8 Hz, respectively. The sampling interval for each wave machine intensity level of 2, 3, 4, 5, and 6 bar was 10 min.

From ADV data the calculation of the wave parameters maximum wave height (H_{max}) and significant wave period (T_s) were made with a modified version of DIWASP (Directional Wave Spectra Toolbox) (Johnson 2004). Wave parameters were calculated for burst intervals of 512 samples (~1.1 min).

Alternatively, the wave parameters were determined from the PS for burst intervals of 1,024 samples (~1.1 min). For this purpose the measured time series of subsurface pressure in each burst interval was converted to a time series of surface elevation using the procedure described in Hofmann et al. (2008a). H_{max} and T_s were calculated by using the zero-upcrossing method (IAHR 1989). Within each burst, the wave amplitude was calculated separately for each time period between two consecutive zero upcrossings. The difference between the maximum elevation in this time period and the mean elevation in the burst interval was used as a measure of wave amplitude. H_{max} was estimated as twice the maximum of all wave amplitudes in the burst interval and T_s is defined as the average period of the highest one-third of wave heights (H_s) in the burst interval (IAHR 1989).

From the VCIS the wave parameters H_{max} and T_s were determined by the analysis of consecutive images (8 Hz). The images showed the propagation of the waves in a graduated mesh grid section around P 2. H_{max} was estimated directly from the observed surface elevation of the wave by determining the vertical distance between its crest and the preceding trough. T_s was calculated from the time needed by a wave to travel the distance of one wave length, where the accuracy was limited by the temporal resolution of the video camera.

H_{max} and T_s values determined for the burst intervals of the ADV, PS, and VCIS were averaged first over the 10 min measuring period for each IL of the wave machine. In a second step, the mean values calculated for the different techniques and for the different IL were averaged again and the standard deviation (SD) was calculated.

The wave-generated current velocities were measured over 10 min by the ADV with a sampling frequency of 8 Hz at all of the 12 stations and for IL set to 2, 3, 4, 5, and 6 bar. The two measured horizontal components of the current velocity were rotated into a longitudinal (in the direction of wave propagation) and a transversal (perpendicular to the direction of wave propagation) component. In the later analysis only the longitudinal component was used, because due to the directed propagation of the waves in the mesocosm the transversal component is negligibly small. For each sample, at each station, and for the five IL of the wave machine the resulting vector of the longitudinal and the vertical wave-generated current velocity component was computed over the 10 min measuring period. Thereof, the mean of the 1% largest current velocities in longitudinal and vertical direction at each station and for the five IL was determined.

Wave-related parameters

As wave-related parameters that characterize the impact of different wave types on the littoral zone the maximum wave-generated near-bottom current velocity (u_{max}), the near-bottom orbital excursion (OE), the wave energy flux to shore (E_F), and the potentially remobilized mean grain size (d_{50}) were used. These parameters were calculated for a wave typically generated in the wave mesocosm at the IL of 5 bar and for different wave types (wind, ship, and catamaran waves) in Lake Constance as described in Hofmann et al. (2008a) at water depths of 0.2, 0.4, and 0.8 m. Behalf the calculation of wave-related parameters the wave height was chosen constant for all wave types and corresponds to the highest possible wave height in the wave mesocosm at the IL of 5 bar (0.12 m). Thereby it was assumed that the wave height and period remain constant at 0.2, 0.4, and 0.8 m water depth. The wave periods used in the calculations were measured in the mesocosm (1.2 s) and in Lake Constance (2.0, 3.3, and 6.3 s for wind wave, the ship wave, and the catamaran wave, respectively (Hofmann et al. 2008a).

The maximum wave-generated near-bottom current velocity u_{max} (m s^{-1}) was calculated by using (Brown et al. 2005):

$$u_{\max} = \frac{\pi \cdot H}{T \cdot \sinh \frac{2 \cdot \pi \cdot h}{\lambda}} \qquad (\text{m s}^{-1}) \qquad (5.1)$$

where H denotes the wave height (m), T the wave period (s), h the water depth (m), and λ the wave length (m). The dispersion relation provided by Fenton and McKee (1990) was used to calculate λ.

The wave-generated orbital excursion (*OE*) is two times the horizontal semiaxis A (m) of the wave orbital defined as follows (CERC 2002):

$$A = a \cdot \frac{\cosh[k \cdot (z+h)]}{\sinh(k \cdot h)} \qquad \text{(m)} \qquad (5.2)$$

where a is the wave amplitude (m), $k = 2\pi/\lambda$ the wave number (m^{-1}), h the water depth (m), and z the position of the orbital above the bottom (m). The orbital excursion was calculated at the bottom ($z = -h$).

The energy flux to shore E_F (W m^{-1}) per unit length of wave crest can be estimated as the product of the group velocity with the wave energy. The latter is solely determined by the wave amplitude. E_F implicitly accounts for the different wave periods since the group velocity of surface waves depends on the wave period (Kundu and Cohen 2002; Hofmann et al. 2008a):

$$E_F = E \cdot c_g \qquad \text{(W m}^{-1}\text{)} \qquad (5.3)$$

$$E = \frac{1}{2}(\rho \cdot g \cdot a^2) \qquad \text{(Ws m}^{-2}\text{)} \qquad (5.4)$$

$$c_g = \frac{c}{2} \cdot \left(1 + \frac{2 \cdot k \cdot h}{\sinh(2 \cdot k \cdot h)}\right) \qquad \text{(m s}^{-1}\text{)} \qquad (5.5)$$

where E is the wave energy (Ws m^{-2}), c_g the group velocity (m s^{-1}), a the wave amplitude (m), c the phase velocity (m s^{-1}), k the wave number (m^{-1}), g the gravitational acceleration (m s^{-2}), and h the water depth (m).

The remobilization of particles under oscillatory flow due to surface waves can be determined from empirical equations. The mean grain size d_{50} of non-cohesive sediments that can be remobilized is (Hallermeier 1980; CERC 2002):

$$d_{50} = \frac{u_{\max}^{\;2}}{8 \cdot \left(\frac{\rho_s}{\rho_w} - 1\right) \cdot g} \qquad \text{(m)} \qquad (5.6)$$

where u_{max} (m s^{-1}) is the wave-generated near-bottom velocity, g the gravitational acceleration (m s^{-2}), ρ_s the sediment density (kg m^{-3}), and ρ_w the density of water (kg m^{-3}). In Lake Constance, potentially available and resuspended sediment has a density ρ_s of ~2,200 kg m^{-3} that was used for later calculations.

Results

Wave heights and periods

The wave parameters H_{max} and T_s were determined independently by the ADV, PS, and the VICS for the five IL of the wave machine. H_{max} increased from 0.065 ± 0.005 m (mean ± SD) at the IL of 2 bar to about 0.12 ± 0.015 m at 5 bar. Further increase in forcing of the wave machine at 6 bar leads to a reduced wave height of about 0.11 ± 0.008 m (Fig. 5.2A). The observed reduction of H_{max} at 6 bar is caused by the extinction of two concurrently generated, phase-shifted waves. The first and higher wave is generated by the forward and the second and smaller by the backward movement of the piston and subsequent reflection at the front wall of the wave mesocosm.

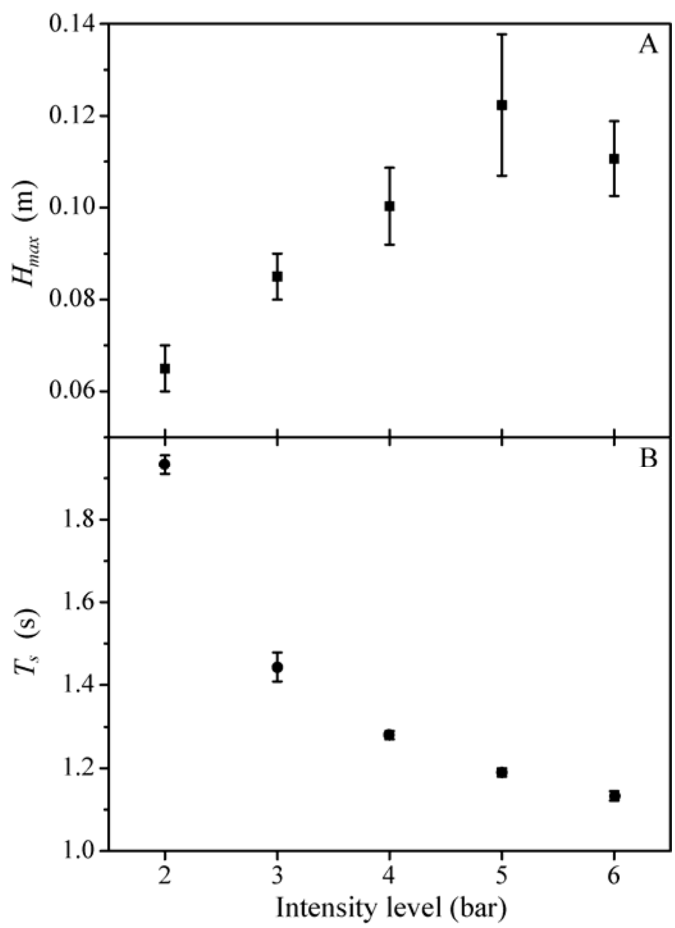

Fig. 5.2 Measured and derived wave parameters for the five intensity levels (IL) of the wave machine. (A) Maximum wave height (H_{max}). (B) Significant wave period (T_s). Both parameters were determined independently by an Acoustic Doppler Velocity Meter (ADV), a pressure sensor (PS), and video camera imaging system (VCIS). The squares and dots in both panels indicate the mean values derived from the different techniques with their standard deviation (SD).

T_s generated in the wave mesocosm continuously decreased from about 1.9 ± 0.02 s at 2 bar to about 1.1 ± 0.01 s at 6 bar (Fig. 5.2B).

The narrow range of the SD for H_{max} and T_s at the different IL expresses the high correspondence between all three measurement techniques and analysis methods.

Wave-generated current velocities

The wave-generated oscillating current velocities (longitudinal and vertical component) are summarized in vector plots and exemplarily shown for the IL of 3 and 5 bar (Fig. 5.3A,B). These results elucidate the shape of the wave orbital in terms wave-generated current velocities at the different stations in the wave mesocosm. Close to the water surface the oscillating current velocities describe a circular orbital that narrows continuously in the vertical component towards the bottom of the mesocosm, where the longitudinal component is the dominant current velocity. Maximum wave-generated current velocities are found at the IL of 5 bar (Fig. 5.3B). The current velocities decreased from about 0.25 m s^{-1} for the longitudinal and vertical component near the water surface to values of about 0.07 m s^{-1} and 0.02 m s^{-1} at the bottom. On the other hand, with decreasing water depth the longitudinal and vertical current velocities at 0.05 m above the bottom increased from 0.07 m s^{-1} and 0.02 m s^{-1} at 0.8 m to about 0.21 m s^{-1} and 0.07 m s^{-1} at 0.25 m (Fig. 5.3B). The wave-generated current velocities at the IL of 3 bar (Fig. 5.3A) are only slightly smaller at most of the measuring stations than the velocities at 5 bar (Fig. 5.3), although H_{max} at 5 bar is about 0.04 m higher than at 3 bar (Fig. 5.2A). The only significant difference is at P 4, where the longitudinal current velocity is increased by about 0.05 m s^{-1} from 3 to 5 bar (~31%).

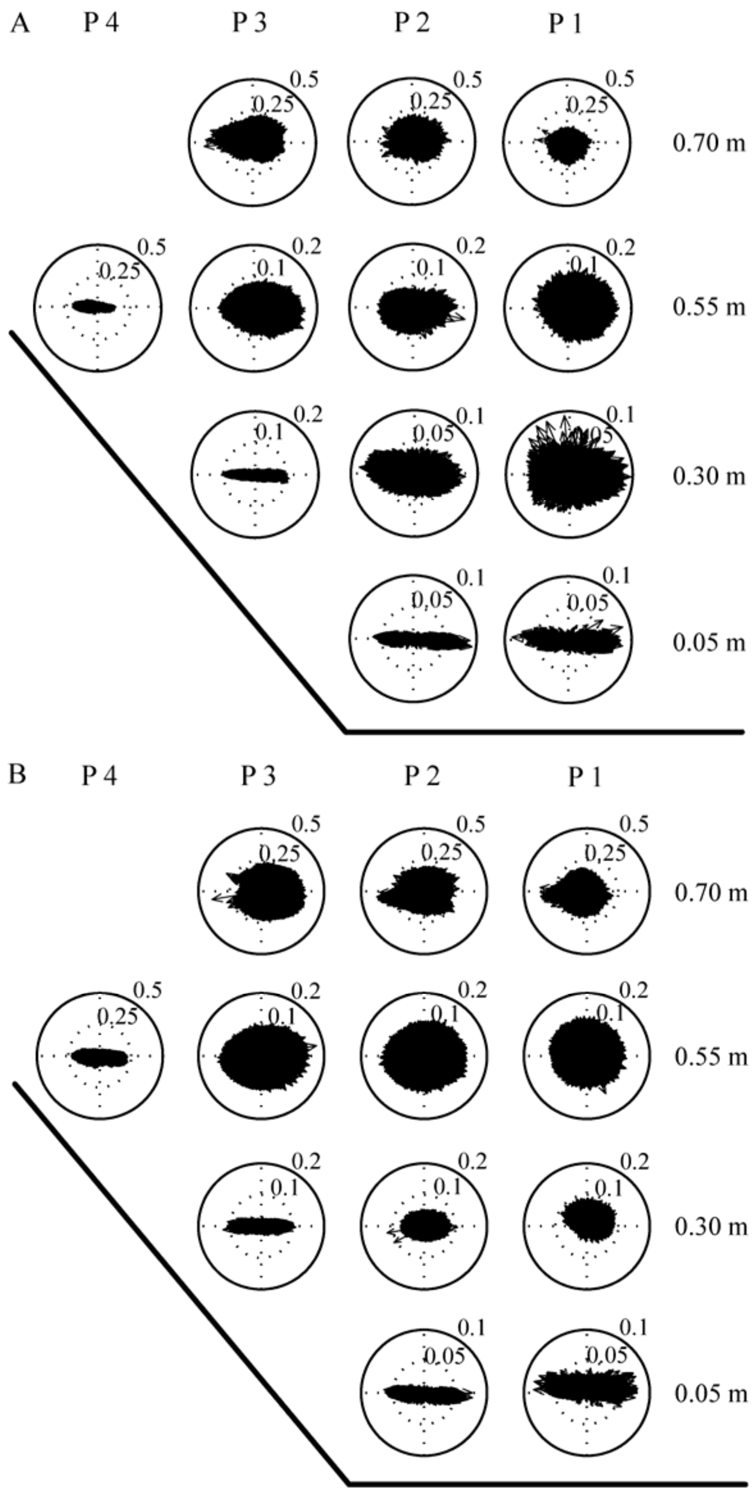

Fig. 5.3 Vector plots of the longitudinal and vertical current velocities (m s^{-1}) at each station measured by an Acoustic Doppler Velocity Meter (ADV). (A) At 3 bar. (B) At 5 bar. Note that the scaling differs. The individual vector plot elucidates the shape of the wave-generated orbital at each station. The vectors at each station were computed from the longitudinal and the vertical wave-generated current velocity component of each sample over the 10 min measuring period.

Discussion

The wave mesocosm of the Limnological Institute at the University of Konstanz covers wave heights between 0.065 and 0.12 m and wave periods between 1.1 and 1.9 s. The wave-generated current velocities range between 0.1 and 0.25 m s^{-1} near the water surface, where the longitudinal and the vertical component are of similar extent. At the bottom the longitudinal and vertical current velocities differed: while the longitudinal component covers a wide range between 0.07 and 0.21 m s^{-1} depending on the specific water depth, the vertical velocity component is much smaller and ranged between 0.02 and 0.07 m s^{-1}. This means that at the surface particles are rotated in orbits with the shape of a circle and at the bottom with the shape of a very flat ellipse, resulting rather in a back- and forward motion of particles and organisms like fishes than in an up- and downward drift at the bottom. In particular, the longitudinal (horizontal) current velocities and the orbital excursion increase rapidly with decreasing water depth (Figs. 5.3, 5.4B). Thus, for example, biofilms, snails and mussels, benthic invertebrates, and juvenile fishes that cannot escape from the shallow littoral, experience an increased hydrodynamic stress at low water depths (Grant and Madsen 1979; Cox and Kobayashi 2000). The wave typically generated in the wave mesocosm at the IL of 5 bar and different wave types (wind, ship, and catamaran waves) observed in the field of Lake Constance were compared to prove to which extent the wave mesocosm covers the situation in the field. The comparison refers to derived wave-related parameters as the maximum wave-generated near-bottom current velocity (u_{max}), the near-bottom orbital excursion (*OE*), the wave energy flux to shore (E_F), and the potentially remobilized mean grain size (d_{50}). Note that the wave generated in the wave mesocosm at the IL of 5 bar was chosen for the comparison because most of the biological experiments were conducted at this IL, where H_{max} and the near-bottom current velocities are found to be the highest. At all water depths and for all four wave-related parameters, the wave generated in the mesocosm shows far lower values compared to the waves in the field. The large differences can be explained by the much shorter period of the wave generated in the mesocosm (1.2 s) compared to the wind, ship, and catamaran waves (2, 3.3, and 6.3 s) in the field (Hofmann et al. 2008a). The short wave periods coincide with short wave lengths causing less bottom shear than longer waves at the same water depth. Thus, ship and catamaran waves that have much higher periods and wave lengths than those in the wave mesocosm cannot be simulated. However, the wave generated in the mesocosm is rather comparable to wind waves in the field that have short periods and small wave heights.

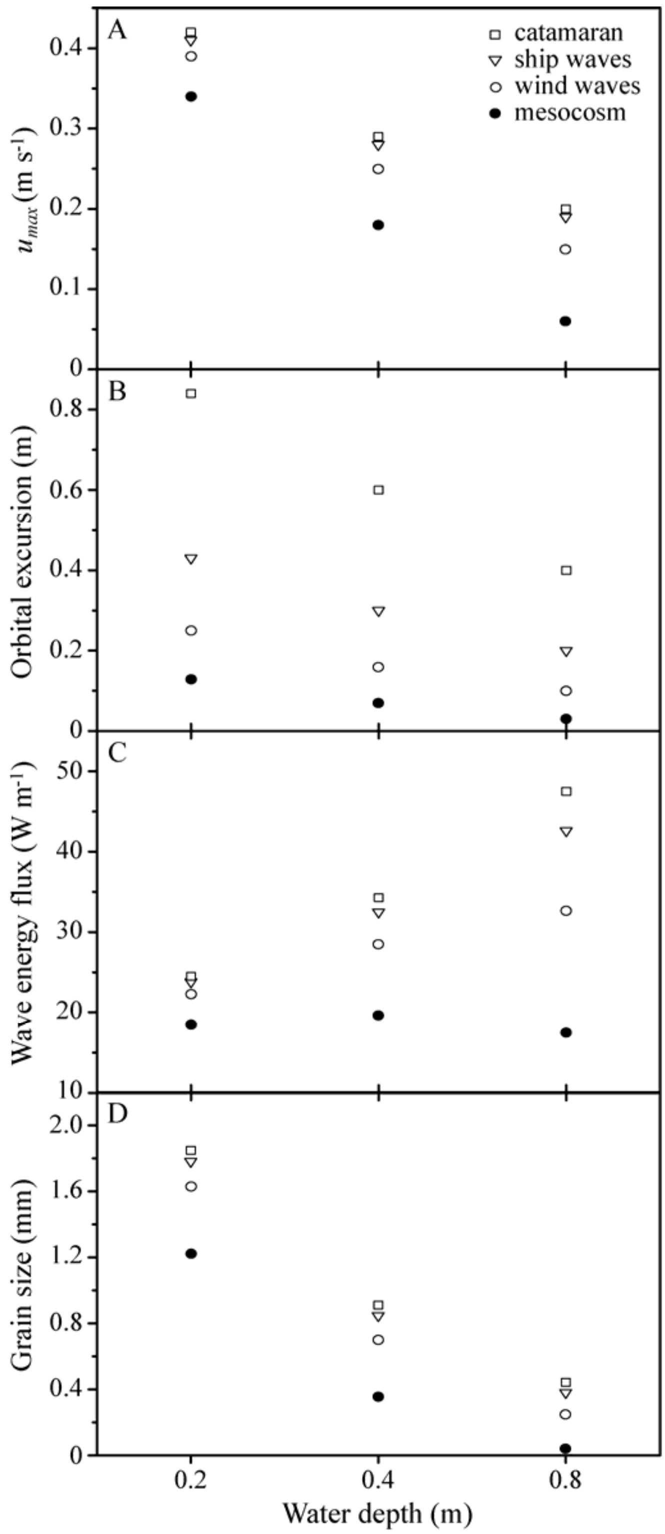

Fig. 5.4 Comparison of wave-related parameters for a wave typically generated in the wave mesocosm at the intensity level (IL) of 5 bar (filled circle) and different wave types [wind (open circle), ship (open triangle), and catamaran (open square) wave] occurring in Lake Constance, as a function of water depth. The wave height was kept constant (0.12 m) for all wave types and water depths, and corresponds to the highest possible wave in the mesocosm. The wave periods used in the calculations are 1.2, 2.0, 3.3, and 6.3 s for the wave in the mesocosm, the wind wave, the ship wave, and the catamaran wave, respectively. (A) Maximum wave-generated near-bottom current velocity (u_{max}). (B) Near-bottom orbital excursion (*OE*). (C) Wave energy flux to shore (E_F). (D) Potentially remobilized mean grain size (d_{50}).

Nevertheless, various investigations during the last years have documented that even these very short-period and low-amplitude waves generated in the mesocosm have considerable implications on biota, for example, the reduction of periphyton biomass (Scheifhacken 2006), a reduced grazing activity of the herbivorous snail *Radix ovata* (Scheifhacken 2006), and a reduced activity of juvenile cyprinids that is accompanied with reduced food uptake (Klahold, pers. comm.). However, since we know that the waves generated in the mesocosm have smaller wave heights, shorter wave periods, and hence smaller near-bottom current velocity, than the waves in the field, the implications on biota determined in the mesocosm experiments underestimate the actual consequences of wave motions on biota in the lake.

Despite these findings, experiments in a wave mesocosm have two main advantages. First, the wave mesocosm allows to trigger the wave exposure with time. This helps to separate, understand, and evaluate the implications of waves that occur sporadically but then continuously over hours or even days from those that occur regularly and periodically. Both temporal patterns cover different situations in the field, where the former is representative for on-shore wind events and the latter for the exposure to ship waves (Hofmann et al. 2008a). Second, mesocosm experiments can investigate systematically the effect of wave exposure since additional factors occurring in the field such as stress through predation, competition, or temperature fluctuations can be excluded or controlled.

Acknowledgments

I thank Nicole Scheifhacken and Petra Klahold for their cooperation and inspiration. I further thank the staff from the electronic and mechanical workshop at the University of Konstanz for technical assistance and for the development of the pressure sensor. I gratefully acknowledge the assistance of Iris Töpfer and Felix Weiß during the measurements and the data analysis. This work was supported by the German Research Foundation (DFG) within the framework of the Collaborative Research Center 454 'Littoral Zone of Lake Constance'.

General discussion and perspectives

General discussion

Surface gravity waves are an important energy source for littoral ecosystems, where most of the wave energy is dissipated. The hydrodynamic disturbances associated with surface waves in the littoral zone affect abiotic as well as biotic processes, as outlined in the introduction. Thus the characterization of wave properties and related processes is of particular importance for an integrated understanding of the environmental conditions in littoral zones. Surface waves can be generated by wind and by ships. Former studies, however, were solely focused on wind waves (e.g., Jin and Wang 1998; Allan and Kirk 2000) or on ship waves (e.g., Bhowmik 1975; Maynord 2005) and covered mostly short time periods only, like the recent studies on the relative importance of fast catamaran ferries in ocean-shelf regions (e.g., Parnell and Kofoed-Hansen 2001; Soomere 2005). The present study is the first that performed long-term measurements and combined analysis of wind and ship waves in a lacustrine ecosystem.

In Lake Constance, the generation of wind waves is strongly dependent on the effective fetch length and wind speed, which are both significant smaller than in the coastal ocean (Komen et al. 1996; CERC 2002; Brown et al. 2005). Hence, in most lakes the wave field is characterized by waves with small amplitudes and high frequencies, which require high-resolution measurements in terms of accuracy and time. The appropriate instrumentation (data acquisition system for a pressure sensor) was developed during this thesis.

The occurrence of wind waves is generally restricted to time periods with relatively strong on-shore directed winds, which are rather sporadically concerning magnitude and duration. The variability of the wave field among different sites at the same lake, however, can be significant as demonstrated by simultaneous measurements of wave parameters at sites with opposing exposures (wind direction and fetch length) to wind. The exposure to wind is reflected by the specific wave properties, like the generated wave heights, as well as by their temporal dynamics. In particular, wind waves measured at the study site Littoral Garden, which is exposed to northeastern winds with a fetch of a few kilometers, are characterized by wave heights below 0.8 m, wave periods between 1.5 and 2.3 s, and wave lengths between 2 and 8 m (Chapter 2). In contrast, the study site Langenargen, which is exposed to western winds with an effective fetch of about 30 km, is characterized by wave heights, periods, and lengths that exceed the ones measured at the site Littoral Garden.

In addition to wind-generated waves, I could also measure a variety of ship-generated waves (Chapter 2). At the main study site Littoral Garden, wind and ship waves differ considerably in their wave lengths and wave periods, whereby wind waves have shorter wave lengths and periods. The characteristic spectral properties of wind and ship waves are used to discriminate them by their respective wave period, whereas wind waves are characterized by wave periods below 2.5 s and ship waves above 2.5 s. Furthermore, three different types of ship waves were distinguished and assigned to the regular car and passenger ferry crossing from Meersburg to Konstanz-Staad, to the passenger ships that cruise all around Lake Constance during the tourist season, and to a newly introduced catamaran ferry connecting Friedrichshafen and Konstanz. At the study site Littoral Garden the ferry, passenger, and catamaran waves are characterized by maximum wave heights between a few centimeters and 0.5 m, wave periods of 3.7 s, 2.9 s, and 6.3 s, and wave lengths of about 20 m, 13 m, and up to 50 m, respectively. Each specific ship generates several wave groups representing divergent and transverse waves (Fig. VA), those are able to propagate over long distances while maintaining their properties (Sorensen 1973; Stumbo 1999; Maynord 2005). As a consequence, ship waves can be observed on shores that are far away from the sailing line (Fig. VB).

Detailed evaluation of the time series of wave field properties allowed for the quantification of the relative importance of wind and ship waves in terms of the respective wave energy flux to shore. Ship-generated waves contribute about 41% of the annual mean wave energy flux to shore and are thus of equal importance as wind-generated waves. In summer, when passenger ships contribute to the overall wave field, ship waves even dominate the wave field in terms of the energy flux to shore and also in terms of their frequency of occurrence. Enhanced ship traffic during daytime and during summer causes a diurnal and a seasonal pattern in the frequency of occurrence and in the heights of surface waves.

Since ship waves are generated all around Lake Constance and are able to travel over long distances, a large proportion of shores at Lake Constance are exposed to a ship-wave-dominated wave field, especially during the tourist season in summer. This observation can be considered as representative for many prealpine and alpine lakes in Europe. Because of their morphometric characteristics and geological exposure (e.g., high length-to-width ratio and shelter of the lake surface from high wind speeds by steep mountain slopes), these lakes have rather short effective fetch lengths and are typically exposed to low wind speeds that limit the wind-generated wave field. Further, most of these lakes are typically located in highly populated areas with diverse recreational and commercial activities, which are associated with intensive ship traffic on the lakes. However, detailed measurements are still required to confirm the significant contribution of ship waves to the overall wave field in these lakes.

The differences between wind and ship waves in respect to the magnitude of their wave parameters (e.g., wave height and wave period) and their temporal dynamics (sporadically occurring wind waves versus frequently and regular occurring ship waves) result in different patterns of disturbance in the littoral ecosystem. So is the resuspension of particles from the sediment surface strongly influenced by the temporal variability of wind and ship waves (Chapter 3). Sediment resuspension induced by wind waves occurs sporadically and less frequently than ship-wave induced resuspension. During wind events the wind-wave generated maximum near-bottom current velocities and the suspended sediment concentrations remain high for hours, where background currents transport the suspended sediment horizontally (Luettich et al. 1990; Lesht and Hawley 2001; Lee et al. 2007). It can be assumed that these major wind events are persistent enough to allow for a steady state between resuspension, settling, and transport of particles. The passage of a single ship, in contrast, increases the near-bottom current velocities drastically and causes a high and distinct peak in the suspended sediment concentration. The just resuspended particles cover a wide range of grain sizes, whereby the coarser particles resettle quickly and finer particles remain in the water column for several minutes. The regular occurrence of ship waves, especially of passenger ships during daytime and in summer, causes a substantial increase in suspended sediment concentration in the shallow littoral and results in a diurnal cycle as well as a seasonal pattern in the suspended sediment concentration and in resuspension.

Regular resuspension events are known to prevent sediment consolidation and the formation of a cohesive sediment layer (Dyer 1986; Schoellhamer 1996). The newly deposited and unconsolidated sediments are more susceptible to resuspension and lead to strong impulse loads of suspended particles due to weak and previously ineffective wind waves (Garrad and Hey 1987; Schoellhamer 1996). Hence, ship waves that maintain such an environment may contribute in combination with wind waves to enhanced erosion of sediments in the littoral zone. Lake-shore erosion is a widely discussed topic in the public, but detailed complementary approaches that consider wind and ship waves in combination with spatially high-resolved sediment properties (e.g., particle density and grain size distribution) are still missing. As a first component to describe sediment erosion in a lake, this study provides data on the temporal dynamics and the relative importance of wind- and ship-induced resuspension. To further study the process of erosion, additional studies that consider also the component of sediment transport have to follow.

Apart from the site-specific exposure of lake shores to wind and ship waves, the degree of sediment resuspension and erosion is also affected by seasonal water level fluctuations and their interplay with surface waves: The latter provide the energy for resuspension and erosion, while the former determine the section of the shore that is exposed to the erosive power (Chapter 1). Thus, wind and ship waves that occur throughout the year have their main impact zone at different sections of the littoral due to seasonal water level fluctuations of 2-3 m in Lake Constance. During the high water level in summer, the substrate exposed to wave motion consists mainly of boulders, cobbles, gravel, where sand and silt are minor components in the interstitial. During the low water levels in winter, the substrate exposed to wave motion consists of much smaller particles like sand, silt, and clay. The continuous interplay of water level fluctuations and surface waves formed the existing shore morphology. However, the mean water level of Lake Constance is decreasing since the recent past. This will increase the wave exposure of finer sediments and thus the resuspension and transport of particles resulting in increasing erosion in the littoral zone. Nowadays, erosion threatens many historic and archeologically important underwater heritages like pile dwellings all around Lake Constance (Bürgi and Schlichterle 1986; Körninger 2005). From the results of this study it can be assumed that ship waves have certainly a pronounced impact on this process.

Another important impact of surface waves in shallow waters is their ability to alter the underwater light climate. In Chapter 1 and 4 it was demonstrated that the amplitudes and temporal scales of the fluctuations in light intensity are related to the process of wave focusing, the change in surface elevation, and sediment resuspension caused by surface waves. The variability of the light climate is maximal at shallow depths, where the light intensity is important for the growth of phytoplankton, biofilms, and macrophytes (Scheffer et al. 1993; Rørslett and Johansen 1995). The strongest amplitudes of fluctuations in light intensity were observed under bright sun and when the surface wave field was dominated by small-amplitude (0.01-0.05 m), high-frequency (1-2 Hz), and short-length (0.4-1.6 m) wind-generated ripple waves. Wave focusing causes flashes of light with intensities that are significantly above the incident light intensity. It was observed that the depth and the intensity of the maximum underwater light intensity are highly dependent on the composition of the surface wave field. This confirms results from theoretical investigations by Zaneveld et al. (2001). By using a modulated surface wave field they have demonstrated that low-frequency waves shift the maximum in light intensity to larger depths whereas the high-frequency waves result in a maximum at shallower depths with higher maximal intensities.

In addition to the observed high-frequent and high-amplitude fluctuations in light intensity due to wave focusing, the wind- and ship-induced resuspension can dramatically reduce the light intensity in the littoral zone on temporal scales ranging from minutes to hours and thus may contribute to light limitation of phytoplankton and biofilm growth. Ship waves that cause resuspension especially during daytime, the most productive time, contribute to this limitation in particular.

On seasonal time scales, not only the seasonal variation in the incident light, but also the variations in water level alter the underwater light climate for biofilms, macrophytes, and sessile organisms. Considerations for Lake Constance revealed that the fluctuations of the light intensity induced by the water level fluctuations have larger amplitudes than seasonal variation of the incident light. Because of high water levels in summer and low ones in winter, where the incident light reaches its maximum and minimum, respectively, both processes counteract and reduce the amplitudes in the variation of the underwater light intensity.

In the preceding sections I demonstrated the importance of surface waves for various physical processes in the littoral zone, but surface waves also interact directly with the biota in terms of wave-generated current velocities and hydrodynamic stress (Scheifhacken 2006; Scheifhacken et al. 2007; Stoll et al. 2008). Studies on the impacts of hydrodynamic stress on biota can be conducted best in a wave mesocosm as it was established at the Limnological Institute of the University of Konstanz. During the last years and very recently various biological experiments were conducted with special emphasis on the effect of waves. The measurements conducted during this study (Chapter 5) may help to evaluate and validate the results of ongoing experiments as well as results obtained in the past, since a detailed knowledge of the wave characteristics in the mesocosm and their comparability with the field conditions was missing in the past. The magnitudes of waves and wave-related parameters generated in the wave mesocosm are much smaller than in the field. Thus, the implications on biota determined during biological experiments underestimate the actual consequences of wave motion in the field. Nevertheless, the main advantages of experiments in a wave mesocosm, as for instance the possibility to trigger the wave exposure with time and to conduct the experiments under controlled conditions, remain and can lead to new findings. For future experiments it would be favorable to plan, conduct, and validate biological experiments together with physical measurements.

Perspectives

Long-term and high-frequent measurements of the surface wave field at the study site Littoral Garden (Lake Constance) revealed that wind and ship waves are of similar importance (Chapter 2). The comparison with another site with different wind exposure further revealed the spatial variability of the wave field. Thus, wave field measurements at a single site are of limited significance for the entire lake especially to a large lake like Lake Constance.

The numerical simulation of the surface wave field with a wave model that is applicable to the shallow littoral zone provides a tool to extrapolate site-specific observations to different sites of interest or even to a basin scale. Such a wave model that has implemented shallow water equations is SWAN (Simulating Waves NearShore) (SWAN 2007). The model provides simulated values of all relevant wave parameters at a high spatial and temporal resolution. Motivated by this study the SWAN model was applied to Lake Constance using a high-resolution bottom-grid topography (20 x 20 m). Preliminary simulations for steady western and northeastern winds of 10 m s^{-1} predict a reasonably wave field of Lake Constance (Fig. VI).

Nested-grid simulations, which are based on preceding basin-scale simulations and applied to specifically confined sites, can provide spatially high-resolution information of wave field parameters and their dynamics in the littoral zone.

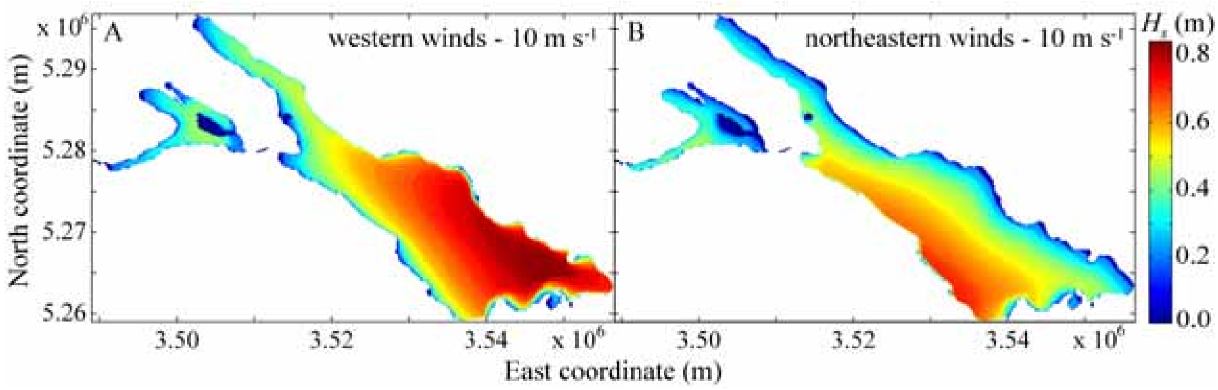

Fig. VI Numerical simulation of the significant wave height (H_s) at Lake Constance by using the SWAN model. (A) For western winds with a wind speed of 10 m s^{-1}. (B) For northeastern winds with a wind speed of 10 m s^{-1}.

However, the current parameter settings of SWAN are adjusted for shallow ocean-shelf regions and have still to be adjusted to the shallow littoral zone in lakes (Jin and Ji 2001; Keen et al. 2007). The preliminary simulations presented here are based on a steady state wind field, but since the natural wind field is usually variable in space and time, the calibration and later validation of the model requires realistic, dynamic, and horizontally heterogeneous wind fields. In addition, ship waves have to be incorporated into the model as well. This requires parallel in situ measurements at the sites of interest to obtain a complete description of the surface wave field and its implications on processes in the littoral zone. Nested-grid simulations can be used for this purpose, since the measured and validated empirical relations between the properties of the surface wave field and its implications on processes such as resuspension and light climate can be assigned to other sites. For example, a detailed characterization of the sediment properties (e.g., grain size, grain size distribution, and particle density) (Schünemann 1993) together with simulated near-bottom current velocities in the entire littoral zone of Lake Constance form the basis for a basin-wide estimate of resuspension.

In the littoral zone surface waves cause not only resuspension of particles, but also an enhanced exchange of pore water due to fluctuating pressure at the sediment surface (Li et al. 1997; Asmus et al. 1998; Precht et al. 2004). Both processes are expected to induce the release of methane and nutrients (phosphate and nitrate) from the sediment pore water into the water column. The release of methane and nutrients is of special importance. Methane is a potent greenhouse gas (Rosa et al. 2004; Giles 2006; IPCC 2007) and the origin of high methane concentrations in the epilimnion compared to the hypolimnion of Lake Constance during summer is widely discussed but still unclear (Thebrath et al. 1993; Schulz et al. 2001). Nutrients are an important resource for primary production (Hutchinson 1967; Wetzel 2001), but become a limiting factor during the summer months in the epilimnion, especially since the re-oligotrophication of Lake Constance (IGKB 2002). Wave-generated disturbances in the littoral zone could provide to some extend an additional source for the limited nutrient phosphorous.

Ship waves that are entering the littoral zone at regular time intervals provide an excellent natural setting to demonstrate and determine the release of methane and nutrients from the sediment pore water in the littoral zone. The importance of ship waves for these processes could be determined in relation to wind waves. A comparison with the dissolved nutrient and methane concentrations in the pelagial could show, whether the littoral zone can act as a source of nutrients and methane. By this comparison it can also be determined whether methane can serve as a tracer to quantify the exchange rate between the littoral zone and the open water.

References

Abdallah, A. M., and D. R. Barton. 2003. Environmental factors controlling the distributions of benthic invertebrates on rocky shores of Lake Malawi, Africa. J. Great Lakes Res. (suppl. 2) 29: 202-215.

Airoldi, L., and F. Cinelli. 1997. Effects of sedimentation on subtidal macroalgal assemblages: An experimental study from a mediterranean rocky shore. J. Exp. Mar. Bio. Ecol. 215 (2): 269-288, doi:10.1016/S0022-0981(96)02770-0.

Airy, G. B. 1845. On the laws of the tides on the coasts of Ireland, as inferred from an extensive series of observations made in connexion with the Ordnance Survey of Ireland (1844). Phil. Trans. R. Soc. Lond.: 1-124.

Allan, J. C., and R. M. Kirk. 2000. Wind wave characteristics at Lake Dunstan, South Island, New Zealand. NZ J. Mar. Freshwater Res. 34: 573-591.

Asmus, R. M., M. H. Jensen, K. M. Jensen, E. Kristensen, H. Asmus, and A. Wille. 1998. The role of water movement and spatial scaling for measurement of dissolved inorganic nitrogen fluxes in intertidal sediments. Estuar. Coast. Shelf Sci. 46 (2): 221-232, doi:10.1006/ecss.1997.0273.

Ball, D. F. 1964. Loss-on-ignition as an estimate of organic matter and organic carbon in non-calcareous soils. J. Soil Sci. 15: 84-92.

Bauer, B. O., M. S. Lorang, and D. J. Sherman. 2002. Estimating boat-wake-induced levee erosion using sediment suspension measurements. J. Waterw. Port C-ASCE 128 (4): 152-162, doi:10.1061/(ASCE)0733-950X(2002)128:4(152).

Bäuerle, E., D. Ollinger, and J. Ilmberger. 1998. Some meteorological, hydrological, and hydrodynamical aspects of Upper Lake Constance. Arch. Hydrobiol. Spec. Issues Advanc. Limnol. 53: 31-83.

Baumgärtner, D., and K.-O. Rothhaupt. 2005. The impact of predation by burbot (*Lota lota* L.) on the macroinvertebrate community in the littoral zone of a large lake. Aquat. Ecol. 39: 79-92.

Bhowmik, N. G. 1975. Boat-generated waves in lakes. J. Hydr. Div., ASCE 101 (HY 11): 1465-1468.

Bhowmik, N. G., T. W. Soong, W. F. Reichelt, and N. M. L. Seddik. 1991. Waves generated by recreational traffic on the upper Mississippi River System, p. 33-35. Research Report 117. Illinois State Water Survey.

Bourne, J. K., K. Joel, and G. Ludwig. 2005. Eccentric Salton Sea. Nalt. Geogra. Mag. 207 (2): 88-107.

Braun, E., and K. Schärpf. 1990. Internationale Bodensee - Tiefenvermessung, p. 98. IGKB - Internationale Gewässerschutzkommission für den Bodensee.

Brennwald, M. S., F. Peeters, D. M. Imboden, S. Giralt, M. Hofer, D. M. Livingstone, S. Klump, K. Strassmann, and R. Kipfer. 2004. Atmospheric noble gases in lake sediment pore water as proxies for environmental change. Geophys. Res. Let. 31: L04202, doi:10.1029/2003GL019153.

Brown, E., A. Colling, D. Park, J. Phillips, D. Rothery, and J. Wright. 2005. Waves, tides and shallow-water processes, 2nd ed. Butterworth-Heinemann.

Bürgi, J., and H. Schlichterle. 1986. Gefährdete Ufersiedlungen am Bodensee. Archäol. Schweiz 9 (2): 34-41.

Bussmann, I. 2005. Methane release through resuspension of littoral sediment. Biogeochemistry 74 (3): 283-302, doi:10.1007/s10533-004-2223-2.

Cattaneo, A. 1990. The effect of fetch on periphyton spatial variation. Hydrobiol. 206: 1-10.

CERC. 2002. Shore protection manual: Volume I. US Army Coastal Engineering Research Center, Books for Business.

Chen, P.-F., and C.-H. Huang. 2004. An inverse hull design approach in minimizing the ship wave. Ocean Eng. 31 (13): 1683-1712, doi:10.1016/j.oceaneng.2003.08.010.

Clark, B. M. 1997. Variation in surf-zone fish community structure across a wave-exposure gradient. Estuar. Coast. Shelf Sci. 44 (6): 659-674, doi:10.1006/ecss.1996.0151.

Coe, M. T., and J. A. Foley. 2001. Human and natural impacts on the water resources of the Lake Chad basin. J. Geophys. Res. 106 (D4): 3349-3356.

Coops, H., M. Beklioglu, and T. L. Crisman. 2003. The role of water-level fluctuations in shallow lake ecosystems - workshop conclusions. Hydrobiol. 506 (1-3): 23-27.

Cox, D. T., and N. Kobayashi. 2000. Identification of intense, intermittent coherent motions under shoaling and breaking waves. J. Geophys. Res. 105 (C6): 14223-14236.

Dean, R. G., and R. A. Dalrymple. 1998. Water wave mechanics for engineers and scientists. World Scientific Publishing.

Dera, J., and H. R. Gordon. 1968. Light fluctuations in the photic zone. Limnol. Oceanogr. 13: 697-699.

Donelan, M. A., F. W. Dobson, H. C. Graber, N. Madsen, and C. McCormick. 2005. Measurement of wind waves and wave-coherent air pressures on the open sea from a moving SWATH vessel. J. Atmos. Oceanic Technol. - Spec. Section 22 (7): 896-908.

Doyle, R. D. 2001. Effects of waves on the early growth of *Vallisneria americana*. Freshwater Biol. 46 (3): 389-397, doi:10.1046/j.1365-2427.2001.00668.x.

Droppo, I. G., N. Ross, M. Skafel, and S. N. Liss. 2007. Biostabilization of cohesive sediment beds in a freshwater wave-dominated environment. Limnol. Oceanogr. 52 (2): 577-589.

Dumont, H. 1995. Ecocide in the Caspian Sea. Nature 377: 673-674.

Duxbury, A. C., A. B. Duxbury, and K. A. Sverdrup. 2003. An introduction to the World's Oceans, 7th ed. McGraw Hill.

Dyer, K. R. 1986. Coastal and estuarine sediment dynamics. Wiley.

Eggleton, M. A., K. B. Gido, W. J. Matthews, and G. D. Schnell. 2004. Assessment of anthropogenic influences on littoral-zone aquatic communities of Lake Texoma, Oklahoma-Texas, USA. Ecohydrol. Hydrobiol. 4 (2): 103-117.

El Ganaoui, O., E. Schaaff, P. Boyer, M. Amielh, F. Anselmet, and C. Grenz. 2004. The deposition and erosion of cohesive sediments determined by a multi-class model. Estuar. Coast. Shelf Sci. 60 (3): 457-475.

Emery, W. J., and R. E. Thomson. 2001. Data analysis methods in physical oceanography, 2nd ed. Elsevier Science.

Eriksson, B. K., A. Sandström, M. Isæus, H. Schreiber, and P. Karås. 2004. Effects of boating activities on aquatic vegetation in the Stockholm archipelago, Baltic Sea. Estuar. Coast. Shelf Sci. 61 (2): 339-349.

Erm, A., and T. Soomere. 2006. The impact of fast ferry traffic on underwater optics and sediment resuspension. Oceanologia (suppl.) 48: 283-301.

Fenton, J. D., and W. D. McKee. 1990. On calculating the lengths of water waves. Coast. Eng. 14 (6): 499-513, doi:10.1016/0378-3839(90)90032-R.

Finger, D., P. Bossard, M. Schmid, L. Jaun, B. Müller, D. Steiner, E. Schäffer, M. Zeh, and A. Wüest. 2007. Effects of alpine hydropower operations on primary production in a downstream lake. Aquat. Sci. 69: 240-256, doi:10.1007/s00027-007-0873-6.

Fischer, P., and R. Eckmann. 1997. Seasonal changes in fish abundance, biomass and species richness in the littoral zone of a large European lake, Lake Constance, Germany. Arch. Hydrobiol. 139: 433-448.

Fonseca, M. S., and J. A. Cahalan. 1992. A preliminary evaluation of wave attenuation by four species of seagrass. Estuar. Coast. Shelf Sci. 35: 565-576.

Francoeur, S., and B. Biggs. 2006. Short-term effects of elevated velocity and sediment abrasion on benthic algal communities. Hydrobiol. 561 (1): 59-69.

Froude, W. W. 1877. Experiments upon the effect produced on the wave-making resistance of ship. Trans. Inst. Naval Arch. 18: 77-87.

Fugate, D. C., and C. T. Friedrichs. 2002. Determining concentration and fall velocity of eatuarine particle concentrations using ADV, OBS and LISST. Cont. Shelf Res. 22: 1867-1886.

Gafny, S., A. Gasith, and M. Goren. 1992. Effect of water level fluctuation on shore spawning of *Mirogrex terraesanctae* (Steinitz), (*Cyprinidae*) in Lake Kinneret, Israel. J. Fish Biol. 41 (6): 863-871.

Gagnon, P., G. Wagner, and J. H. Himmelmann. 2003. Use of a wave tank to study the effects of water motion and algal movement on the displacement of the sea star *Asterias vulgaris* towards its prey. Mar. Ecol. Prog. Ser. 258: 125-132.

Garrad, P. N., and R. D. Hey. 1987. Boat traffic, sediment resuspension and turbidity in a Broadland River. J. Hydrol. 95 (3-4): 289-297.

Garrison, T. S. 2005. Essentials of oceanography, 4th ed. Thompson Brooks/Cole.

Giles, J. 2006. Methane quashes green credentials of hydropower. Nature 444: 524-225.

Grant, W. D., and O. S. Madsen. 1979. Combined wave and current interaction with a rough bottom. J. Geophys. Res. 84 (C4): 1797-1808.

Guan, C., and L. Xie. 2004. On the linear parameterization of drag coefficient over sea surface. J. Phys. Oceanogr. - Notes and Correspondence 34 (C5): 2847-2851.

Güde, H., M. Seidel, P. Teiber, and M. Weyhmüller. 2000. P-release from littoral sediments in Lake Constance. Verh. Internat. Verein. Limnol. 27: 1-4.

Guganesharajah, K., and E. M. Shaw. 1984. Forecasting water levels for Lake Chad. Water Resour. Res. 20 (8): 1053-1065.

Guy, H. P. 1969. Laboratory theory and methods for sediment analysis, p. 58. Techniques of water-resources investigations of the United States Geological Survey. US Geological Survey.

Håkanson, L. 2005. A new dynamic model for Suspended Particulate Matter (SPM) in lakes. Int. Rev. Hydrobiol. 90 (5-6): 603-636, doi:10.1002/iroh.200510790.

Hallermeier, R. J. 1980. Sand motion initiation by water waves: Two asymtotes. J. Waterw. Port C. Div. 106: 299-318.

Hamblin, P. F. 1989. Observations and model of sediment transport near the turbidity maximum of the upper Saint Lawrence Estuary. J. Geophys. Res. 94 (C10): 14419-14428.

Hawley, N., and C. H. Lee. 1999. Sediment resuspension and transport in Lake Michigan during the unstratified period. Sedimentology 46 (5): 791-805.

Hawley, N., and B. M. Lesht. 1992. Sediment resuspension in Lake St. Clair. Limnol. Oceanogr. 37 (8): 1720-1737.

Hawley, N., B. M. Lesht, and D. J. Schwab. 2004. A comparison of observed and modeled surface waves in southern Lake Michigan and the implications for models of sediment resuspension. J. Geophys. Res. 109: C10S03, doi:10.1029/2002JC001592.

Heyer, J., and U. Berger. 2000. Methane emission from the coastal area in the Southern Baltic Sea. Estuar. Coast. Shelf Sci. 51: 13-30, doi:10.1006/ecss.2000.0616.

Hofmann, H., A. Lorke, and F. Peeters. 2008a. The relative importance of wind and ship waves in the littoral zone of a large lake. Limnol. Oceanogr. 53 (1): 368-380.

---. 2008b. Temporal and spatial scales of water level fluctuations in lakes and their ecological implications. Hydrobiol. 613 (1): 85-96, doi:10.1007/s10750-008-9474-1.

---. in press. Wave-induced variability of the underwater light climate in the littoral zone. Verh. Internat. Verein. Limnol.

Holdaway, G. P., P. D. Thorne, D. Flatt, S. E. Jones, and D. Prandle. 1999. Comparison between ADCP and transmissometer measurements of suspended sediment concentration. Cont. Shelf Res. 19: 421-441.

Hollan, E., D. B. Rao, and E. Bäuerle. 1980. Free surface oscillations in Lake Constance with an interpretation of the 'wonder of the rising water' at Konstanz in 1549. Arch. Met. Geoph. Biokl. Series A, 29: 301-325.

Hunt, P. C., and J. W. Jones. 1972. The effect of water level fluctuations on a littoral fauna. J. Fish Biol. 4: 385-394.

Hutchinson, G. E. 1967. A treatise on limnology - Vol II: Introduction to lake biology and the limnoplankton. Wiley.

IAHR. 1989. IAHR working group on wave generation and analysis: List of sea-state parameters. J. Waterw. Port C-ASCE 115: 793-808.

IFM-GEOMAR. 2005. Methods: Determination of density in solid samples [Internet]. Available from: http://www.ifm-geomar.de/index.php?id=1916&L=1.

IGKB. 2002. Tolerierbare Phosphor-Fracht des Bodensee-Obersees 54, p. 81. *In* H. Bührer [ed.], Bericht der Internationalen Gewässerschutzkommission für den Bodensee.

IPCC. 2007. Fourth assessment report [Internet]. IPCC. Available from: http://www.ipcc.ch/.

Ippen, A. T. 1966. Estuary and coastline hydrodynamics. McGraw-Hill.

James, M. R., C. Weatherhead, C. Stanger, and E. Graynoth. 1998. Macroinvertebrate distribution in the littoral zone of Lake Coleridge, South Island, New Zealand: Effects of habitat stability, wind exposure, and macrophytes. NZ J. Mar. Freshwater Res. 32: 287-305.

Jin, K., and K. Wang. 1998. Wind generated waves in Lake Okeechobee. J. Am. Water Res. Assoc. 34 (5): 1099-1108.

Jin, K. R., and Z. G. Ji. 2001. Calibration and verification of a spectral wind wave model for Lake Okeechobee. Ocean Eng. 28 (5): 571-584, doi:10.1016/S0029-8018(00)00009-3.

Jöhnk, K. D., D. Straile, and W. Ostendorp. 2004. Water level variability and trends in Lake Constance in the light of the 1999 centennial flood. Limnologica 34: 15-21.

Johnson, D. 2004. DIWASP: Directional wave spectra toolbox for MATLAB: User manual [Internet]. Available from: http://www.metocean.co.nz/webcontent/software/DIWASP_manual.pdf.

Kawamata, S. 2001. Adaptive mechanical tolerance and dislodgement velocity of the kelp *Laminaria japonica* in wave-induced water motion. Mar. Ecol. Prog. Ser. 211: 89-104.

Keddy, P. A. 1982. Quantifying within lake gradients of wave energy: interrelationships of wave energy, substrate particle size and shoreline plants in Axe Lake, Ontario. Aquat. Bot. 14: 41-58.

Keen, T. R., W. E. Rogers, J. Dykes, J. M. Kaihatu, and K. T. Holland. 2007. Determining heterogeneous bottom friction distributions using a numerical wave model. J. Geophys. Res. 112: C08008, doi:10.1029/2005JC003309.

Khodorevskaya, R. P., and Y. V. Krasikov. 1999. Sturgeon abundance and distribution in the Caspian Sea. J. Appl. Ichthyol. 15 (4-5): 106-113.

Kinsman, B. 1965. Wind waves: Their generation and propagation on the ocean surface. Prentice-Hall.

Kirk, J. T. O. 1994. Light and photosynthesis in aquatic ecosystems, 2nd ed. Cambridge University Press.

Klige, R. K., and M. S. Myagkov. 1992. Changes in the water regime of the Caspian Sea. GeoJournal 27 (3): 299-307, doi:10.1007/BF02482671.

Komen, G. J., L. Cavaleri, M. A. Donelan, K. Hasselmann, S. Hasselmann, and P. A. E. M. Janssen. 1996. Dynamics and modelling of ocean waves. Cambridge University Press.

Körninger, J. 2005. Unterwasserarchäologie am Überlinger See. NAU Nachrichtenblatt Arbeitskreis Unterwasserarchäologie 11/12: 63-70.

Kosarev, A. N., and E. A. Yablonskaya. 1994. The Caspian Sea. SPB Academic Publishing.

Kotowski, W., and H. Piorkowski. 2005. Competition and succession affecting vegetation structure in riparian environments: Implications for nature management. Ecohydrol. Hydrobiol. 5 (1): 51-57.

Kristensen, P., M. Søndergaard, and E. Jeppesen. 1992. Resuspension in a shallow eutrophic lake. Hydrobiol. 228: 101-109.

Krogstad, H. E., and O. A. Arntsen. 2000. Linear wave theory - Part A: Regular waves [Internet]. Norwegian University of Science and Technology. Available from: http://folk.ntnu.no/oivarn/hercules_ntnu/LWTcourse/lwt_new_2000_Part_A.pdf.

Kundu, P. K., and I. M. Cohen. 2002. Fluid mechanics. Academic Press.

Lawrence, P. L., and R. G. D. Davidson-Arnott. 1997. Alongshore wave energy and sediment transport on Southeastern Lake Huron, Ontario, Canada. J. Coast. Res. 13 (4): 1004-1015.

Le Blond, P. H., and L. A. Mysak. 1978. Waves in the ocean, 1st ed. Elsevier.

Lee, C., D. J. Schwab, D. Beletsky, J. Stroud, and B. M. Lesht. 2007. Numerical modeling of mixed sediment resuspension, transport, and deposition during the March 1998 episodic events in southern Lake Michigan. J. Geophys. Res. 112: C02018, doi:10.1029/2005JC003419.

Lerman, A., D. M. Imboden, and J. R. Gat. 1995. Physics and chemistry of lakes, 2nd ed. Springer.

Lesht, B. M., and N. Hawley. 2001. Using wave statistics to drive a simple sediment transport model. Proceedings of the International Symposium on Ocean Wave Measurement and Analysis 2: 1366-1375.

Li, Y., A. J. Mehta, K. Hatfield, and M. S. Dortch. 1997. Modulation of constituent release across the mud-water interface by water waves. Water Resour. Res. 33 (6): 1409-1418.

Lindholm, T., M. Svartström, L. Spoof, and J. Meriluoto. 2001. Effects of ship traffic on archipelago waters off the Långnäs harbour in Åland, SW Finland. Hydrobiol. 444 (1-3): 217-225, doi:10.1023/A:1017518131889.

Lorke, A., B. Müller, M. Maerki, and A. Wüest. 2003. Breathing sediments: The control of diffusive transport across the sediment-water interface by periodic boundary-layer turbulence. Limnol. Oceanogr. 48 (6): 2077-2085.

Lou, J., T. Wolf, and W. Rosenthal. 1999. Modeling sediment resuspension in coastal areas, p. 23-35. *In* J. Harff, W. Lemke and K. Stattegger [eds.], Computerized modeling of sedimentary systems. Springer.

Luettich, Jr., R. A., D. R. F. Harleman, and L. Somlyody. 1990. Dynamic behavior of suspended sediment concentrations in a shallow lake perturbed by episodic wind events. Limnol. Oceanogr. 35 (5): 1050-1067.

Luft, G., and G. van den Eertwegh. 1991. Long-term changes in the water level of Lake Constance and possible causes, p. 31-44. *In* G. Schiller, R. Lemmel and M. Spreafico [eds.], Hydrology of natural and manmade lakes. IAHS Press.

Luft, G., and H. Vieser. 1990. Veränderung der Bodensee-Wasserstände von 1887 bis 1987. Dtsch. Gewässerkundl. Mittl. 34 (5/6): 148-156.

Lynch, J. F., J. D. Irish, C. R. Sherwood, and Y. C. Agrawal. 1994. Determining suspended sediment particle size information from acoustical and optical backscatter measurements. Cont. Shelf Res. 14 (10/11): 1139-1165.

Madsen, J. D. 1976. Wave climate of the continental margin: Elements of its mathematical description, p. 65-87. *In* D. J. Stanley and D. J. P. Swift [eds.], Marine sediment transport and environmental management. Wiley.

Maynord, S. T. 2005. Wave height from planning and semi-planning small boats. River Res. Appl. 21 (1): 1-17, doi:10.1002/rra.803.

McGowan, S., P. R. Leavitt, and R. I. Hall. 2005. A whole-lake experiment to determine the effects of winter droughts on shallow lakes. Ecosystems 8 (6): 694-708, doi:10.1007/s10021-003-0152-x.

Meadows, G. A., L. A. Meadows, W. L. Wood, J. M. Hubertz, and M. Perlin. 1997. The relationship between Great Lakes water levels, wave energies, and shoreline damage. Bull. Am. Meteorol. Soc. 78 (4): 675-683.

Mortimer, C. H. 1974. Lake hydrodynamics. Mitt. Int. Ver. Limnol. 20: 124-197.

Naselli-Flores, L., and R. Barone. 2005. Water-level fluctuations in Mediterranean reservoirs: setting a dewatering threshold as a management tool to improve water quality. Hydrobiol. 548: 85-99, doi:10.1007/s10750-005-1149-6.

Nielson, P. 1994. Coastal bottom boundary layers and sediment transport, 2nd ed. World Scientific Publishing.

Ostendorp, W., K. Schmieder, and K. Jöhnk. 2004. Assessment of human pressures and their hydromorphological impacts on lakeshores in Europe. Ecohydrol. Hydrobiol. 4 (4): 379-395.

Pahl-Wostl, C. 1992. Dynamic versus static models for photosynthesis. Hydrobiol. 238: 189-196.

Parchure, T. M., W. H. McAnally, and A. M. Teeter. 2001. Desktop method for estimating vessel-induced sediment suspension. J. Hydraul. Eng.-ASCE 127 (7): 577-587.

Parnell, K. E., and H. Kofoed-Hansen. 2001. Wakes from large high-speed ferries in confined coastal waters: Management approaches with examples from New Zealand and Denmark. Coast. Manage. 29 (3): 217-237, doi:10.1080/08920750152102044.

Peeters, F., D. Finger, M. Hofer, M. Brennwald, D. M. Livingstone, and R. Kipfer. 2003. Deep-water renewal in Lake Issyk-Kul driven by differential cooling. Limnol. Oceanogr. 48 (4): 1419-1431.

Peeters, F., R. Kipfer, D. Achermann, M. Hofer, W. Aeschbach-Hertig, U. Beyerle, D. M. Imboden, K. Rozanski, and K. Fröhlich. 2000. Analysis of deep-water exchange in the Caspian Sea based on environmental tracers. Deep-Sea Res. - Part I 47: 621-654.

Peters, L. 2005. Periphyton as a habitat for meiofauna - a case of a neglected community. Ph.D. Thesis. University of Konstanz.

Peters, L., and W. Traunspurger. 2005. Species distribution of free-living nematodes and other meiofauna in littoral periphyton communities of lakes. Nematology 7 (2): 267-280.

Pierson, D. C., H. Markensten, and N. Strombeck. 2003. Long and short term variations in suspended particulate material: the influence on light available to the phytoplankton community. Hydrobiol. 494: 299-304.

Piroth, K., and E. Plate. 1993. The wave climate, an important factor in lakeshore deterioration - concept and measurements at Lake Constance, p. 77-92. *In* W. Ostendorp and P. Krumscheid-Plankert [eds.], Seeuferzerstörung und Seeuferrenaturierung in Mitteleuropa. Limnol. Akt.: 5. Gustav Fischer Verlag.

Pond, S., and G. L. Pickard. 1983. Introductory dynamical oceanography. Pergamon Press.

Precht, E., U. Franke, L. Polerecky, and M. Huettel. 2004. Oxygen dynamics in permeable sediments with wave-driven pore water exchange. Limnol. Oceanogr. 49 (3): 693-705.

Precht, E., and M. Huettel. 2003. Advective pore-water exchange driven by surface gravity waves and its ecological implications. Limnol. Oceanogr. 48 (4): 1674-1684.

Rasmussen, J. B., and D. J. Rowan. 1997. Wave velocity thresholds for fine sediment accumulation in lakes, and their effect on zoobenthic biomass and composition. J. N. Am. Benthol. Soc. 16: 449-465.

Rodionov, S. N. 1994. Global and regional climate interaction: The Caspian Sea experience. Kluwer Academic Publisher.

Rolinski, S. 1999. On the dynamics of suspended matter transport in the tidal river Elbe: Description and results of a Lagrangian model. J. Geophys. Res. 104 (C6): 26043-26057.

Roman, M. R., and K. R. Tenore. 1978. Tidal resuspension in Buzzards Bay, Massachusetts, I. Seasonal changes in the resuspension of organic carbon and chlorophyll-a. Estuar. Coast. Shelf Sci. 6: 37-46.

Romero, J. R., and J. M. Melack. 1996. Sensitivity of vertical mixing in a large saline lake to variations in runoff. Limnol. Oceanogr. 41 (5): 955-965.

Rørslett, B., I. Hawes, and A. M. Schwarz. 1997. Features of the underwater light climate just below the surface in some New Zealand inland waters. Freshwater Biol. 37 (2): 441-454.

Rørslett, B., and S. W. Johansen. 1995. Dynamic response of the submerged macrophyte, *Isoëtes lacustris*, to alternating light levels under field conditions. Aquat. Bot. 51 (3-4): 223-242, doi:10.1016/0304-3770(95)00473-D.

Rosa, L. P., M. A. dos Santos, B. Matvienko, E. O. dos Santos, and E. Sikar. 2004. Greenhouse gases emissions by hydroelectric reservoirs in tropical regions. Clim. Change 66 (1-2): 9-21.

Rosenthal, W. 1993. Flächenhafte Seegangsuntersuchungen in der Friedrichshafener Bucht des Bodensee-Obersees, p. 66. GKSS - Forschungszentrum Geesthacht GmbH.

Scheffer, M., S. H. Hosper, M.-L. Meijer, B. Moss, and E. Jeppesen. 1993. Alternative equilibria in shallow lakes. Trends Ecol. Evol. 8 (8): 275-279.

Scheifhacken, N. 2006. Life at turbulent sites: benthic communities in lake littorals interacting with abiotic and biotic constraints. Ph.D. Thesis. University of Konstanz.

Scheifhacken, N., C. Fiek, and K.-O. Rothhaupt. 2007. Complex spatial and temporal patterns of littoral benthic communities interacting with water level fluctuations and wind exposure in the littoral zone of a large lake. Fundam. Appl. Limnol. 169 (2): 115-129.

Schleuter, D. 2006. Competition for food between perch (*Perca fluviatilis* L.) and invasive ruffe (*Gynocephalus cernuus* (L.)) in re-oligotrophic Lake Constance. Ph.D. Thesis. University of Konstanz.

Schleuter, D., and R. Eckmann. 2006. Competition between perch (*Perca fluviatilis*) and ruffe (*Gymnocephalus cernuus*): the advantage of turning night into day. Freshwater Biol. 51: 287-297, doi:10.1111/j.1365-2427.2005.01495.x.

Schmieder, K., M. Dienst, W. Ostendorp, and K. Jöhnk. 2004. Effects of water level variations on the dynamics of the reed belts of Lake Constance. Ecohydrol. Hydrobiol. 4 (4): 469-480.

Schoellhamer, D. H. 1996. Anthropogenic sediment resuspension mechanisms in a shallow microtidal estuary. Estuar. Coast. Shelf Sci. 43 (5): 533-548, doi:10.1006/ecss.1996.0086.

Schubert, H., S. Sagert, and R. M. Forster. 2001. Evaluation of the different levels of variability in the underwater light field of a shallow estuary. Helgol. Mar. Res. 55: 12-55, doi:10.1007/s10150000064.

Schulz, M., E. Faber, A. Hollerbach, H. G. Schroeder, and H. Guede. 2001. The methane cycle in the epilimnion of Lake Constance. Arch. Hydrobiol. 151 (1): 157-176.

Schünemann, B. 1993. Litoralsedimente des Bodensees: Mineralogie - CS Analytik - Granulometrie (Sedimentuntersuchungen im Rahmen der Kartierung der Makrophytenvegetation des Bodensees 1993), p. 146. ISF Langenargen.

Snyder, R. L., and J. Dera. 1970. Wave-induced light-field fluctuations in the sea. J. Opt. Soc. Am. 60 (8): 1072-1079.

Søndergaard, M., P. Kristensen, and E. Jeppesen. 1992. Phosphorus release from resuspended sediment in the shallow and wind-exposed Lake Arresø, Denmark. Hydrobiol. 228: 91-99.

Soomere, T. 2005. Fast ferry traffic as a qualitatively new forcing factor of environmental processes in non-tidal sea areas: A case study in Tallinn Bay, Baltic Sea. Environ. Fluid Mech. 5 (4): 293-323, doi:10.1007/s10652-005-5226-1.

Soomere, T., and J. Engelbrecht. 2005. Extreme elevations and slopes of interacting solitons in shallow water. Wave Motion 41 (2): 179-192, doi:10.1016/j.wavemoti.2004.06.006.

Soomere, T., R. Põder, K. Rannat, and A. Kask. 2005. Profiles of waves from high-speed ferries in the coastal area. Proc. Est. Acad. Sci. Eng. 11: 245-260.

Sorensen, R. M. 1973. Ship-generated waves. Adv. Hydrosci. 9: 49-83.

Stephens, D. W. 1990. Changes in lake levels, salinity and the biological community of Great Salt Lake (Utah, USA), 1847-1987. Hydrobiol. 197: 139-146.

Stokes, G. G. 1847. On the theory of oscillatory waves. Trans. Cambridge Philos. Soc. 8: 441-455.

Stoll, S., P. Fischer, P. Klahold, N. Scheifhacken, H. Hofmann, and K.-O. Rothhaupt. 2008. Effects of water depth and hydrodynamics on the growth and distribution of juvenile cyprinids in the littoral zone of a large pre-alpine lake. J. Fish Biol. 72: 1001-1022, doi:10.1111/j.1095-8649.2007.01780.x.

Stramska, M., and T. Dickey. 1998. Short-term variability of the underwater light field in the oligothrophic ocean in response to surface waves and clouds. Deep Sea Res. Part I 45: 1393-1410.

Stramski, D., C. R. Booth, and G. B. Mitchell. 1992. Estimation of downward irradiance attenuation from a single moored instrument. Deep Sea Res. Part A: Oceanogr. Res. Pap. 39 (3-4): 567-584, doi:10.1016/0198-0149(92)90089-C.

Stramski, D., and L. Legendre. 1992. Laboratory simulation of light-focusing by water-surface waves. Mar. Biol. 114 (2): 341-348.

Stumbo, R. M. 1999. The prediction, measurement, and analysis of wake wash from marine vessels. Mar. Technol. SNAME N. 36 (4): 248-260.

SWAN. 2007. Simulating Waves NearShore [Internet]. Delft University of Technology. Available from: http://www.citg.tudelft.nl/live/pagina.jsp?id=f928097d-81bb-4042-971b-e028c00e3326&lang=en.

Thebrath, B., F. Rothfuss, M. J. Whiticar, and R. Conrad. 1993. Methane production in littoral sediment of Lake Constance. FEMS Microbiol. Ecol. 102 (3-4): 279-289.

Thevenot, M. M., and N. C. Kraus. 1993. Comparison of acoustical and optical measurements of suspended material in the Chesapeake Esturary. J. Mar. Env. Eng. 1: 65-79.

Thomson, W. L. K. 1887. On ship waves. Proc. Inst. Mech. Eng.: 409-433.

Tsigelnaya, I. D. 1995. Issyk-Kul Lake, p. 199-229. *In* A. F. Maudych [ed.], Enclosed seas and large lakes of Eastern Europe and Middle Asia. SPB Academic Publishing.

Tucker, M. J., and E. G. Pitt. 2001. Waves in ocean engineering. Elsevier.

Ursell, F. 1960. On Kelvin's ship waves pattern. J. Fluid Mech. 8: 418-431.

Usmanova, R. M. 2003. Aral Sea and sustainable development. Water Sci. Technol. 47 (7-8): 41-47.

Utne-Palm, A. C. 2004. Effects of larvae ontogeny, turbidity, and turbulence on prey attack rate and swimming activity of Atlantic herring larvae. J. Exp. Mar. Bio. Ecol. 310: 147-161.

van Duin, E. H. S., G. Blom, F. J. Los, R. Maffione, R. Zimmermann, C. F. Cerco, M. Dortch, and E. P. H. Best. 2001. Modeling underwater light climate in relation to sedimentation, resuspension, water quality and autotrophic growth. Hydrobiol. 444: 25-42.

Vittori, G. 2003. Sediment suspension due to waves. J. Geophys. Res. 108 (C6): 3173, doi:10.1029/2002JC001378.

Voulgaris, G., and S. T. Meyers. 2004. Temporal variability of hydrodynamics, sediment concentration and sediment settling velocity in a tidal creek. Cont. Shelf Res. 24: 1659-1683.

Walsh, P., and L. Legendre. 1983. Photosynthesis of natural phytoplankton under high frequency light fluctuations simulating those induced by sea surface waves. Limnol. Oceanogr. 28 (4): 688-697.

Weggel, J. R., and R. M. Sorensen. 1986. Ship wave prediction for port and channel design, p. 797-814. Ports '86 Conference. American Society of Civil Engineers (ASCE).

Wetzel, R. G. 2001. Limnology - Lake and river ecosystems. Academic Press.

Wiegel, R. L. 1964. Oceanographical engineering. Prentice-Hall.

Wilson, S. D., and P. A. Keddy. 1985. The shoreline distribution of *Juncus pelocarpus* along a gradient of exposure to waves: an experimental study. Aquat. Bot. 21: 277-284.

Wüest, A., and A. Lorke. 2003. Small-scale hydrodynamics in lakes. Annu. Rev. Fluid Mech. 35: 373-412, doi:10.1146/annurev.fluid.35.101101.161220.

Zaneveld, R. J. V., E. Boss, and A. Barnard. 2001. Influence of surface waves on measured and modeled irradiance profiles. Appl. Opt. 40 (9): 1442-1449.

Zavialov, P. O., A. G. Kostianoy, S. V. Emelianov, A. A. Ni, D. Ishniyazov, V. M. Khan, and T. V. Kudyshkin. 2003. Hydrographic survey in the dying Aral Sea. Geophys. Res. Let. 30 (13): 1659.

Acknowledgments

Sincere thanks are given to all the people who helped me to accomplish this thesis during the last years.

First of all, I want to thank my supervisor, Prof. Dr. Frank Peeters for offering me this topic and for his outstanding support during the last years. I especially thank him having always an open door for my questions and the long, helpful, and very fruitful discussions. This greatly improved my way of working and this thesis in particular. His enthusiastic and creative nature in practicing science was very inspiring. I further thank Prof. Dr. habil. Karl-Otto Rothhaupt and Dr. habil. Klaus Jöhnk for the evaluation of this thesis and for being on my defense committee.

I am grateful to everybody in the Environmental Physics Group for the good time during the last years.

Many thanks to Dr. Andreas Lorke, who contributed to this thesis with good ideas, scientific discussions, valuable comments, and helpful corrections. I am also grateful for many other things I could learn from him, and which helped me to understand lakes from a physical perspective. Apart from this, Andreas and Manuela became special friends to me. Thanks for the pleasant time and the inspiring discussions that were always thought-provoking.

Beatrix Rosenberg and Josef Halder I thank for the support in the field and for being always up to date with the computer. I acknowledge their helpful hands and commitment also at the end of a long working day. Bea, thanks for the familiar atmosphere in the room.

Thanks to Stefan Stoll, Dr. Nicole Scheifhacken, Petra Klahold, and Nik Probst for their collaborations and discussions during joint projects that combined biological and physical knowledge.

The scientific workshop at the University of Konstanz in particular Georg Heine and Bruno Erne constructed lots of my measuring devices that formed an important basis for the long and very accurate data sets. Many thanks!

I also thank the people at the ISF Langenargen for their help and assistance in the field and laboratory, in particular Dr. Thomas Wolf, Dr. Martin Wessels, Klaus Weih, and Karin Popp.

This work was supported by the assistance of many students. Sincere thanks to Roland Cerna, David Fischer, Johannes Giesecke, Heinrich Grabmayr, Stefan Heinze, Falk Hildebrant, Julia Kleinteich, Matthias Kohlndorfer, Tobias Merz, Johannes Sutter, Iris Töpfer, and Felix Weiß.

I thank all the colleges from the Limnological Institute for their support, services, and nice time at the institute, in particular my fellow PhD students, the secretaries Silvia Berger and Karin Huppertz, and Martin Wolf, Alfred Sulger, Christine Gebauer, Gisela Richter, and Petra Merkel for technical support and help in the laboratory.

I am very grateful to my parents, who always supported me during this thesis, and to Diana for her help, confidence, and for lots of great experiences full of happiness.

This study was financed by the German Research Foundation (DFG) within the framework of the Collaborative Research Center 454 'Littoral Zone of Lake Constance' and the European Science Foundation with a travel grant.

Curriculum vitae

Name	Hilmar Hofmann
Date	27 September 1976
Place of birth	Hoyerswerda
Nationality	German
2004 - 2007	Doctoral thesis entitled 'Characteristics and implications of surface gravity waves in the littoral zone of a large lake (Lake Constance)' at the Limnological Institute, Environmental Physics Group, University of Konstanz, supervisor Prof. Dr. Frank Peeters
2003 - 2004	Research associate at the Chair of Freshwater Conservation, Brandenburg University of Technology Cottbus
2003	Diploma thesis entitled 'Morphometrische, hydrologische und hydrogeologische Charakterisierung des Tagebausees Plessa 117 (Grünewalder Lauch)' at the Chair of Freshwater Conservation, Brandenburg University of Technology Cottbus Award for the best Diploma thesis of the Faculty of Environmental Sciences and Process Engineering at Brandenburg University of Technology Cottbus
1999 - 2003	Study of Environmental and Process Engineering at Brandenburg University of Technology Cottbus
2001	Research project entitled 'Factor analysis of environmental data sets' at Delft University of Technology, The Netherlands
1998 - 1999	Socrates-Erasmus-Student in Civil Engineering and Environmental Chemistry at Delft University of Technology, The Netherlands
1996 - 1998	Basic studies of Environmental and Process Engineering at Brandenburg University of Technology Cottbus

List of publications

Hofmann, H., A. Lorke, and F. Peeters. 2008. The relative importance of wind and ship waves in the littoral zone of a large lake. Limnol. Oceanogr. 53 (1): 368-380.

Hofmann, H., A. Lorke, and F. Peeters. 2008. Temporal scales of water level fluctuations in lakes and their ecological implications. Hydrobiol. 613 (1): 85-96, doi:10.1007/s10750-008-9474-1.

Hofmann, H., A. Lorke, and F. Peeters. *in press*. Wave-induced variability of the underwater light climate in the littoral zone. Verh. Internat. Verein. Limnol.

Hofmann, H., A. Lorke, and F. Peeters. *in revision*. Wave-induced resuspension in the littoral zone of a large lake. Water Resour. Res.

Lorke, A., A. Weber, **H. Hofmann**, and F. Peeters. 2008. Opposing diel migration of fish and zooplankton in the littoral zone of a large lake. Hydrobiol. 600 (1): 139-146, doi:10.1007/s10750-007-9183-1.

Stoll, S., P. Fischer, P. Klahold, N. Scheifhacken, **H. Hofmann**, and K.-O. Rothhaupt. 2008. Effects of water depth and hydrodynamics on the growth and distribution of juvenile cyprinids in the littoral zone of a large pre-alpine lake. J. Fish Biol. 72: 1001-1022, doi:10.1111/j.1095-8649.2007.01780.x.

Probst, W. N., S. Stoll, **H. Hofmann**, P. Fischer, and R. Eckmann. *in press*. Spawning site selection of Eurasian perch *Perca fluviatilis* L. in relation to temperature and wave exposure. Ecol. Freshw. Fish.

Scheifhacken, N., P. Klahold, and **H. Hofmann**. *submitted*. Wave mesocosm experiments as tool for behavioral and ecological studies in lake littorals. Hydrobiol.

Manuscripts in preparation

Hofmann, H., E. Bäuerle, P. Fischer, and F. Peeters. *in preparation*. Observation of resuspension-induced density plumes in the littoral zone of Lake Constance.

Stoll, S., P. Fischer, and **H. Hofmann**. *in preparation*. The effect of habitat exposure and temperature on the young-of-the-year fish community in littoral habitats.

Conference and workshop presentations

Hofmann, H., A. Lorke, and F. Peeters. 2007. Wave-induced variability of the underwater light climate in the littoral zone. 30th Congress of the International Association of Theoretical and Applied Limnology (SIL), Montreal, Canada.

Hofmann, H., A. Lorke, and F. Peeters. 2006. The impact of water level fluctuations at different temporal and spatial scales on abiotic and biotic processes. 10th Workshop on Physical Processes in Natural Waters. Granada, Spain.

Hofmann, H., A. Lorke, and F. Peeters. 2005. Temporal and spatial scales of water level fluctuations. Workshop: Water level fluctuations in lacustrine systems: ecological impacts and prospects of future climate change. Konstanz, Germany

Hofmann, H., A. Lorke, and F. Peeters. 2005. Wave-induced resuspension in the littoral zone of Lake Constance. 9th Workshop on Physical Processes in Natural Waters. Lancaster, UK.

Hofmann, H., E. Bäuerle, P. Fischer, and F. Peeters. 2005. Observation of resuspension-induced density plumes in the littoral zone of Upper Lake Constance. Aquatic Science Meeting 2005 of the American Society of Limnology and Oceanography (ASLO). Salt Lake City, Utah, USA.